MODELING FATE AND TRANSPORT OF *CRYPTOSPORIDIUM PARVUM* AND ROTAVIRUS IN OVERLAND FLOW

BY

RABIN BHATTARAI

DISSERTATION

Submitted in partial fulfillment of the requirements
for the degree of Doctor of Philosophy in Agricultural and Biological Engineering
in the Graduate College of the
University of Illinois at Urbana-Champaign, 2011

Urbana, Illinois

Doctoral Committee:

Professor Prasanta K. Kalita, Chair
Professor Marcelo H. Garcia
Associate Professor Richard A. Cooke
Associate Professor Timothy R. Ellsworth

ABSTRACT

In the United States, there have been at least 1870 outbreaks associated with drinking water during the period of 1920 to 2002, causing 883,806 illnesses. Most of these outbreaks are resulted due to the presence of microbial pathogens in drinking water. *Cryptosporidium parvum* (*C. parvum*) has been recognized as one of the most frequently occurring microbial contaminants that can cause infection and diarrhea in many mammalian hosts, including humans. About 403,000 of an estimated 1.61 million residents in the Milwaukee area became ill with the stomach cramps, fever, diarrhea and dehydration caused by the outbreak of *C. parvum* in 1993. It was the largest waterborne disease outbreak in documented United States history. Similarly, rotavirus is the leading cause of death among children around the world. Each year more than two million children are hospitalized due to rotavirus infection and more than 500,000 children die from diarrheal disease caused by rotavirus. Past studies have demonstrated that environmental factors such as rainfall intensity and duration, slope, soil type and surface cover conditions significantly affect the transport of *C. parvum* oocyst and rotavirus in surface flow. Laboratory experiments conducted at the University of Illinois have demonstrated *C. parvum* oocysts and rotavirus transport is greatly influenced by climatic and soil-surface conditions like slope, soil types, soil texture, and ground cover.

The objective of this study was to simulate the fate and transport of *C. parvum* and rotavirus in overland flow in different ground cover and slope conditions. Transport of pathogens in overland flow can be simulated mathematically by including terms for the concentration of the pathogens in the liquid phase (in suspension or free-floating) and the solid phase (adsorbed to the soil solid particles like clay, sand and silt). Advection, adsorption, and decay processes have been considered in the physically-based model. The mass balance equations have been solved

using numerical technique to predict spatial and temporal changes in pathogen concentrations in two phases. In order to capture the dynamics of sediment-bound pathogen, the Water Erosion Prediction Project (WEPP) is coupled with the pathogen transport model. Outputs from WEPP simulations (flow velocity, depth, saturated conductivity and the soil particle fraction exiting in flow) are transferred as input to the pathogen transport model. Altogether four soil types (Alvin, Catlin, Darwin and Newberry), four slope conditions (1.5, 2.5, 3.0 and 4.5%), three rainfall intensities (2.54, 6.35 and 9.0 cm/hr), and three different surface cover conditions (bare, Brome grass and Fescue) have been used in the experimental investigations. Results of *C. parvum* and rotavirus transport from these conditions have been used in calibrating and validating the model simulation results.

Model simulation results of *C. parvum* and rotavirus transport through soil surface with and without any ground cover (bare soil) have produced very good agreement between observed and predicted results in most cases. Experimental data on pathogen transport showed multiple peaks in few cases. It was noted that the model results could capture only first observed peak in pathogen break through curve but could not replicate multiple peaks in pathogen transport that were found in experimental results. Additionally, there were more parameters used in model calibration for vegetated surface compared to surface without ground cover. This study provides both success and challenges of the *Cryptosporidium parvum* and rotavirus modeling and list future activities so that a pathogen transport model can be reasonably used under different climatic and soil conditions.

ACKNOWLEDGMENTS

The successful completion of this dissertation became possible only because of the unrestricted accessibility, meaningful and result driven guidance and always encouraging nature of my adviser Prof. Prasanta K Kalita. I express my deep sense of gratitude to Prof. Kalita for his continuous assistance, valuable suggestions, and encouragement provided throughout the research. My sincere gratitude also goes to Dr. Richard A. Cooke for his valuable guidance, support, suggestions throughout the period of my study and also serving as a member of my doctoral committee. I am grateful to Prof. Marcelo H. Garcia and Dr. Timothy R. Ellsworth for their cognitive suggestions, critical comments and constructive criticism, and serving as the members of my doctoral committee.

I would like to acknowledge the valuable support from my research group members Dr. Paul Davidson, Daniel Koch and Jennifer Trask for providing the necessary data to calibrate and validate the model that I developed in this study. Supports from the Construction Engineering Research Laboratory (CERL) and Illinois Department of Transportation are highly appreciated for providing the research grants which funded my graduate research assistantships. I would like to extend my gratitude to all my fellow graduate students at the Department of Agricultural and Biological Engineering, especially Siddhartha Verma, Joseph Monical, Carlos Bulnes Garcia and Dr. Goutam Nistala for their generous support and cooperation in various stages of this study.

Above all, I wholeheartedly dedicate this thesis study to my beloved parents and loving brother who are always behind my success. Last but not the least, despite my best efforts and all the generous help I received, errors may exist. However, any errors that may remain are entirely my own.

TABLE OF CONTENTS

CHAPTER 1: INTRODUCTION

After air, water is one of the most important essentials for life. Not only is water necessary for the digestion and absorption of food, but it also helps to maintain proper muscle tone, supplies oxygen and nutrients to cells, purges the body of wastes and regulates the body temperature. Chaplin (2006) has summarized the importance of water in human life as “Liquid water is not a 'bit player' in the theatre of life - it's the headline act”.

Most of the developed world perceives clean drinking water from the tap as an ordinary and standard part of life, not a luxury. But even today, over one billion people across the world do not have access to clean water and over two billion people lack access to improved sanitation (WHO, 2009). About 3.5 million people (including 3 million children) die worldwide due to water related diseases every year (Prüss-Üstün *et al*., 2008). Majority of these deaths, about 98%, occur in the developing countries where water-borne outbreaks are prevalent. Diarrheal illnesses alone causes more than 1.5 million deaths annually making it worse health threat than cancer or AIDs in terms of death toll (Prüss-Üstün *et al*., 2008). A report published by Pacific Institute in 2002 predicts that approximately 135 million people will die worldwide from water related diseases by 2020 if no action is taken to address basic human needs for safe drinking water (Gleick, 2002). The report also projects that between 34 and 76 million people will die from water-related diseases by 2020 even with the accomplishment of Millennium Goals (by 2015, halve the proportion of people who are unable to reach or to afford safe drinking water) announced by the United Nations in 2000.

A water source can be contaminated in many ways by municipal sewage, polluted urban runoff, pesticides and fertilizers from agricultural fields, animal waste from feedlots and farms,

industrial pollution from factories, mining waste, hazardous waste sites, spills and leaks of petroleum products, and industrial chemicals etc. Like the rest of the world, contamination of water sources by harmful chemicals and infectious pathogens also affects the health of millions of residents in the United States. In order to monitor the outbreak of water related diseases in US, the Centers for Disease Control and Prevention (CDC) in partnership with the Council of State and Territorial Epidemiologists (CSTE), and the Environmental Protection Agency (EPA) initiated a national surveillance system known as the Waterborne Disease and Outbreak Surveillance System (WBDOSS) in 1971. As documented by WBDOSS, there have been 794 waterborne disease outbreaks making more than 575,000 people sick from 1971 to 2006. If we take the annual average for the same duration, about 20 drinking water-related disease outbreaks are reported to CDC, affecting an average of 15,000 people per year. Center for Disease Control and Prevention (CDC) has placed water safety threats as category B bioterrorism threats in USA (CDC, 2009).

The United States has over 300 million acres of land that produces an abundant supply of low-cost, nutritious food and other products. And, the state of Illinois alone has more than 28 million acres of agricultural land. American agriculture is noted worldwide for its productivity, quality, and efficiency in delivering goods to the consumer. However, improperly managed, agricultural activities can affect water quality. The National Water Quality Inventory, published in 2000, reports agricultural Non-Point Source (NPS) pollution as the leading source for deteriorating water quality in surveyed rivers and lakes, the third largest source of impairments to surveyed estuaries, and also a major contributor to ground water contamination and wetlands degradation (EPA, 2000). Runoff from animal production facilities may contain high levels of nutrients, solids, and microorganisms that have the potential to degrade the quality of surface

water sources. This issue becomes a primary concern when there is a substantial risk for disease transmission by waterborne microorganisms, especially pathogens. Microbial pathogens present in agricultural runoff impose a significant hazard on human health when acquired directly via the fecal-oral route or indirectly as a waterborne contaminant.

Cryptosporidium parvum (*C. parvum*) is one of those microbial pathogens, which are found in large quantities in the feces of diseased animals. *Cryptosporidium parvum,* a protozoan parasite, is excreted in the form of an oocyst. Livestock and concentrated animal facilities have been associated with high concentrations of *C. parvum*. Infected animals have been known to pass as many as 10 billion oocysts per gram of feces. Therefore, only a few infected animals can produce enough oocysts to potentially contaminate a large water source (Fayer *et al*., 2000). The remarkable infective potential *Cryptosporidium* is illustrated by the largest outbreak of waterborne disease in US history in Milwaukee, Wisconsin in the spring of 1993. About 403,000 people were affected from the outbreak, which also caused more than 100 casualties (MacKenzie *et al*., 1994; Kramer *et al*., 1996; Hoxie *et al*., 1997). Many conventional measures used in water treatment techniques, such as chlorination, are not very effective in disinfecting the oocyst due to its resistive nature (LeChevallier *et al*., 1991). Due to the unique structure of the oocyst, *C. parvum* is resistant to diverse environmental conditions and various chemicals that make it a significant concern from a water quality perspective. As watercourses are the most common pathways for the oocyst transport, the removal of *C. parvum* from runoff can contribute to alleviating water quality and addressing health concerns.

Rotavirus is among the smallest of pathogens but a leading cause of death of children around the globe. Rotavirus infection kills more than 500,000 children under the age of 5 every year, most of them in developing countries (Feng *et al*., 2002). Even in a developed country like

the United States, rotavirus was estimated to be the cause of about 60,000 hospitalizations and 37 deaths annually during the period of 1993–2003 Fischer *et al*., 2007). Apart from human, rotaviruses have a wide host range including many mammalian species like pigs (Ferrari and Gualandi, 1986), lambs (Wray *et al*., 1981), foals (Conner and Darlington, 1980), rabbits (Conner *et al*., 1988) and deer (Smith and Tzipori, 1979).

Vegetative filter strips (VFS) is one of the most popular Best Management Practices (BMP) in controlling the movement of polluted agricultural runoffs into source waters. Vegetative filter strips are maintained areas of vegetation placed down slope of potential pollutant sources. The filter strips reduce runoff velocity allowing more water detention on the surface, which promotes more infiltration into the soil profile, adsorption to the vegetation and sediment, and deposition of suspended solids. Many studies have suggested that a VFS can be an effective tool in removing pathogens including *C. parvum* oocysts and rotavirus from surface runoff (Brush *et al*., 1999; Atwill *et al*., 2002, Trask, 2002, Trask *et al*., 2004; Davidson, 2007; Davidson, 2010).

The risk of large microbial pathogenic contamination is not only a human health hazard but also a potential threat to the continued existence of small to medium-sized dairy farms and feedlots. To design and develop control mechanisms, microbial transport processes in surface and near-surface runoff need to be properly understood and quantified along with various factors that affect pathogen transmission to the environment. While some information exists for *C. parvum* oocyst (Brush *et al*., 1999; Atwill *et al*., 2002; Tate *et al*., 2004; Trask *et al*., 2004) and rotavirus (Goyal and Gerba, 1979; Davidson, 2007; Davidson, 2010) transport in soil using small scale experiments hardly any attempts have been made to model transport and fate of oocysts in surface and near-surface flow conditions. Similarly, no information is available on the effects of

various environmental factors such as duration and intensity of precipitation, snowmelt, vegetation and land-use condition, watershed topography, and actual watershed management practices on pathogen loads from dairy/cattle farms to the water supply. These factors dominate pathogen transport rates to the environment (Brown *et al*., 1980; Medema *et al*., 1998), and the information is essential for developing strategies and designing BMP for source control of microbial pathogens. Otherwise, the risk of water contamination by dairy/cattle farms will continue unabated, thereby putting cattle and dairy operations at risk.

A model is an abstraction and simplification of a real system. Apart from replicating present condition, models also allow prediction and simulation of future scenarios, both in time and space. Hence, models can be both cost-effective and time-saving tool if used appropriately. In the area of hydrology and water quality, models simulate the natural process of water flow, sediment movement along with chemical, nutrient and microbial pathogen transport. These models not only help in addressing a range of environmental problems but also play an important role in quantifying the effect of human activities on the flow processes. To name few, Agricultural NonPoint−Source pollution model or AGNPS (Young *et al*., 1987; Young *et al*., 1995; Bingner and Theurer, 2001; Shamshad *et al*., 2008), Areal Nonpoint Source Watershed Environment Response Simulation or ANSWERS (Beasley *et al*., 1980; Connolly *et al*., 1997; Bouraoui *et al*., 2002), CASCade of planes in 2−Dimensions or CASC2D (Ogden and Julien, 2002), Hydrological Simulation Program – Fortran or HSPF (Bicknell *et al*., 1993), KINematic runoff and EROSion model or KINEROS (Woolhiser *et al*., 1990), the European Hydrological System model or MIKE SHE (Refsgaard and Storm, 1995), and Soil and Water Assessment Tool or SWAT (Arnold *et al*., 1998) are few popular water quality models. Generally, these models are focused on surface water hydrology rather than subsurface hydrology and also require a

significant amount of data and empirical parameters for development and calibration. Apart from SWAT, most of these models can simulate runoff, sediment yield, and nutrient losses within and from a watershed but not pathogen transport.

Monitoring real-world transport of pathogenic microorganisms such as *C. parvum* and rotavirus on a continuous basis is difficult, expensive and not feasible for many water resources systems. Additionally, there is also a need for the ability to predict the levels of specific pathogens as a result of non-point sources of contamination. Many waterborne disease outbreaks have occurred following periods of intense rainfall (Hrudey *et al*., 2002; Hunter, 2003), suggesting a link between watershed hydrology and disease transmission. A better understanding of the connection between microbial occurrence and watershed hydrology is greatly needed. Since it is very difficult to monitor the influence of several environmental factors on pathogen fate and transport, modeling can provide a quantitative and consistent approach to estimate pathogen loading under a wide range of conditions. Models can also predict the extent of movement along with the time required for the microorganisms to move to the target location.

As noted by Jamieson *et al*. (2004), there have been few attempts to simulate microbial pathogen in surface waters at watershed scale such as "loading" models like MWASTE (Moore *et al*., 1989), COLI (Walker *et al*., 1990), and SEDMOD (Fraser *et al*., 1998). Similarly, models are also developed to simulate survival and transport of fecal bacteria in receiving waters such as lakes (Canale *et al*., 1993) and rivers (Wilkinson *et al*., 1995) and there also exists model that incorporate both landscape and in-stream microbial processes like Soil and Water Assessment Tool (SWAT) (Sadeghi and Arnold, 2002) and a watershed model developed by Tian *et al*. (2002). These models simulate the survival and transport of indicator organisms, typically *Fecal coliform*. Although overland flow is recognized as the primary transport mechanism of

microorganisms to receiving streams in these models, the physical processes involved in the movement of microorganisms on the land surface has received little attention. Apart from SWAT, no other models explicitly attempt to partition microorganisms into adsorbed and non-adsorbed fractions in sediments. Unfortunately, reliable data on bacteria partitioning is currently not available, which also imposes a challenge to validate SWAT's partitioning approach. In current models, sediment-associated microorganism resuspension and deposition rates in streams are simulated as simple empirical functions of discharge. No attempt has been made to assess the movement of microorganisms by directly modeling the sediment particles to which they are attached.

This study intends to bridge the knowledge gap in pathogen transport modeling by developing a simulation tool for *C. parvum* oocysts and rotavirus transport in surface and near-surface flow considering partitioning of pathogens into adsorbed and non-adsorbed fractions.

CHAPTER 2: OBJECTIVES

The overall objective of this study is to understand microbial pathogen transport and transport processes, characterize critical environmental factors affecting microbial transport and control in runoff and near-surface runoff, and develop a predictive model for microbial transport in surface and near-surface runoff. The results obtained from this study can be used for translating basic research results into designing agricultural BMPs that will prevent transport of microbial pathogens to the water supply. In order to achieve this overall objective, the following specific research aims were proposed:

1. Review the literatures related to models developed to simulate microbial pathogens transport processes and characterize the effects of various environmental factors such as duration and intensity of precipitation, vegetation and land-use condition on overland (surface) and near-surface (shallow sub-surface) transport of *Cryptosporidium parvum* and rotavirus.
2. Develop a predictive model for *Cryptosporidium parvum* and rotavirus transport in surface and near-surface flow.
3. Calibrate and validate the model using observed data.
4. Analyze the observed and predicted results and develop recommendation on further use of the model for designing BMP (such as VFS) to control microbial pathogen transport.

The study also intends to test the following hypothesis regarding *Cryptosporidium parvum* and rotavirus transport in surface and near-surface flow:

1. Vegetation reduces pathogen transport drastically by reducing flow velocity providing more time for pathogens to interact with soil and vegetation surface.

2. Rainfall intensity, bed slope and soil type are important factors affecting pathogen transport in surface and near-surface flow.

CHAPTER 3: REVIEW OF LITERATURE

This chapter is divided into 4 sections: section 1 describes about pathogens in general (outbreaks and regulations); section 2 describes about *Cryptosporidium* in general (life cycle and experimental studies); section 3 describes about rotavirus in general (life cycle and experimental studies); and section 4 provides the details of modeling studies related to all microbial pathogens including *C. parvum*.

3.1 Microbial pathogens: an introduction

Potential waterborne pathogenic microorganisms include bacteria, viruses and prions, fungi and microsporidia, protozoa and helminths (Cotruvo *et al*., 2004). Many grow in the human or animal intestinal tract and are transmitted through the feces of infected individuals. Others, such as prions (e.g. the pathogen causing bovine spongiform encephalopathy, also known as mad cow disease) have not been ruled out as being capable of causing disease through waterborne transmission (Cotruvo *et al*., 2004), although initial estimates suggested negligible risk (Gale, 2001). Fecal pollution of water can result in new infections if the water is not adequately treated. *C.parvum* has largely been the pathogen driving drinking water treatment regulations because of its resistance to conventional treatment (including chlorine disinfection) (e.g. Korich *et al*., 1990) and its role in waterborne disease outbreaks in the United States and around the world (Hoxie *et al*., 1997; Craun *et al*., 2006; Karanis *et al*., 2007), but many other known and emerging pathogens have been identified.

Zoonotic pathogens (pathogens transmissible between vertebrate animals and humans) comprise 75% of the emerging infectious diseases in humans. Many of these emerging zoonoses are transmitted indirectly through water, foods, or environmental contamination (Bolin *et al*.,

2004). Evidence suggests that zoonotic waterborne pathogens will continue to be recognized as an increasing public health concern worldwide because of a multitude of driving forces that include changing pattern in water use, climate change leading to severe weather events, increasingly concentrated livestock operations, and international trade in animal products (Cotruvo *et al*., 2004). Pathogens may reemerge because of their ability to adapt, mutate or recombine in response to changing environmental pressures (Cotruvo *et al*., 2004). In the United States, *Giardia*, *Campylobacter*, *Cryptosporidium*, *Salmonella*, and *E. coli* have been the most commonly identified zoonotic agents of waterborne disease outbreaks from contaminated drinking water (Craun *et al*., 2004).

Craun *et al*. (2006) reported that at least 1870 outbreaks were associated with drinking water, an average of 22.5 per year, during the period of 1920 to 2002. In terms of illness, 883,806 illnesses were reported, an average of 10,648 cases per year during the same period. During the same period (1920-2002), 1165 deaths were reported, an average of 14 deaths per year. As shown in Figure 3.1 below, the average annual number of Water borne disease outbreaks (WBDOs) ranged from a low of 11.1 during 1951–1960 to as many as 32.4 WBDOs during 1971–1980. The average annual number of illness cases ranged from a low of 1249 during 1951–1960 to a high of 36,162 cases during 1991–2002. In the 12-year period from 1991to 2002, 207 WBDOs causing 433,947 illnesses and 73 deaths were reported; slightly more WBDOs occurred in non-community water systems (42%) than either community (36%) or individual systems (22%). During 1991–2002, *Giardia* (16%) and chemical contaminants (12%) were two main important causes of WDOs along with a number of other pathogens including *Cryptosporidium* (7%), *norovirus* (6%), *E. coli* O157:H7 (5%), *Campylobacter* (3%), and *Legionella* (3%).

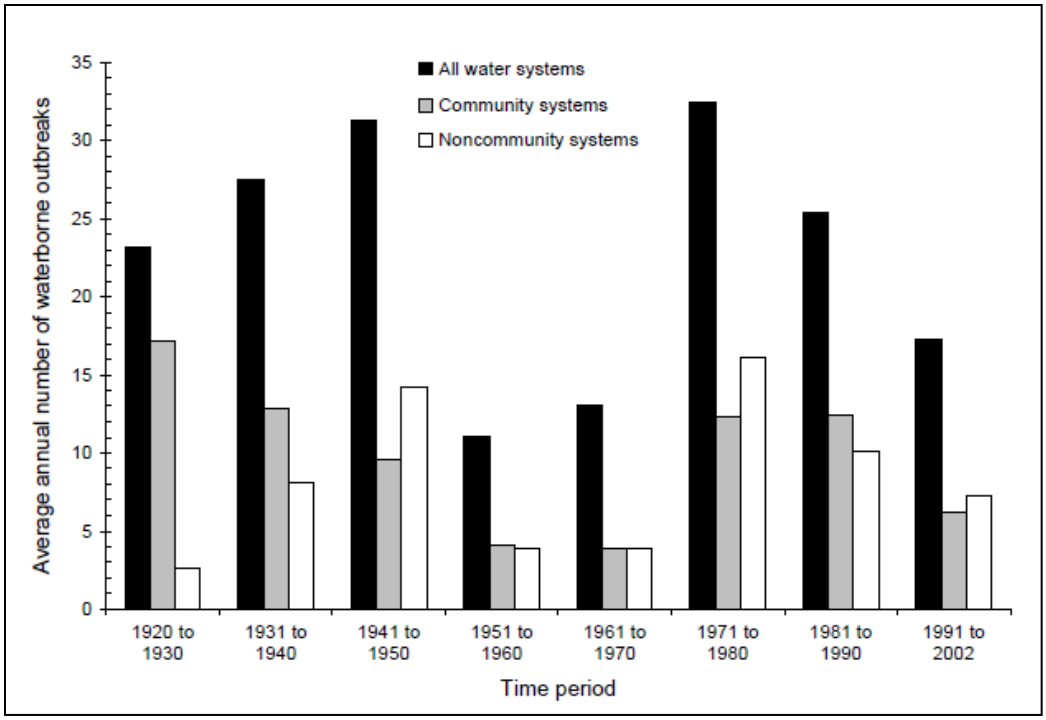

Figure 3.1 Reported waterborne outbreaks, 1920-2002 (Craun *et al*., 2006).

In 1914, federal regulation of drinking water quality started as the U.S. Public Health Service set standards for the bacteriological quality of drinking water (USEPA, 1999). This standard was applicable to water systems which provided drinking water to interstate carriers like ships, trains, and buses, and only applied to contaminants capable of causing contagious disease only. These standards were revised and expanded in 1925, 1946 and 1962 by the Public Health Service. The 1962 standards regulated 28 substances and are considered the most comprehensive federal drinking water standards in existence before the Safe Drinking Water Act came into the existence in 1974 (USEPA, 1999). These days, public water systems are regulated under the Safe Drinking Water Act (SDWA) of 1974, which was amended in 1986 and 1996 and administered by the U.S. Environmental Protection Agency's Office of Ground Water and Drinking Water and its partners. The 1996 amendments required Environmental Protection

Agency (EPA) to publish every five years a list of contaminants known or anticipated to occur in public water systems and possibly needing regulation. Microbial contamination is regulated under the Surface Water Treatment Rule (SWTR) of 1989 and the Total Coliform Rule (TCR) of 1989. United States Environmental Protection Agency introduced the Interim Enhanced Surface Water Treatment Rule (IESWTR) on December 1998, which provides additional protection against *C. parvum* and other waterborne pathogens.

In 1998, the United States Environmental Protection Agency developed a Drinking Water Contaminant Candidate List which comprised 60 contaminants and contaminant classes, including 10 microbial contaminants and groups of related microorganisms and 50 chemicals and chemical groups (USEPA, 1998). The group of 10 microorganisms included in the list was *Acanthamoeba,* Adenovirus, *Aeromonas hydrophila,* Caliciviruses, Coxsackieviruses, Cyanobacteria, Echoviruses, *Helicobacter pylori*, Microsporidia, and *Mycobacterium avium* intracellulare. The American Water Works Association Research Division Microbial Contaminant Committee reviewed the importance of several emerging pathogens for the drinking water industry in 1999. Three viral, four bacterial, three protozoan microorganisms, and one set of bacterial toxins were examined (LeChevallier *et al.*, 1999a; LeChevallier *et al.*, 1999b). They were enteroviruses, calicivirus, Norovirus, and hepatitis A virus; *Mycobacterium avium* complex, *Helicobacter pylori*, pathogenic *Escherichia coli*, *Campylobacter jejuni*; *Cyclospora cayetanensis*, Microsporidia, and *Toxoplasma gondii*; and cyanobacteria toxins, respectively. It should be noted that there are five pathogenic groups of *E. coli*. A frequently found strain *E. coli* O157:H7 is a member of the enterohemorrhagic group (EHEC). Other groups include enteropathogenic *E. coli* (EPEC), enterotoxigenic *E. coli* (ETEC), enteroinvasive *E. coli*

(EIEC), enteroaggregative *E. coli* (EAggEC), and diffuse adherent *E. coli* (DAEC) (LeChevallier *et al.,* 1999a).

Ferguson *et al*. (2003) have tried to fulfill the knowledge gap concerning precise mechanism of pathogen transport and provided extensive review of numerous studies related to fate and transport of surface water pathogens in watersheds. Pathogens considered in the study were *E. coli, Campylobacter, Salmonella, Cryptosporidium* and *Giardia*. The study has also proposed a conceptual model for pathogen transport in different watershed processes.

It is of critical importance to control or eliminate runoff-mediated contamination of agricultural watersheds for the preservation of safe water resources and sustainable agriculture. To design and develop these control mechanisms, microbial transport processes in surface and near-surface runoff need to be properly understood and quantified. Little information is available on the environmental or physicochemical factors governing microbial pathogens like *C. parvum* and rotavirus transport in surface and near-surface runoff. In case of *C. parvum*, its unique biological characteristics and highly resistant nature in the environment makes the environmental survival and disease transmission issues even more complicated. In order to understand the transport of *C. parvum*, knowledge about its biological characteristics, prevalence in the environment, disease, contamination sources, potential factors associated with transport, the current removal of *C. parvum* from drinking water and different model developed to characterize fate and transport is needed. Therefore, these issues, in addition to previous research using vegetative filter strips as a control measure for pathogen transport, are discussed.

3.2 *Cryptosporidium parvum*

Cryptosporidium parvum is a coccidia protozoan from the phylum Apicomplexa, family Cryptosporidiidae (Fayer *et al*., 1997). There are eight species of *Cryptosporidium* that are

considered legitimate, though most of the research has focused on *Cryptosporidium parvum*. The interest in *C. parvum* is greater than that of the other seven species because *C. parvum* has been identified as the cause of clinical disease in humans and zoonotic infections in livestock, and other mammals (Robertson and Smith, 1992). *C. parvum* is a unique parasite found in a very robust form in the environment. This form, called an oocyst, is resistant to most natural environmental conditions (Gajadhar and Allen, 2004). This resistance gives the oocyst a long survival time in the environment and the potential to travel long distances, most commonly transported in water. Studies have shown that some oocysts can survive up to 32 days at a temperature of -22^{o}C and still remain viable (Robertson *et al*., 1992).

3.2.1 Sources of *C. parvum*

There are numerous sources of *C. parvum* in the environment; some have bigger impact on water supplies than others. The impact of livestock on contamination as well as the impact of other major wildlife that contribute to possible contamination of water courses are discussed in the next section.

C. parvum can cause gastrointestinal illness in a wide variety of mammals, including humans, cattle, sheep, goats, pigs, horses, deer, raccoons, opossums, and rabbits (Ungar, 1990). Hence, the potential for other animals to produce oocysts that infect humans is high. Farm animals, especially livestock, which include beef and dairy cattle, sheep, horses and pigs, are susceptible to *C. parvum* infection. Cattle are thought to be a major source of oocysts among these groups because of their numbers, distribution, and incidence of infection and also they are capable of producing up to 10 billion oocysts per gram of feces (Olson *et al*., 1999; Kuczynska and Shelton, 1999). Infections have developed in young ruminants around calving times as well as asymptomatically in adults, usually in the warmer months (Mawdsley *et al*., 1995; Graczyk *et*

al., 2000). Infection can occur in animals and humans with ingestion of as little as 10 oocysts from a contaminated water supply (Harter *et al*., 2000). In 2007, confined beef and dairy cows produced over 160 million tons of manure in the U.S. (Capper *et al.*, 2009). With this type of production and the potential for just a few infected cattle to contaminate a large water supply, the potential for infection is great.

Most birds do not pose a threat to humans because it is unlikely that they carry *C. parvum*. An exception to this is gulls, which tend to feed at animal production facilities and wastewater treatment plants (Fayer *et al*., 1997). Canadian geese are another bird species that can carry and produce oocysts (Graczyk *et al*., 2000). Deer and other ranging animals such as zebras and buffalo may also be potential reservoirs for *C. parvum* (Fayer *et al*., 1997). A study in Spain that examined the infectivity of small mammals (i.e. rodent and insectivore species) to *C. parvum* showed that all types of species became infected during the trial. These findings show that small mammals may become an important source of oocysts in the absence of humans and livestock (Torres *et al*., 2000).

Many studies have looked at the rates of infection among cattle. Graczyk *et al*. (2000) studied dairy and beef cattle in Pennsylvania that were allowed to wade and graze near streams and found that 64% of the farms (n=50) tested positive for the presence of oocysts in at least one manure sample and 44% were positive in all samples. Livestock were allowed direct access to watercourses without barriers present (i.e., vegetative filter strips). To compound the problem, these farms and their manure storage areas are located on a 100-year floodplain and are at risk for inundation. Starkey *et al.* (2005) reported that 747 samples, out of the 9914 fecal samples collected from 39 study farms in Catskill/Delaware watershed of New York City, were found to

contain *C. parvum*. Garber *et al*. (1994) concluded that with herds over 100 head, virtually all have been infected with *C. parvum* at some time in their lifetimes.

3.2.2 Life Cycle of *Cryptosporidium*

The life cycle of *C. parvum* consists of several stages followed by a final excretion stage of mature oocysts into the environment. The initial endogenous stage commences when a host ingests the oocyst. Sporozoites within the oocyst are released (excysted) from the suture end and adhere to epithelial cells that line the gastrointestinal tract. For most parasites, excystation requires reducing internal conditions, exposure to pancreatic enzymes, and bile salts. However, *C. parvum* is one parasite that can survive in normal physiological conditions. Once the cell's microvilli encapsulate the sporozoites, there is a parasite/host cell relationship. The four sporozoites from the oocyst form trophozoites, which undergo asexual reproduction (merogony). After asexual reproduction, six to eight nuclei are formed and mature into a merozoite of type I meront, a similar structure to the sporozoite. At this point, the type I meront has the capability to infect another epithelial cell and repeat asexual reproduction producing more merozoites or undergo sexual reproduction to form a type II meront. The type II meronts formed after sexual reproduction either become microgamonts or macrogamonts. Microgamonts, which consists of about 20% of the type II meronts, are thin-walled oocysts that maintain the parasite's survival within the host. They are responsible for continuing the infection in the gastrointestinal tract. It is the fertilized macrogamonts that develop into thick-walled oocysts and are excreted as mature oocysts in the host's feces (Fayer *et al*., 1997). Each mature oocyst has a two-layered outer wall, contains four sporozoites, and is approximately 5-μm in diameter (Clark, 1999). Once the oocysts are excreted into the environment, they are viable, completely sporulated, infective, and await a new suitable host. It is at this time that other mammals such as cattle, sheep, and humans

can become infected with *C. parvum* via fecal-oral route. A schematic showing different stages of *C. parvum* life cycle is presented in Figure 3.2.

Cryptosporidiosis is the disease caused by *C. parvum* infection. It was first reported in cattle in 1971, which caught the interest of the veterinary medical profession (Rose, 1997; Current and Garcia, 1991). Cryptosporidiosis was first reported in humans in 1976. At present, cryptosporidiosis has been identified on all continents, excluding Antarctica, totaling at least 95 countries and has been found to be infective to 79 different species of mammals, including humans (Current and Garcia, 1991; Fayer *et al*., 1997). This leads to the belief that the transmission of *C. parvum* can cross host species barriers quite easily (Current and Garcia, 1991).

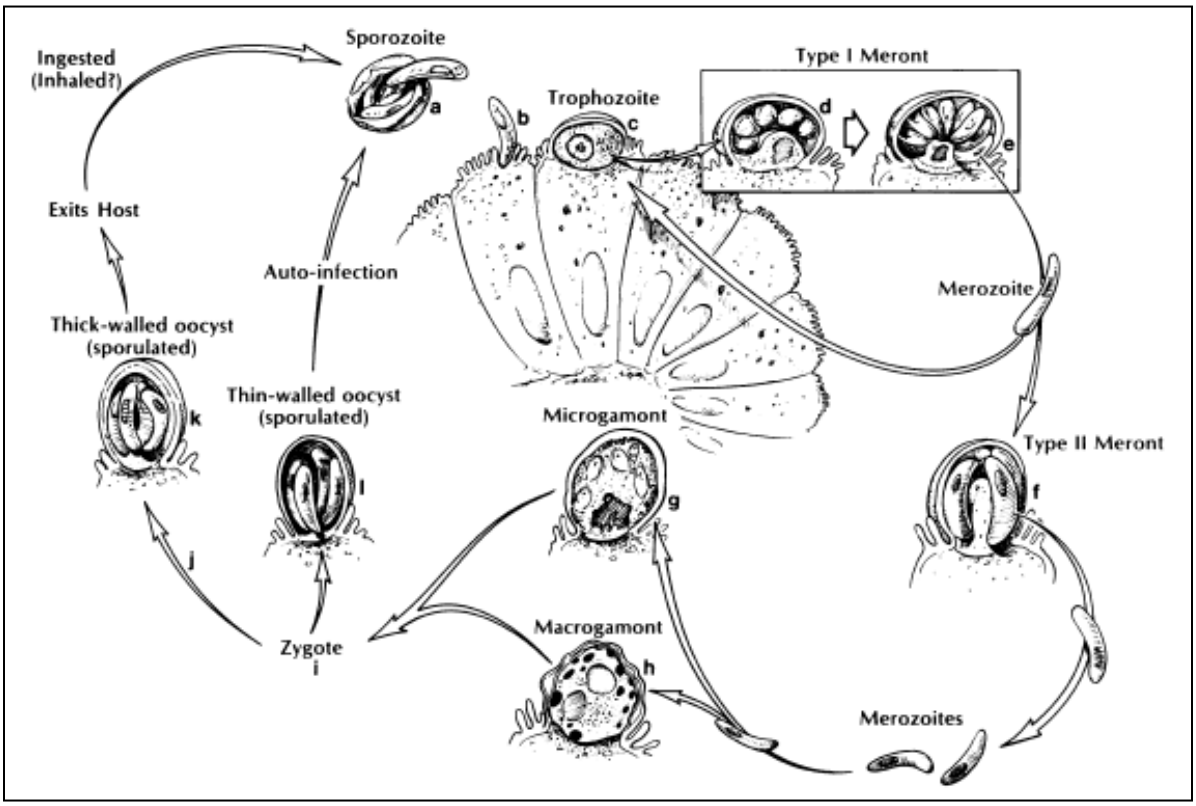

Figure 3.2 Life cycle of *Cryptosporidium parvum* (Current and Garcia, 1991).

3.2.3 Transmission between hosts

Animal and zoonotic transmission of *C. parvum* can occur in different ways. Infection can occur directly via the fecal-oral route (zoonotic transmission), through waterborne transmission and possibly with other parasitic protozoa through food-borne transmission (Current and Garcia, 1991; Widmer *et al*., 1996; Fayer *et al*., 1997).

Transmission between humans can occur several ways. These include low hygiene levels, sexual activities and close contact with infants (Rose, 1997). Most commonly, transmission will occur with younger children (pre-school) because hygiene levels are not yet fully developed. Outbreaks in settings where children are prevalent, like day care centers, are common (Current and Garcia, 1991; Mawdsley *et al*., 1995; DuPont *et al*., 1995). Transmission can also occur when caring for infected livestock, zoo animals and domestic animals. Studies have reported that 155 species of mammals have been found to be infected with *C. parvum* or *C. parvum*-like organisms (Fayer, 2004).

Water is thought to be the predominant route of oocysts to expose new hosts (Rose, 1997). There are also various ways that *C. parvum* can reach watercourses, including direct leakage to a drainage system from a storage facility or barn, application of contaminated manure as a fertilizer to agricultural fields, direct runoff from animal production facilities and direct contamination by animals (Mawdsley *et al*., 1995; Kuczynska and Shelton, 1999; Graczyk *et al*., 2000). Runoff may also occur because of excessive amounts of precipitation or snowmelt. This form of transport may become more prevalent with shifting rainfall patterns. For instance, the precipitation trend in the contiguous United States has shown that up to a 20% increase in annual snowfall and rainfall over the past century (Groisman and Easterling, 1994; Groisman *et al*., 2001). Climatologists are also projecting that flooding events will become more severe and

happen more frequently (Bates *et al*., 2008). In addition, treated or untreated discharge from a water treatment plant may contain oocysts. Untreated water can then be transported to an area where new hosts come into contact with the oocysts. These areas include recreational waters, drinking water wells for humans and animals, and bathing areas (Medema *et al*., 1998).

Fayer *et al*. (1997) reported that *C. parvum* oocysts are the most important biological contaminant in the United States. *C. parvum* infection is widespread exceeding several million cases worldwide (Casemore *et al*., 1997). Higher rates of infection and transmission occur more frequently in underdeveloped countries. In the developed regions like North America and Europe, cryptosporidiosis infection rate is between 1 and 3% and is more prevalent in urban areas with close human contact than in the lower density rural areas. Studies have shown that about 25-35% of the population in developed countries (including the United States) has had cryptosporidiosis at some time in their lives (Sureshbabu *et al*., 2010). Mead *et al*. (1999) estimated that there are about 300,000 cases of diarrhea annually resulting from cryptosporidiosis in the United States. On the other hand, cryptosporidiosis accounts for approximately 10% of cases of acute diarrheal illness in developing countries (Chen *et al*., 2002). The higher rate can be attributed to the lack of sanitary facilities and clean water, as well as crowded housing conditions. Diarrhoea is the leading cause of death in children younger than five years of age in developing countries, where *Cryptosporidium* infection accounts for 30 to 50 percent of those deaths (Snelling *et al*., 2007).

3.2.4 Effects of Infection

A majority of reported *C. parvum* infections have occurred in the gastrointestinal tract. When infection occurs in the gastrointestinal tract, symptoms will begin to persist anywhere from 2-10 days following infection and generally last 1 to 2 weeks (Current and Garcia, 1991; Fayer *et al*.,

1997; Mawdsley *et al*., 1996a). Most of those infected experienced multiple symptoms including watery diarrhea, nausea and vomiting, abdominal pain, mild fever, anorexia, malaise, fatigue and respiratory problems. Oocyst excretion can last 1 to 4 weeks after most symptoms have subsided. General feelings of fatigue and malaise may last up to a month after symptoms cease. In addition, weight loss and dehydration are extremely common when bowel movements are frequent and voluminous (Fayer *et al*., 1997; Mawdsley *et al*., 1996a).

Although majority of reported cryptosporidiosis infections are related to gastrointestinal track, the infection does not always take place in the intestinal tract. Infections can occur in the respiratory tract, gallbladder, biliary tree, and pancreatic duct. Respiratory infections in particular are becoming more common; symptoms include coughing, wheezing, croup, hoarseness and shortness of breath. Oocysts have been identified in sputum and tracheal aspirates. Infections in the gallbladder, bile duct, and pancreas have similar symptoms as intestinal cryptosporidiosis, although diarrhea may not occur (Current and Garcia, 1991; Fayer *et al*., 1997). The health implications of cryptosporidiosis at any infection site vary from person to person and depend on many factors.

The severity of the disease depends on the immunological status or health of the individual and the amount of oocysts ingested or absorbed at the time of infection (Mawdsley *et al*., 1996a; Current and Garcia, 1991; Fayer *et al*., 1997; Rose, 1997). In a study that was conducted by DuPont *et al*. (1995), 29 healthy volunteers were infected with different doses of oocysts ranging from 30 to 1,000,000. Results from the study showed that 18 people became infected, mostly from a dose of 100 or more. The data demonstrated that dosage affects the time and the duration of the oocyst excretion, but not the severity of the disease or symptoms. The

mean ID_{50} (infective dose for 50% of the population) of this particular bovine strain was found to be 132 oocysts.

Immunocompromised or immunosuppressed people are at high risk for more severe and potentially life threatening infection because if impaired T cell functions (Rose, 1997). Immunocompromised people include those that are HIV positive, have cancer, are transplant patients, are on immunosuppressive chemotherapy, require renal dialysis or have other viral infections including chicken pox and the measles (Current and Garcia, 1991, MacKenzie *et al*., 1994). Because of *C. parvum*'s ability to autoinfect, the disease takes a much greater toll on the individuals with an already weakened immune system. The mortality rate for HIV infected people with cryptosporidiosis is 50% (Rose, 1997). Fluid replacement which is a primarily a supportive treatment is essential in patients with severe diarrhea. Normally 3 to 6 liters per day of fluid loss is expected, whereas HIV patients can lose up to 17 liters of fluid per day (Current and Garcia, 1991).

3.2.5 Environmental Resistance

C. parvum can be a major health concern because of its resistance to many environmental stresses for long periods of time. Studies have suggested that the oocyst has evolved to survive in harsh environmental conditions, which is the key factor for its transport and survivability within the environment (Robertson *et al*., 1992; Fayer and Nerad, 1996). Its resistance to temperature and various chemicals has made it a major concern from a public health perspective. Studies have also shown that oocysts remain infective in both cold and warm water temperatures as well as after freeze-thaw. A study found that after snap freezing, all oocysts were nonviable; however, as temperatures were gradually decreased over time to -22ºC, a small percentage of oocysts were still viable up to 750 hours (Robertson *et al*., 1992). Fayer and Nerad (1996)

examined oocyst viability at room temperature after freezing oocysts at -10, -15, -20, and -70 degrees Celsius (ºC). For all temperatures, oocysts were viable from 5 to 168 hours except for at -70ºC. For a temperature of 5ºC, all oocysts were viable for 168 hours. This may allow extended survival in surface waters during the winter season. Not only can oocysts survive under low and freezing conditions, they are also viable in warm temperatures. It has been shown that oocysts can survive in warm water temperatures from 25 to 64ºC (Fayer, 1994). However, the survival time of oocysts in warm water is much lower than that in cold-water temperatures. A study by Olson *et al*. (1999) showed the effects of temperature on oocyst viability in various media. It was found that at -4 and 4ºC, oocysts remained infectious for more than 12 weeks in water and autoclaved soil, whereas oocyst survival in cattle feces varied from more than 12 weeks at -4ºC to 8 weeks at 4ºC. Oocyst survival was less at 25ºC than at -4 and 4ºC. Even though similar results were reported in soil and cattle feces for various temperatures, water still provides the best survival medium for *C. parvum* oocysts in the environment. Therefore, even at low temperatures, oocysts can be transported in runoff to water sources causing a major risk of contamination. Unlike other pathogens, *C. parvum* can remain viable under a variety of environmental conditions.

The size and structure of the oocyst is another key survival characteristic of *C. parvum*. Due to the small size, near neutral buoyancy and negative surface charge resulting in low hydrophobicity, oocysts can remain suspended in water with the potential to travel long distances (Drozd and Schwartzbrod, 1996; Walker *et al*., 1998). Medema *et al*. (1998) found that both free and attached oocysts remained in suspension due to their relatively slow settling velocities over larger particle sizes, thus increasing the chances of transport in water. The outer membrane structure of the oocyst wall may also change its chemical composition over time increasing its

survival rate in the environment (Brush *et al*., 1999). The structure and composition of the oocyst also prevents inactivation by various chemical treatments. Many chlorine-based chemicals such as chlorine, monochloramine, and chlorine dioxide at typical applied concentrations and conventional treatment disinfection times have little effect on oocyst inactivation (Fayer *et al*., 1997). Therefore, conventional drinking water treatment alone cannot guarantee the complete inactivation of the oocysts from drinking water supplies, thus increasing the risk of disease transmission.

3.2.6 *Cryptosporidium parvum* transport studies

Many studies have looked into the biological characteristics of *C. parvum* since its discovery. However, extensive research on *C. parvum* did not commence until there were several reported major outbreaks of human infection, especially the Milwaukee outbreak in 1993. Since that time, many studies have investigated various environmental factors affecting oocyst viability such as temperature, chemical disinfectants, and survival in different media, but characteristics of oocyst transport within the watershed are limiting (Robertson *et al*., 1992; Fayer, 1994; Olson *et al*., 1999; Bukhari *et al*., 2000; Davies *et al*., 2003; Davies *et al*., 2004; Kaucner *et al*., 2005; Ferguson *et al*., 2007a). Similarly, several studies have been studied the vertical transport of *C. parvum* with and without vegetation. Brush *et al*. (1999) measured the vertical transport of *C. parvum* through three different media. The results indicated that there was significant removal of *C. parvum* from the sand followed by glass and shale. Harter *et al*. (2000) also measured the vertical transport of *C. parvum* using three different sands and two pore velocities representing a sandy aquifer and saturated soil following a heavy rain storm event. It was found that medium sands retained the greatest percent of oocysts within the soil column. Another study investigated vertical transport of *C. parvum* using perennial ryegrass vegetation and three soil types: silt-

loam, clay-loam, and loamy sand (Mawdsley *et al*., 1996a). The study showed that oocysts were found in the subsurface flow for the silt-loam and clay-loam but not for the loamy sand. The remaining oocysts in the soil were still viable for transport in subsurface and overland flow. Even though studies have shown that there is a potential risk of groundwater contamination by vertical transport of oocysts, the potential migration of oocysts through soil seems to be small and much lower than bacteria and viruses. This is mainly due to the larger size and adsorption properties of the oocysts to soil particles (Mawdsley *et al*., 1996a). Vertical transport of *C. parvum* causing groundwater contamination is an issue, but most contamination has resulted from surface water sources, indicating overland flow as the major source of oocysts posing a greater public health risk. Mawdsley *et al*. (1996b) studied the vertical and horizontal movement of *C. parvum* using three soil-tilting beds after simulated rainfall. The beds were placed at a 7.5% slope and contained silty clay-loam with perennial ryegrass. The runoff and leachate analyzed for oocyst concentration indicated that movement of the pathogen lasted for at least 21 days in surface runoff and in one case for 70 days for subsurface flow. The difference in oocyst transport times was explained by the variation of the intact soil cores taken from the field. For two of the tilting soil chambers, more water volume was lost as subsurface flow than surface runoff while the third soil chamber had approximately the same volumes from surface and subsurface flow. They suggested the need for further studies using different slopes, varying the distance of application, and different methods of application to enhance understanding of oocyst transport in overland flow.

Atwill *et al*. (2002) examined the efficiency of vegetated buffer strips to remove *C. parvum* from surface and shallow subsurface flow using simulated rainfall rates of 15 or 40 mm/h. The experiments were conducted using buffers set at 5 to 20% slope having 85 to 99%

Fescue cover with soil textures of either silty clay (19:47:34 sand-silt-clay), loam (45:37:18), or sandy loam (70:25:5). One of the findings of the study was vegetated buffers constructed with sandy loam soil (or higher soil bulk densities) were less effective at removing *C. parvum* compared to buffers constructed with silty clay or loam soil. The study also concluded that a vegetated buffer strip comprised of similar soils at a slope of ≤20% and a length of ≥3 m should function to remove ≥99.9% of *C. parvum* oocysts from agricultural runoff generated during events involving mild to moderate precipitation. Trask (2002) studied the effects of ground cover conditions (bare and vegetated surfaces), slopes and rainfall intensities on *C. parvum* oocyst transport in overland and near-surface (shallow subsurface) flow using a horizontal tilting soil chamber in a controlled laboratory environment. Oocyst transport was investigated for three slope conditions (1.5, 3.0, and 4.5%) in conjunction with two rainfall intensities (2.54 and 6.35-cm/hr). Results from the study the surface runoff from the vegetated surface had much lower total percent recoveries of oocysts than those from the bare-ground conditions for all slope and rainfall conditions. McLaughlin (2003) studied the adsorption kinetics of *C. parvum* with individual soil particles (sand, silt and clay) and vegetation. Using a Coulter Counter and photomicrographs, soil adsorption were conducted which indicated that oocysts primarily adhere to or become entrapped within aggregating clay particles and do not adhere substantially to either silt or sand. Results from the vegetation adsorption experiment showed that the oocysts were transported more readily on bare soil than vegetated soil. Koch (2009) carried out a series of small scale laboratory experiments to investigate the effect of vegetation, slope and rainfall intensity on surface and near-surface transport of *C. parvum*. The experiments were performed at 3.0% slope and 90 mm/hr rainfall intensity and 2.5% slope and 65 mm/hr intensity. The study reported that the oocyst recovery in runoff was substantially lower from the vegetated surface

condition when compared to those from the bare surface condition for all the cases. Davidson (2010) examined the kinetics of *C. parvum* transport in overland flow with the help of series of small scale laboratory experiments. For the transport studies, three soil types were tested (Catlin silt-loam, Alvin fine sandy-loam, Darwin silty-clay) with and without vegetation cover. The results from bare soil experiments showed that a higher recovery of *C. parvum* oocysts from the Alvin soil compared to other soil types and vegetation greatly reduced the recovery of infective oocysts, in addition to delaying the time to the peak recovery.

3.3 Rotavirus

Rotavirus is 65-75 nm in diameter which makes it one of the smallest microorganisms (Ansari et al., 1991). It belongs to the family *Reoviridae* and causes inflammation of stomach and intestines, the medical condition commonly known as gastroenteritis. The rotavirus infection causes severe watery diarrhea, often with vomiting, fever, and abdominal pain (CDC, 2011). The virus is the leading cause of severe diarrhea in infants and the most frequently detected pathogen in children under two years of age in developing countries. The virus accounts for about 5% of all deaths among children less than five years of age and about one-third of deaths from diarrhea around the world. It is also estimated that almost every child around the globe has been infected with rotavirus at least once by the age of three (Velázquez *et al*., 1996; Feng *et al*., 2002). The rates of infection are similar in developed and developing countries but the severity of rotavirus infections differs between those two settings. Improvements in clean drinking water supplies and good hygiene are unlikely to prevent the infection since they have little effect on the transmission of infection (Dennehy, 2008). Although the mortality rates are low in developed countries, rotavirus infections account for more than 500,000 deaths annually in young children primarily in developing countries (Bishop, 1996; Feng *et al*., 2002). In addition, rotavirus causes

approximately 111 million episodes of gastroenteritis requiring only home care, 25 million clinic visits and 2 million hospitalizations each year (Parashar *et al*., 2003). Based on the studies published between 1986 and 1999, it was estimated that rotaviruses caused approximately 22% of childhood diarrhea hospitalizations worldwide (Parashar *et al*., 2003). However, this proportion increased to 39% from 2000 to 2004, as reported by Parashar *et al*. (2006).

Taxonomically, rotaviruses are classified into seven groups: A, B, C, D, E, F and G (Santos and Hoshino, 2005). Rotavirus A is the most common among them and causes more than 90% of infections in humans. Although the first infection of rotavirus can be fatal in children, immunity develops with each infection and subsequent infections are less severe (Linhares *et al*., 1988). A study showed that intestinal mucosal IgA responses are responsible for protecting immunity against rotavirus reinfection (Feng *et al*., 2002).

Because of the large numbers of rotavirus infections around the world, researchers started to develop a vaccine against rotavirus infection in 1990s. RotaShield, the first rotavirus vaccine developed by Wyeth, was licensed for use in the United States in 1998. Clinical trials of the vaccine in the United States, Finland, and Venezuela reported the vaccine to be 80 to 100% effective at preventing severe diarrhea caused by rotavirus A. Although these trials also showed no statistically significant serious adverse health effects, the vaccine was withdrawn from the market in 1999 when it was discovered that the vaccine may have contributed to an increased risk for intussusception, or bowel obstruction, in one of every 12,000 vaccinated infants. The experience provoked debate about the relative risks and benefits of a rotavirus vaccine (Bines, 2006). Recently two live oral rotavirus vaccines (RotaTeq and Rotarix) have been recommended by the WHO for inclusion into the national immunization programs of countries worldwide in 2009 (Patel *et al*., 2009).

As reported by McNulty (1978), the name "rotavirus" was proposed by Flewett *et al*. (1974), although the first case of rotavirus infection was documented by Mebus *et al*. (1969). Rotavirus infection is very common in humans (Flewett *et al*., 1973; Bishop *et al*., 1974; Middleton *et al*., 1974; Bishop, 1996; Feng *et al*., 2002; Parashar *et al*., 2003, Parashar *et al*., 2006) and calves (Mebus *et al*., 1969; Woode *et al*., 1974; McNulty and Logan, 1983). In addition, rotavirus infections have been detected in other mammals including pigs (Rodger *et al*., 1975; Woode *et al*. 1976; Ferrari and Gualandi, 1986), lambs (McNulty *et al*., 1976; Snodgrass *et al*., 1977; Wray *et al*., 1981), foals (Flewett *et al*., 1975; Conner and Darlington, 1980), rabbits (Bryden *et al*., 1976; Conner *et al*., 1988) and deer (Tzipori *et al*., 1976, Smith and Tzipori, 1979) making it a wide-spread infectious agent.

3.3.1 Rotavirus life cycle

Rotaviruses have a complex architecture with double stranded RNA. Microscopic analyses reveal that they consist of three concentric capsid layers surrounding a genome of 11 segments of double-stranded RNA (Feng *et al*., 2002). The double stranded RNA (dsRNA) in rotavirus can be separated into eleven distinct bands by gel electrophoresis. Each of these eleven distinct bands represents a distinct rotavirus gene that is responsible for synthesis of a single structural or non-structural viral protein (Estes, 1990). These doube stranded RNA also serve as templates for the synthesis of the segmented double-stranded RNA (dsRNA) genome (Silvestri *et al*., 2004).

The complete infectious particle is composed of six structural proteins assembled as a triple layer as shown in Figure 3.3. The inner core of virus proteins 1, 2, and 3 (VP1, VP2, VP3) contains the genetic information in the form of 11 double-stranded RNAs along with the enyzmes necessary for replication. This is protected by a second shell of VP6, the group antigen

that defines a rotavirus as being group A, B, C, etc. The outer shell carries the antigens involved in protective immunity. The VP4 is the spike protein involved in cell attachment. A glycoprotein, VP7, is the dominant target of the antibody response. Immunity against VP4 or VP7 is protective (Shaw, 2006). Group A rotaviruses have been further subdivided on the basis of antigens on VP6 (subgroup I, II), on VP7 (G-types), and on VP4 (P types). Human infections with Groups A, B, and C viruses have been recorded. Most severe acute diarrhea in children is caused by rotaviruses of Group A, subgroups I or II, G types 1-4, and P types 1A (Bishop, 1994) or 1B (Bartlett *et al.*, 1985).

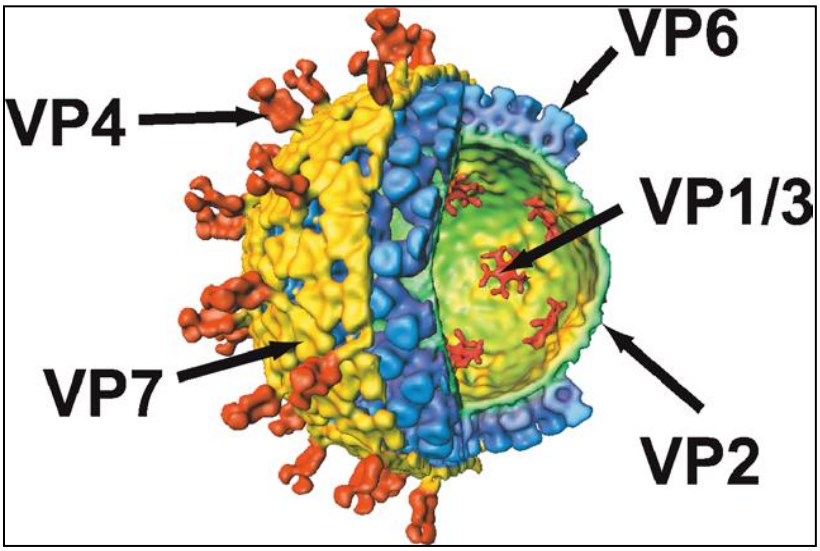

Figure 3.3 The triple-layered particle rotavirus virion (Shaw, 2006).

The rotavirus replication cycle is cytoplasmic as the cycle completes within cytoplasm of the cell (Estes, 1990). Figure 3.4 shows a simplified life cycle, in which the features critical to understanding genetics are emphasized (for simplicity, only one of the 11 genome segments is shown). Upon entry of the virion, the outer capsid is removed which activates the virion-associated transcriptase. The resulting mRNAs function either as templates for replication of

progeny genomes or as messengers for translation into protein. Subviral particles are formed that contain a mixture of structural and nonstructural proteins, together with one copy of each of the 11 template RNAs after sufficient viral protein is translated. In this cycle, polymerase activities and dsRNA are always particle-associated and mRNA is the only viral nucleic acid that is free for genetic interaction (Ramig, 1997).

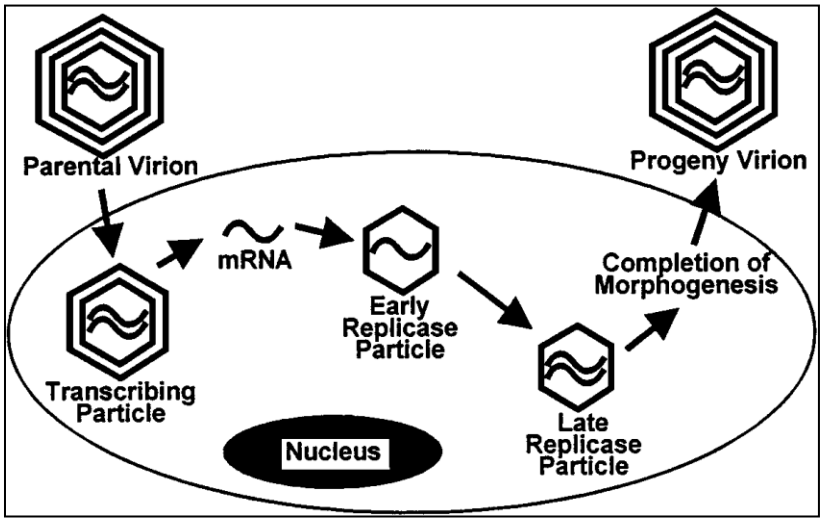

Figure 3.4 Essential elements of the rotavirus life cycle (Ramig, 1997).

3.3.2 Rotavirus transmission

Rotavirus transmission occurs when a new host comes in contact with contaminated stool and the pathogen is ingested orally. This is known as a fecal-oral route of transmission. Direct contact with contaminated surfaces and ingestion of contaminated food or water are two most frequent pathways of transmission. Factors such as the large number of virus shed by infected mammals, the very low infectious dose required, and a high degree of resistance to physical inactivation make the transmission easily spreadable through environmental sources. Rotaviruses are resistant to environmental stresses and they can survive up to four hours on human hands, 10

days on solid, dry surfaces and for weeks on wet surfaces and water (Ansari *et al.*, 1988; Ansari *et al*., 1991; Sattar *et al.*, 1984). The rapid nature of rotavirus transmission has been reported by a number of studies (Foster *et al*., 1980; Kapikian and Chanock, 1985; Santosham *et al*., 1985).

It has been reported that rotaviruses can be highly infectious when transmitted within the same species. Replication within the intestinal tract can result in shedding of 10^{10} plaque forming units (PFU) per milliliter of feces (Ansari et al., 1991). The infectious dose for the human small intestine has been reported as approximately 1 PFU per milliliter (Graham *et al.*, 1987). Although rotaviruses are generally species-specific, cross-species transmission is also possible (Cook *et al.*, 2004). Transmission of animal rotavirus to humans is possible because human infection with rotavirus mutants possessing bovine (or occasionally porcine or avian) genes has been recorded in Italy, India, Indonesia, Finland, Thailand and the U.S. (Nakagomi and Nakagomi, 1993).

3.3.3 Rotavirus in the environment

It should be noted that there are more than 120 different virus types that are known to be excreted in human feces by infected persons and not all of them are pathogenic. Studies have reported that a number of human enteric viruses may be present even in treated wastewater effluents (Gerba *et al*., 1975; Hoadley and Goyal, 1976), suggesting that the application of wastewater on land may spread the contamination of viruses. The different soil type may exhibit different virus adsorption characteristics but the effects of different soil type on of viruses during land treatment of wastewater have not been studied extensively. Similarly, very little is known about the survival or fate of human viruses applied to the soil or vegetation. Because of their size, viruses migrate vertically, resulting in groundwater contamination if they are not retained

by the soil or vegetation. In fact, few studies have reported the detection of enteroviruses in groundwater after land treatment (Schaub and Sorber, 1977; Vaughn et al., 1978; Wellings et al., 1974; Wellings *et al*., 1975). A study by Abbaszadegan *et al.* (2003) found that about one-third of the groundwater drinking wells, out of 448 sites across 35 states, contained human pathogenic enteric viruses.

Goyal and Gerba (1979) studied comparative adsorption pattern of a number of human enteroviruses, rotaviruses and bacteriophages to nine different soil types was studied. They reported that greater than 90% of all viruses adsorbed to a sandy loam soil except echovirus types 1, 12, and 29 and a simian rotavirus (SA-11), which adsorbed to a considerably lower degree. The study also observed a great deal of variability between adsorption of different strains of echovirus type 1, indicating that viral adsorption to soils is highly strain dependent. The adsorption was found to be influenced also by soil type, in addition to being dependent on type and strain of virus. Thus, soils having a saturated pH of less than 5 were generally good adsorbers. Sagar and Gerba (1979) studied the effect of soil characteristics on different virus strains. They found that the nature of virus adsorption to soil is highly dependent on the strain of virus. The variability in the configuration of proteins in the outer capsid of the virus can influence the net charge on the virus. The net charge on the virus would affect the electrostatic potential between virus and soil, and thereby could influence the degree of interaction between them. They also reported that a low soil pH (below 5) appeared to favor virus adsorption of all the viruses studied. In addition, they found that percent clay, percent sand, percent organic matter, total phosphorus, resin-extractable phosphorus, total iron, total aluminum, exchangeable aluminum, and exchangeable magnesium all influenced virus adsorption.

In another study, LaBelle and Gerba (1979) investigated the adsorption of enteric viruses estuarine sediment. Their finding suggested that the viruses are dependent upon the sediment particle for transport. The study concentrated primarily on clay sediment particles because clay sediments are the slowest to settle and more easily transported due to the smaller size and mass. However, the study from Davidson (2007) suggested that rotavirus preferentially interacts with sand particles. Although some interaction was observed with clay particles, the extent of interaction was very less as compared to sand particles. Therefore, if rotavirus is bound to the much larger sand particles, the opportunity for transport is greatly reduced.

3.4 Microbial pathogen transport fate and transport modeling

A model can be defined as an abstract representation of an item or a concept which help us better understand real world systems. Models can be broadly divided into two categories: physical and mathematical. A physical model is one that physically represents an object. In most cases, the physical model either zooms in or zooms out the real object to better understand the different phenomenon associated with it. In contrast, a mathematical model doesn't have any physical presence and uses mathematical language to describe the behavior of a system. In hydrology, there exist different types of mathematical models based on their formulation. A hydrologic model can be classified into either lumped or distributed based on spatial discretization. A model treats a watershed as a single homogeneous element while a distributed model divides the watershed into many small units such as grid cells. Similarly, a model can be classified into event-based, continuous time, and large time-scale model based on time scale. Based on solution techniques, models can be classified as analytical, numerical, and or analog solution model. Based on the way different hydrologic processes are represented in a model, it can be further

classified into data-driven or process-based model. Data-driven models, also known as black-box models, are usually driven by the raw or processed data and the formulation may not be conceptually supported by the mechanism of the phenomenon under consideration (Elshorbagy and Ormsbee, 2006). Process-based models, also known as mechanistic or physically-based models, describe different processes associated with the phenomenon under consideration and are parameter-intensive in general.

During the last two decades, computer simulation models for water quality have been developed to simulate numerous components of pollution from watersheds. These components include surface runoff, sediment, nutrients, and pesticides. However, little has been done to address fate and transport of pathogens from watersheds. It is a common practice where pathogens like fecal coliform bacteria are considered to be associated with surface water flow and flow-associated constituents like pathogens are assumed to be accumulated on the land surface until the occurrence of a rainfall event (Paul *et al*., 2004). Pachepsky *et al.* (2006) have reviewed the status and challenges in modeling the fate and water transport of manure-borne pathogens in the environment. The study included models for the pedon, the hillslope, and the watershed scales. Jamieson *et al.* (2004) have reviewed current approaches in modeling the microbial quality of surface waters at watershed scale. The study has reviewed "loading" models like MWASTE (Moore *et al*., 1989), COLI (Walker *et al*., 1990), and SEDMOD (Fraser *et al*., 1998). Similarly, other models developed to simulate survival and transport of fecal bacteria in receiving waters such as lakes (Canale *et al*., 1993) and rivers (Wilkinson *et al*., 1995) have been included in the study along with models that incorporate both landscape and in-stream microbial processes like Soil and Water Assessment Tool (SWAT) (Sadeghi and Arnold, 2002) and a watershed model developed by Tian *et al*. (2002). These models simulate the survival and

transport of indicator organisms, typically FC. Moore *et al*. (1989), Fraser *et al*. (1998) and Tian *et al*. (2002) all estimate surface transport of bacteria using simple empirical equations which relate bacteria transport to runoff rate or depth. The empirical transport equations within these models have not been well tested and validated. The empirical transport parameters have no physical basis and must be obtained through calibration. The model which have been developed in past for modeling bacterial fate and transport to the streams such as the revised Agricultural Runoff Model (ARM II): Animal Waste Version (Overcash *et al*., 1983), UTAH State (Springer *et al*., 1983); MWASTE (Moore *et al*., 1989); COLI (Walker *et al*., 1990); Hydrologic Simulation Program Fortran - HSPF (Bicknell *et al*., 1997); Spatially Explicit Delivery Model – SEDMOD (Fraser *et al*., 1998); and PROMISE and WATNAT (Medema and Schijven, 2001) have not proven to very effective tool as most of them have limitation in their capabilities.

In 2000, a microbial sub-model was developed and added to the Soil and Water Assessment Tool (SWAT) to address fate and transport of both more persistent and less persistent fecal bacteria (Neitsch *et al*., 2002; Sadeghi and Arnold, 2002). Currently for hydrologic simulations, a significant amount of research is being done using the SWAT model because it appears to be the most inclusive of the numerous variables needed to make accurate predictions of hydrologic systems. A microbial sub-model considers sources of bacteria and their fate and transport (Sadeghi and Arnold, 2002) and it has been in a continual development process since that time. The most recent update was released in 2005 (Neitsch *et al*., 2005).

Tian *et al*. (2002) developed and applied a modeling system for assessing microbial contaminants like fecal coliform on animal-grazed farmlands. The model identified the sources, sinks, transport processes, and fate of E. coli contaminants in catchments and associated streams including grazing location, land topography, distance to a nearby stream, distance through the

stream network to the outlet, population dynamics on the land surface, in flow, and on streambeds. The model applies the principles of conservation of mass balance on grid cells on land surfaces and networked stream segments. In order to improve the prediction of the effects of different land management strategies on the fecal contamination of waterways, the model characterizes the movement of fecal contaminants from land to streams and in-stream mobilization. The model was applied to a hill land catchment with an area of 140 ha, predominantly used for animal grazing. The sensitivity of the model predictions was analyzed for effect of stock rate (grazing intensity), attenuation rate, and flow volumes and it was found that the controlling diffusion rate and *E. coli* rate per pat were the most sensitive parameters. The authors concluded that further experiments were required to expand the model's functionality for covering more mitigation options.

Collins and Rutherford (2004) developed a model to predict concentrations of the fecal bacteria indicator *E. coli* in streams and applied the model to a small grazed watershed of 259 hectare area in New Zealand. In order to estimate *E. coli* inputs to the catchment, a daily record of grazing livestock was used and transport of bacteria to the stream network was simulated within surface and subsurface flows including in-stream processes of deposition and entrainment and die-off on land and in water. Although the authors reported that uncertainty existed with a number of the processes represented in the model, it model broadly reproduced observed *E. coli* concentrations in the hill-country catchment grazed by sheep and beef cattle. They also reported that the model was sensitive to the amount of excretion direct to streams and seepage zones along with the distance over which surface runoff delivered bacteria to a stream. The study concluded that riparian buffer strips may improve bacterial water quality both by trapping of bacteria by the riparian vegetation and by eliminating livestock defaecation in and near streams.

Haydon and Deletic (2006) developed two conceptual continuous pathogen models and evaluated them using *E. coli* as a pathogen indicator to model pathogen discharges from three catchments in Australia. The first model, known as the EG model, included surface and subsurface pathogen transport processes by means of wash-off and loss equations and an existing hydrologic model (SimHyd) model was coupled with. For flow simulation, EG model was coupled to an existing hydrologic model (SimHyd). The second model, named ASP, was simpler than EG as it took into account only surface pathogen transport processes. To drive pathogen transport, EG model was coupled to a stormflow-baseflow separation model. Both the models were calibrated and validated using baseflow and storm event E. coli concentrations measured at three dissimilar catchments from southern Australia. The model results comparison showed that the prediction of pathogen peak concentrations by the EG model was reasonably better than those from ASP model.

Wu *et al*. (2009) developed, calibrated, and validated a watershed scale *Escherichia coli* fate and transport model. *Escherichia coli* densities in water and sediments from the Blackstone River Watershed, Massachusetts, were measured at three sites for a total of five wet weather events and three dry weather events covering three seasons. Results showed that there were significant correlations between *E. coli* and total coliforms in water and sediments. In addition, *E. coli* concentrations in water were weakly correlated with sediment particle size and sediment concentrations. A hydrologic model, WATFLOOD⁄SPL9 (Kouwen and Mousavi, 2002), was used to predict the temporal and spatial variation of *E. coli* in the Blackstone River. The rapid rise of stream *E. coli* densities was more accurately predicted by the model with the inclusion of sediment resuspension, thus demonstrating the importance of the process.

Parajuli *et al*. (2008) applied SWAT model to explore effectiveness of vegetative filter strip (VFS) lengths applied at the edge of fields to reduce non-point source pollution in the Upper Wakarusa watershed in northeast Kansas. The study tested the effectiveness of VFS lengths (0, 10, 15 and 20 m) for reducing sediment and fecal bacteria concentration in overland flow and also ranked sub-watersheds based on sediment and fecal bacteria contribution of each sub-watershed. They reported that the 15-m VFS reasonably reduced fecal bacteria concentration in the watershed.

Apart from the watershed scale models mentioned above, small scale models have been developed based on break-through curve for porous media. Tufenkji (2007) reviewed traditional modeling approaches used to predict the migration and removal of microorganisms (e.g., viruses, bacteria, and protozoa) in saturated porous media along with their weaknesses or inconsistencies. The study found that the inappropriate use of the equilibrium adsorption approach, the observed breakdown of classical filtration theory, the inability of existing theories to predict microbial attachment rates, and omission of physical straining and microbe detachment were some limitations of modeling methods reviewed. The paper also discusses recently proposed improvements to the most commonly used filtration model, with particular consideration of straining and microbe detachment.

Oates *et al*. (2005) studied reactive microbial transport in saturated translucent porous media using the bacteria *Pseudomonas fluorescens* 5RL genetically engineered to carry a plasmid with bioluminescence genes inducible by salicylate. They also modeled bacterial transport with the advection dispersion equation and oxygen concentration was modeled assuming bacterial consumption via Monod kinetics with consideration of additional effects of rate-limited mass transfer from residual gas bubbles. Using the observed bioluminescence, model

parameters were fit that were consistent with literature values and produced results in good agreement with the experimental data.

3.4.1 *Cryptosporidium parvum* transport fate and transport modeling

Although the prediction of fate and transport of pathogens including *C. parvum* in surface and subsurface system has the great practical importance, the mathematical modeling of the phenomenon has been illustrated in very few literatures. Similarly, there has been a very few physically-based modeling attempts specially focused to simulate the fate and transport of *C. parvum* in surface and near-surface flow.

Walker and Stedinger (1999) developed a numerical model to describe the fate and transport of oocysts from dairy farms to the water supply reservoirs that serve New York City. The model includes dairy calf wastes and human sewage effluent discharged to the watercourses as the only sources of *Cryptosporidium*. Manure and *Cryptosporidium* oocysts were modeled as surface pollutants and assumed to move in response to runoff events in the six reservoir systems within the Catskill-Delaware watershed, New York. Oocyst degradation in manure and in water was modeled with first-order kinetics along with rudimentary stream routing and reservoir modeling with a first-order decay function to model the fate and transport of oocysts in the watercourse.

In Netherlands, Medema and Schijven (2001) modeled the discharge of *Cryptosporidium* and *Giardia* into surface water and the dispersion into rivers and streams using an emission model (PROMISE) and a dispersion model (WATNAT). However, the authors noted that both models were unable to account for the impact of diffuse agricultural pollution and pointed out that the modeling framework needed further improvement by increasing the number and time frame of input monitoring data.

Neelakantan *et al*. (2001) developed a simple feed-forward artificial neural network, trained by error backpropagation algorithm to relate peak *Cryptosporidium* and *Giardia* concentrations with other biological, chemical and physical parameters in surface water. A range of water quality parameters (alkalinity, pH, turbidity, suspended solids, dissolved solids, river flow, precipitation, total coliphage, male-specific coliphage, total coliform, faecal coliform, *E. coli* and *Clostridium perfringens)* were evaluated as inputs to the neural network models. They found that the best prediction performance was found when the number of internal nodes was twice that of the input parameters in single hidden-layer architecture. The use of neural network approach has been criticized in hydrologic modeling since the approach is closer to black-box modeling than physically-based.

Elshorbagy and Ormsbee (2006) developed an object-oriented simulation environment for surface water quality management, based on the concepts of system dynamics (OO-SD). The proposed model, which combines both process-based and data-driven techniques to handle the issue of pathogen transport and fate, was applied to seven watersheds in southeastern Kentucky, USA. The study also identifies the potential use of the proposed approach, especially in data-poor conditions, and the challenges that lie ahead of hydrologists to fully exploit such a modeling approach.

Dorner *et al*. (2006) developed a watershed-scale fate and transport model for Escherichia coli and several waterborne pathogens: *Cryptosporidium spp.,Giardia spp.,Campylobacter spp*, and *E. coli* O157:H7. They extended an existing hydrologic model, WATFLOOD, to incorporate pathogen transport to predict the levels of indicator bacteria and pathogens in surface water and tested on a watershed in Southwestern Ontario, Canada. The pathogen model considered transport as a result of overland flow, subsurface flow to tile

drainage systems, and in-stream routing. The model predicted that most microorganisms entering the stream from land-based sources enter the stream from tile drainage systems rather than overland transport.

Ferguson *et al*. (2007b) developed and applied a process-based mathematical model to predict *Cryptosporidium, Giardia* and *E. coli* loads from a drinking water catchment in Australia. The model uses a mass-balance approach and predicts *Cryptosporidium* and *E. coli total* loads generated and the total loads exported from each sub-catchment. The model considered the processes affecting the generation and transport of microorganisms based on land use and flow data, and catchment specific information including point sources such as sewage treatment plants and on-site systems. A sensitivity analysis of the model demonstrated that pathogen excretion rates from animals and humans, and manure mobilization rates were significant factors determining the output of the model.

Coffey *et al*. (2010) used SWAT model to simulate *Cryptosporidium* populations at Fergus catchment in the west of Ireland. After calibrating the model for water flow, the *Cryptosporidium* simulations were run using data from January 2004 until December 2006. The results indicated that the model can be used to predict oocyst concentrations in water catchments, and manure application was identified as being a significant source of the pathogen to which management strategies could be focused to reduce potential levels of *Cryptosporidium* in catchment waters.

Most of the studies mentioned above are related to the development and application of watershed scale models. The models developed by Walker and Stedinger (1999) and Ferguson *et al*. (2007b) can be used to prioritize the implementation of control measures for the reduction of pathogen risks to drinking water. Apart from the watershed scale modeling attempts, there are

few studies in smaller scales like Darnault *et al*. (2004), Cortis *et al*. (2006) and Yeghiazarian *et al*. (2006). Darnault *et al*. (2004) have investigated and modeled the transport of oocysts through preferential flow paths in the vadose zone considering preferential or fingered flow to groundwater. The study was carried out by adding calves feces containing *C. parvum* oocysts with a Cl^- tracer to undisturbed silt loam columns and disturbed sand columns during a simulated steady-state rain. The sand columns exhibited preferential flow in the form of fingers whereas macropore flow occurred in the undisturbed cores. They also developed a simulation model for the transport of oocysts via preferential flow on the basis of an existing preferential flow model for nonadsorbing solutes, with addition of a first-order sink term for adsorbance of the *C. parvum* to the air–water–solid (AWS) interfaces, and with velocity and dispersivity parameters derived from Cl^- transport. The break-through of *C. parvum* oocysts could be described realistically for the sand columns. However, the model could not describe oocyst transport in the columns with macropores.

Kim and Corapcioglu (2004) applied a transport model to simulate laboratory column data for *C. parvum* oocyst. The model incorporated sorption, filtration and inactivation processes. Similarly, the model also looked into the suitability of a kinetic model to describe *C. parvum* oocyst transport and removal in porous media by comparing the result with an equilibrium model. The results indicated that the kinetic model was more suitable than the equilibrium one at simulating the fate and transport of the oocysts in porous media. The model successfully simulated the concentration peak and the late time tailing effect appeared in the break-through curves. The study concluded that sorption caused retardation along with a tailing in the break-through curve and filtration acted as a major mechanism of removing the oocysts

from the aqueous phase, whereas the role of inactivation in reducing the viable oocyst concentration was minimal.

Cortis *et al*. (2006) carried out a series of saturated column experiments to measure the break-through and long-term elution of *Cryptosporidium parvum* in medium sand for a few thousand pore volumes after the initial source of oocysts was removed. They also proposed a new filtration model based on the continuous time random walk (CTRW) theory. Continuous time random walk which is a stochastic transport theory based on local-scale ensamble averages. The study demonstrates that physicochemical heterogeneities at the scale of transported colloids, collector grain surfaces, and pore size have a major impact on the attachment and detachment behavior of the oocysts at the macroscopic scale of the column experiments which can help in understanding the oocysts transport mechanism in groundwater.

Yeghiazarian *et al*. (2006) have developed a stochastic Markov model of *Cryptosporidium* transport, with distinct states of microorganism behavior capturing the microbial partitioning between solid and aqueous phases in runoff and soil surface, including the partitioning among soil particles of various sizes. Although the study is more focused on microscopic behavior of oocyst, there is a room to expand the framework to larger scale.

Table 3.1 provides an overview of recent studies involving pathogen (including *C. parvum*) transport modeling. This table shows historical efforts in development of pathogen transport model by various authors. Although several of these models show good agreement with observed data, there are still challenges for these models when applied to other condition. Therefore, there is a need for development of a process-based model or models that can be applied to a broader climatic, soils, and management conditions.

Table 3.1 Pathogen transport modeling: a review of recent literature.

Study	Pathogen	Scale	Type of model	Flow regime
Walker and Stedinger (1999)	*Cryptosporidium*	Watershed	Deterministic	Surface flow
Medema and Schijven (2001)	*Cryptosporidium*, *Giardia*	Watershed	Deterministic	Surface flow
Sadeghi and Arnold (2002)	Fecal bacteria	Watershed	Deterministic	Surface flow
Tian *et al*. (2002)	*E. coli*	Watershed	Deterministic	Surface flow
Collins and Rutherford (2004)	*E. coli*	Watershed	Deterministic	Surface flow
Darnault *et al*. (2004)	*C. parvum*	Soil Column	Deterministic	Vertical sub-surface flow
Kim and Corapcioglu (2004)	*C. parvum*	Soil Column	Deterministic	Vertical sub-surface flow
Oates *et al*. (2005)	*Pseudomonas fluorescens*	Soil Column	Conceptual	Horizontal/vertical flow
Cortis *et al*. (2006)	*C. parvum*	Saturated soil column	Stochastic	Horizontal/vertical flow
Yeghiazarian *et al*. (2006)	*C. parvum*	Hill slope, plot	Stochastic	Surface flow
Elshorbagy and Ormsbee (2006)	*Fecal coliform*	Watershed	Deterministic	Surface water
Dorner *et al*. (2006)	*E. coli*, *Cryptosporidium*, *Giardia*, *Campylobacter*	Watershed	Deterministic	Surface water
Haydon and Deletic (2006)	*E. coli*	Watershed	Conceptual	Surface and subsurface flow
Ferguson *et al*. (2007b)	*E. coli*, *Cryptosporidium*, *Giardia*	Watershed	Deterministic	Surface flow
Wu *et al*. (2009)	*E. coli*	Watershed	Deterministic	Surface flow

CHAPTER 4: EXPERIMENTAL STUDIES

The specific mechanisms that affect the transmission and attenuation of microorganisms in soil and water include both physical/chemical and biological factors. However, factors that affect the soil migration of different organisms differ significantly and experimental designs must be accordingly flexible. Although the effects of slope and vegetation on water quality parameters like sediments and nutrients are relatively well understood, their influences on overland transport of pathogens, e.g., the relative amounts of these pathogens which partition as attached to clay, mineral and/or organic matter in the soil and vegetation versus unattached, suspended particles in overland flow, have yet to be quantified. The experiments are aimed at delineating important mechanisms that effect transport, and die-off of *C. parvum* oocysts and rotavirus in surface and near-surface runoff. The experimental emphasis is on laboratory experiments where the hypothesized parameters that potentially affect the migration and attenuation can be closely controlled. The experiments were conducted at the University of Illinois at Urbana-Champaign (UIUC) which includes laboratory experiments on inclined soil-beds.

The data used to calibrate and validate the model developed in this study were obtained from two sets of experimental studies: a large scale laboratory studies conducted by Trask (2002) and a small scale laboratory studies conducted by Koch (2009) and Davidson (2010).

4.1 Large scale laboratory experiment

A tilting soil-chamber with dimensions 3.6 m by 1.5 m in surface area and 0.3 m deep was used to monitor the overland and near-surface flow of *C. parvum*. A sheet metal divider separated the soil bin into two equal compartments (3.6 m by 0.75 m). The both compartments were filled with soil, one compartment was planted with Brome grass and the other one was left

to simulate bare-ground condition as shown in Figure 4.1. The laboratory experiments were conducted using three slopes (1.5, 3.0, and 4.5%) which represent the low, medium and high slope conditions in central Illinois.

Rainfall was applied to the soil chamber using a microcomputer-controlled laboratory rainfall simulator which could provide a fairly even distribution of rainfall over the entire simulator basin. The rainfall simulator is located 10 m above from the soil bed to ensure that most of the drops attain terminal velocity upon impact with the simulator test floor, thus simulating natural rainfall events. Two rainfall intensities of 2.54 and 6.35 cm/hr were applied during the experiments representing 1 yr and 10 yr events in Champaign, IL. The rainfall duration of 40 minutes was selected such that ample runoff volume could be collected for sample analysis.

There were two soils selected for the experimental trials that were deemed a good representation of Illinois soils. A moderately well drained silt-loam (Catlin series, mesic Oxyaquic Argiudolls) soil and a poorly drained silt-loam from southern Illinois (Newberry series, mesic Mollic Endoaqualfs) were used to prepare the soil bed for the experimental studies. Catlin soil was obtained from a site located just south of the Windsor Pond along south 1st Street in Champaign, IL while Newberry soil was obtained from a farm field with a corn-bean rotation located in Effingham, IL.

The overland sample collection system included a trough with an aluminum divider plate to separate surface runoff from each compartment. Surface runoff from each compartment was directed to collection bottles through a hole with a funnel mounted directly below the hole. Near-surface flow was collected separately from each compartment. Each compartment had twelve holes at the bottom of the bed in the last one-third section (i.e. bottom of the slope). A steel tray

was placed beneath each compartment spanning one-half the length of the soil chamber which facilitated collection of subsurface or near-surface flow. The collection bottles used were 23 liter glass carboys with one-liter increment markers.

Once grass was fully grown, oocysts were applied to the tilting bed and the bed placed under the laboratory. Runoff samples from both compartments (with and without grass) were collected to quantify the effects of vegetation on oocysts transport. Shallow lateral sub-surface flow that was exfiltrated from the bottom of the soil chamber at the outlet was collected to investigate near-surface transport of oocysts. The different parameters to be examined in the inclined soil-bed experiments were the effect of slopes, vegetation, rainfall intensity, and flow regime on oocysts migration on overland and near-surface flow. Known amount of oocysts was applied to the soil in aqueous suspensions prior to rainfall simulation and mass balances of viable oocysts and infective virus particles was made on various components of surface and near-surface flow. Control solutions "spiked" with oocysts were used to test the effects of natural solute conditions on survival and viability (or infectivity) of the organisms. The oocysts were applied by two different techniques; surface application and injection at the upper end of the sloped surface. Runoff samples were collected at every five minutes intervals for transport kinetics measurements. Once experiments were conducted on all slopes with one soil type, experiments were conducted with other soil type. At the end of each experiment, soil samples were collected from the inclined-beds for *C. parvum* quantity and viability (infectivity) analyses. Because of the well-known environmental stability of oocysts, determination of oocysts concentration in water and soil samples was done using an antigen-capture enzyme immunoassay (EIA). Oocyst viability was determined by differential vital dye staining and oocyst excystation assays. Similarly, oocyst viability in selected samples, e.g., those showing relatively high oocyst

concentrations, was confirmed by measuring oocyst infectivity in HCT-8 cells using modifications of a previous method (Schets *et al.*, 2005). The experimental results were used to parameterize and validate the results obtained from this modeling study.

Figure 4.1 Tilting soil chamber with surface and subsurface sample collection systems (Trask, 2002).

4.2 Small scale laboratory experiments

Overland and near-surface transport of *C. parvum* and rotavirus was investigated through small-scale laboratory experiments were conducted at the Department of Pathobiology of the College of Veterinary Medicine at the University of Illinois from 2007-2009. The following sections provide the details of experimental setup, trials, and sample analysis.

A small-scale tilting frame and soil bed were used to investigate *C. parvum* and rotavirus transport in surface and subsurface flow. This system allowed flexibility for additional experiments in a more practical manner than the large-scale systems that were previously constructed. A Plexiglass frame measuring 0.305 m (1 ft) wide by 0.610 m (2 ft) long by 0.153 m

(0.5 ft) deep was used to prepare the soil bed. The soil bed rested on a wooden frame with hinges and a handle to adjust the soil bed to any desired slope condition. The experiments carried out by Koch (2009) used two slope conditions: 2.5 and 3% while the experiments conducted by Davidson (2010) used only 2.5% slope condition.

Surface runoff from the soil bed was diverted to runoff collection system through an aluminum tray, located down-slope end of the wood frame. A vinyl tube was attached to the aluminum tray so samples could be collected in the sampling jars. Another aluminum tray collected near-surface runoff and diverted it to sampling jars through a vinyl tube.

The rainfall simulator system used for these experiments was made up of PVC pipes. Because of their ability to supply a very low rate of water, three different nozzles mister nozzles were used in the system which also allowed small increments of rainfall intensity. In order to increase the drop size of simulated rain, fiberglass window screen was placed below the nozzle system. The nozzles sprayed water onto the screen which helped in forming the bigger droplets on the screen which eventually fell onto soil bed below, more closely mimicking natural rainfall droplets. Experiments conducted by Koch (2009) used two rainfall intensities, 63.5 and 90 mm/hr to investigate the effect of vegetation on *C. parvum* transport. 90 mm/hr intensity was the highest rainfall intensity that the simulator was capable of delivering. 63.5 mm/hr intensity was previously tested by Trask *et al*. (2004) allowing for comparison between the two data sets. The experiments conducted by Davidson (2010) were conducted under a rainfall intensity of 63.5 mm/hr applied for 20 minutes. In case of Koch (2009) experiments, simulated rainfall duration was 10 minutes since the duration resulted in adequate runoff volumes during preliminary trials without *C. parvum* application.

The experiments carried out by Koch (2009) investigated the transport of *C. parvum* on Catlin soil beds. A moderately drained silt-loam (Catlin series, mesic Oxyaquic Argiudolls: 24% sand, 50% silt, 26% clay) soil was packed in the soil beds. Rainfall was applied to the chambers on a regular basis to simulate natural climatic conditions and approach natural soil compaction after a few weeks (Fohrer *et al*., 1999). Brome grass was established on two of the constructed soil beds while the surface of two other beds was left bare. Smooth Brome grass was chosen as the vegetation cover since it is a grass species commonly used for VFS in Illinois (McLaughlin, 2003).

Davidson (2010) used three types of soil bed (Catlin, Alvin and Darwin soils) and three surface conditions: bare, Brome grass and Fescue to study fate and transport of *C. parvum* and rotavirus. The experimental procedure was similar to Koch (2009) experiments. Once experiments were completed with Catlin soil beds, the same procedure was repeated for other two soil types: a well-drained fine sandy loam (Alvin series: 60% sand, 25% silt, 15% clay) soil and poorly-drained silty clay (Darwin series: 5% sand, 50% silt, 45% clay). For more details on the experimental set up, please refer to Koch (2009) and Davidson (2010).

4.2.1 Pathogen transport experiments

Experiments began after adequate grass cover was established on the vegetated soil beds. To ensure the initial surface moisture conditions were similar for each experiment, simulated rainfall was applied to the soil bed until flow began. The soil bed was then allowed to drain until surface and near-surface flow ceased prior to *C. parvum* application. At that time the moisture content of the soil is near field-capacity. *C. parvum* oocysts were applied as fecal slurry as opposed to purified oocysts in order to more closely represent natural oocyst shedding in the environment by a calf. For all experiments, surface and subsurface runoff samples were collected

throughout the entire flow event. In addition, soil samples were collected to examine the transport of *C. parvum* oocysts in the soil.

For the bare condition experiments, the soil bed was placed on the tilting frame at desired slope. After the desired moisture condition was reached and flow stopped (near field-capacity), 15 mL of the *C. parvum* slurry was applied in a band approximately 50 mm from the upper end (up-slope) of the soil bed with a pipet. Immediately following the oocyst application, rainfall was simulated over the soil bed at desired intensity for ten minutes. No sooner the surface flow started, samples were taken every 30 seconds until flow ceased. Soil cores were then taken as described previously after all runoff stopped.

Experiments with vegetated covers started after the vegetation was grown to more than adequate height and coverage. Prior to running the experiment, the grass was cut to an average height of 15.2 cm (6 in). This is the minimum cutting height recommended by the Environmental Protection Agency (EPA) (McLaughlin, 2003). The vegetated soil bed was placed at a desired slope on the tilting frame. First, the bed was brought to near-saturation condition using the rainfall simulator and allowed to drain. When all runoff stopped (near-field capacity), 15 mL of the *C. parvum* oocyst slurry was applied to the vegetated soil bed in a band approximately 50 mm from the upper end (up-slope) of the soil bed as previously described.

Figure 4.2 Complete laboratory-scale rainfall simulator and tilting soil bed system **(**Davidson, 2010).

Following the *C. parvum* slurry application, rainfall was simulated at desired intensity for desired duration (10 minutes for Koch (2009) experiments and 20 minutes for Davidson (2010) experiments). As soon as surface flow started, samples were collected every 30 seconds until the flow stopped by Koch (2009). The sampling duration was 1 minute for Davidson (2010) experiments. A very similar experimental procedure was applied during rotavirus transport studies.

4.2.2 Detection and quantification of *C. parvum*

Two methods for *C. parvum* quantification were used in this study. An ELISA assay used in previous larger-scale studies (Trask *et al*., 2004) was chosen to allow the data from the small-scale system to be used for comparison with exiting published data. A second infectivity assay was employed in order to determine the actual viability of oocysts in the surface runoff, near-surface flow, and soil core fractions.

Runoff samples from both the bare and vegetated conditions were collected every 30 seconds as described above. Each sample contained a dilute concentration of *C. parvum* oocysts, requiring a concentration of the samples for detection. The total volume of each sample was measured and 50 mL of each sample (the entire volume was used if less than 50 mL was collected) was placed in 50 mL conical tubes. The 50 mL extracts were centrifuged for 10 minutes at 4 ºC and 1260 x g (2500 rpm). The centrifugation forced the sediment and oocysts into a pellet at the bottom of the conical tubes. A 45 mL volume of supernatant was removed from each conical tube, leaving 5 mL of a 10x concentrated runoff sample.

Each sample was analyzed for the presence of *C. parvum* using an enzyme-linked immunosorbent assay (ELISA) (Premier *Cryptosporidium* enzyme immunoassay, Meridian Diagnostics, Inc), detecting an antigen specific to *C. parvum*. Microwells pre-coated with a polycolonal anti-*Cryptosporidium* capture antibody were used to specifically capture an antigenic determinant of *C. parvum*. An aliquot of each concentrated runoff sample (50 μL) was allowed to rest in the microwells for 30 minutes to ensure complete antigen bonding. After adequate bonding time, a second antibody (monoclonal anti-*Cryptosporidium*)/enzyme conjugate (peroxidase) was added to tag the captured antigen. Following the addition of peroxidase substrates, the absorbance values were determined for each well in an ELISA plate reader. The

absorbance values were compared to a standard curve, produced by testing various known dilutions of the same *C. parvum* slurry that was applied to the beds.

The infectivity assay results are more beneficial since it provides the actual oocyst infectivity per runoff sample but it is more complicated than the ELSIA assay. Initially, a sucrose floatation procedure was performed on all runoff and soil core samples in order to purify the oocysts in the samples to minimize soil contamination to cells in the assay. Results showed that while fewer oocysts were found in the vegetated surface samples than the bare surface samples when analyzed with the ELISA assay, the difference was not nearly as apparent as in the infectivity assay. So, the runoff samples were prepared with the exact same method omitting the sucrose floatation procedure. Soil core samples were still treated with the sucrose floatation procedure since analyzing the raw soil cores was not possible.

4.2.3 Detection and quantification of rotavirus

Since the collected samples contained a relatively high concentration of rotavirus particles, a dilution of the samples was required for analysis. The procedure for diluting the samples involved measuring the total volume, shaking the samples and allowing soil particles to settle, and then taking a given amount from each sample. A 1/5 dilution was then prepared by combining 200 µL of each sample with 800 µL of serum-free MEM and applying 500 µL directly to the plate wells.

For the quantification of rotavirus in samples, the focus forming unit (FFU) assay was performed following the method described by Rolsma *et al*. (1998). The rotavirus FFUs were quantified by counting the number of FFUs present in a given sample. The FFUs (stained viral-antigen-positive cells) were quantified 100 times using a Nikon TS 100 inverted microscope

equipped with a computer-controlled electronic stage and Spot RT-slider CCD camera. Twenty five digital images were automatically collected from each plate well using Metamorph software (Molecular Devices, Inc) to develop and capture images within a scan grid which covered >80 % of the well surface area. The number of FFU in each of these images were then counted either by hand or automatically using integrated morphometric parameters within the software to recognize FFU. The ability to automatically count FFU was dependent on the degree of background staining, which varied between different antibody lots.

4.3 Rainfall - Runoff induced erosion: large scale laboratory experiments

A series of laboratory experiments were carried out to compare the erosion pattern from a bare soil bed subjected to rainfall with the same bed subjected to surface runoff only. The experimental set up was similar to the system used by Trask (2002). The soil chamber (3.6 m long, 1.5 m wide and 0.3 m deep) was made up of 10-gauge (3.4 mm thickness) sheet metal. The soil chamber was divided into two separate compartments with a steel plate divider placed at the center of the 1.5 m wide chamber across its 3.6 m length and sealed. Similarly, the bottom and edges of each compartment were sealed completely. Both chambers were filled with Dana silt loam series soil, which is predominantly found on slopes (from 2 to 5 percent) in central Illinois. The soil has bulk density ranging from 1.40 to 1.55 g/cc, permeability ranging from 1.5 to 5.1 cm/h, clay content ranging from 18 to 27 percent, pH ranging from 5.6 to 7.3 and contained approximately 4% organic matter (USDA, 2008). For rainfall induced erosion experiments, two rainfall intensities (2.54 cm/hr and 6.35 cm/hr) were applied for 20 minutes with 1.5 and 4.5%

bed slope conditions. For runoff induced erosion experiments, two runoff rates 0.00235 cfs (4 liter/min) and 0.00470 cfs (8 liter/min) were selected based on measured runoff that was generated by 2.54 and 6.35 cm/hr rainfall, respectively. Due to the facility constraints, higher runoff rate experiments were not feasible. The desired runoff rate was applied for 20 minutes using rain gutter placed at the top of the bed to ensure the even distribution of applied flow. The rain gutter was supported by wooden frames. The flow input to rain gutter was measured before the experiment began. The samples were collected in 5 minutes duration to measure runoff rate and sediment concentration at the bottom of the bed. The total runoff volume was also measured for both set of experiments. Figure 4.3 below shows the experimental set up to investigate the erosion pattern due to overland flow only.

Figure 4.3 Experimental set up to study erosion pattern from overland flow.

CHAPTER 5: DEVELOPMENT OF A PHYSICALLY-BASED MODEL FOR TRANSPORT OF PATHOGEN IN OVERLAND FLOW

In this study, a model to simulate *C. parvum* oocysts and rotavirus transport in surface flow is developed. The model is coupled with a soil erosion model in order to capture the dynamics of sediment-bound oocysts. Selected outputs from the soil erosion model, Water Erosion Prediction Project or WEPP (Nearing *et al.*, 1989; Cochrane and Flanagan, 1999) served as input for the oocyst transport model. A brief schematic of modeling framework is presented in Figure 5.1.

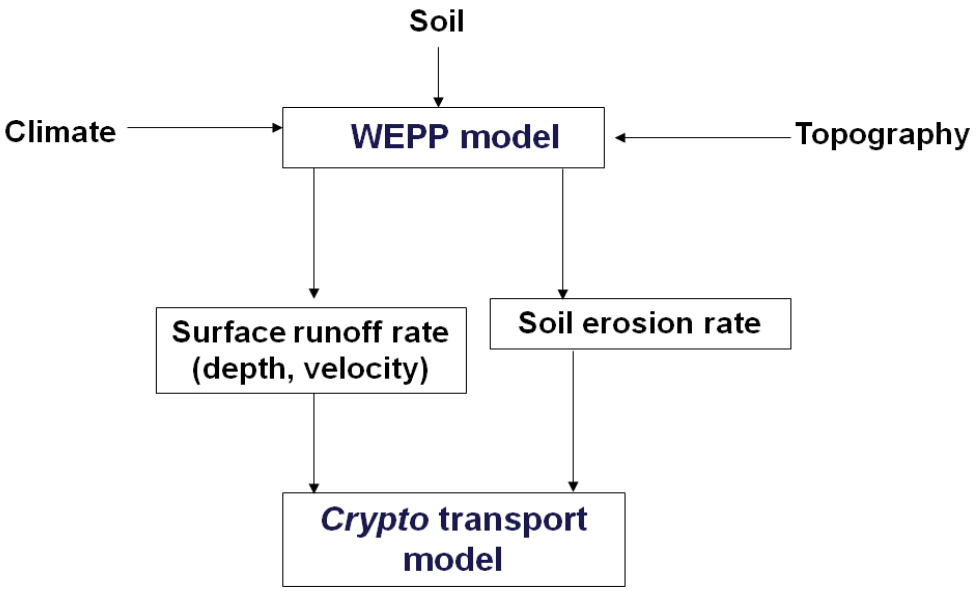

Figure 5.1 Overview of modeling framework.

Water Erosion Prediction Project (WEPP) is a physically-based erosion prediction model developed by the United States Department of Agriculture (USDA) and applicable to erosion processes on single hillslope and small watersheds (Nearing *et al.*, 1989; Laflen *et al*., 1991; Cochrane and Flanagan, 1999). Water Erosion Prediction Project (WEPP) model represents an erosion prediction technology based on fundamentals of stochastic weather generation, infiltration theory, hydrology, soil physics, hydraulics, and erosion mechanics (Cochrane and Flanagan, 1999). There are two versions of WEPP available: hillslope and watershed. The hillslope or landscape profile version of WEPP is capable of estimating spatial and temporal distributions of soil loss (net soil loss for an entire hillslope or for each point on a slope profile can be estimated on a daily, monthly, or average annual basis). In watershed applications, the model can predict soil loss and sediment deposition from overland flow on hillslopes, soil loss and sediment deposition from concentrated flow in small channels, sediment deposition in impoundments, and sediment yield from entire fields and watershed (Flanagan and Nearing, 1995). The WEPP has been widely applied to simulate soil erosion and sediment yield in different geographic and climatic conditions (Renschler, 2003; Flanagan *et al*., 2007; Dun *et al*., 2009; Singh *et al*., 2009). The hillslope version of WEPP model is used in this study. A flow chart showing different processes incorporated in WEPP model is shown in Figure 5.2.

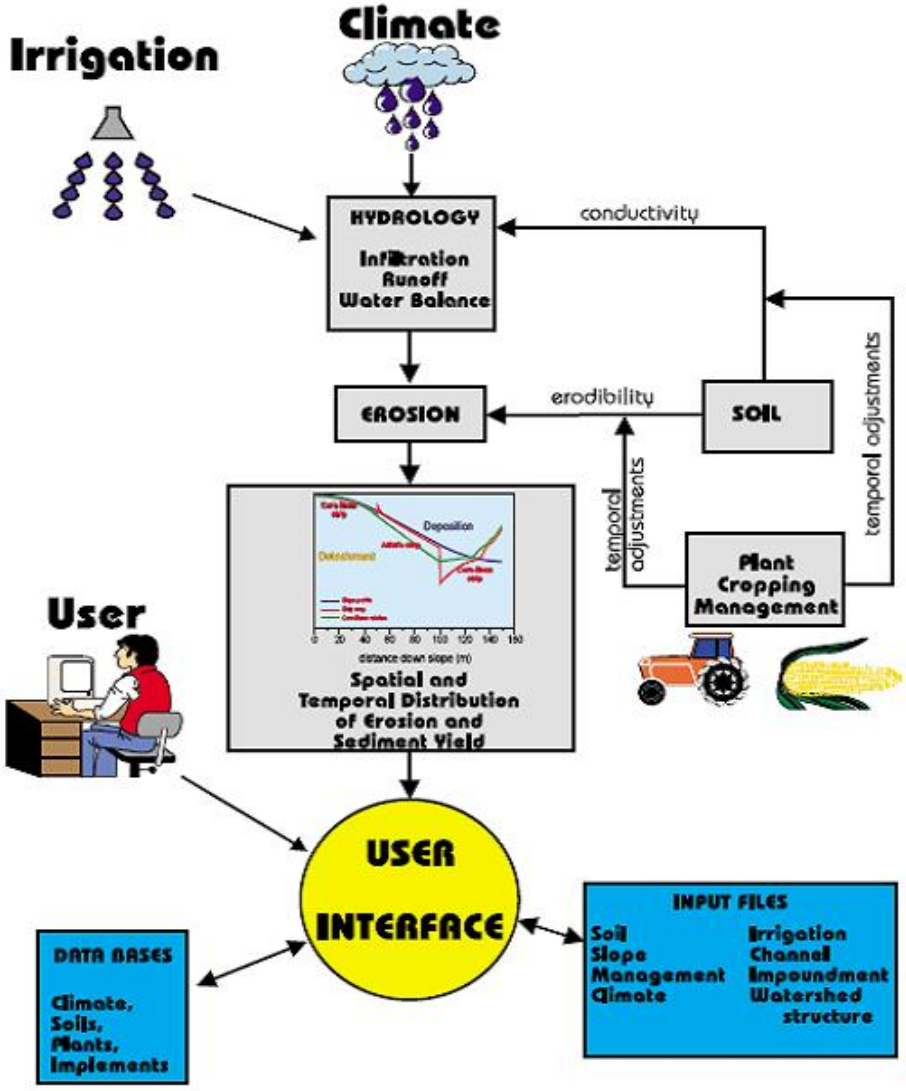

Figure 5.2 Flow chat for the WEPP erosion model system (Laflen *et al*., 1991).

The following possible states of pathogen transport in overland flow were considered following the stochastic modeling framework proposed by Yeghiazarian *et al.* (2006):

(1) Pathogens attach to soil particles with attachment rate K_{12}

(2) Pathogens attached to soil particles (soil + oocyst aggregate) are removed by surface flow velocity (u) with rate constant K_{23}

(3) Pathogens attached to soil particles gets liberated with the detachment rate K_{21}

(4) Pathogens become inactivated with decaying rate K_d

(5) Pathogens are removed by infiltration with the rate equal to f/D (f is saturated hydraulic conductivity, and D is flow depth).

The different stages of pathogen transport considered in the model are shown in Figure 5.3 below.

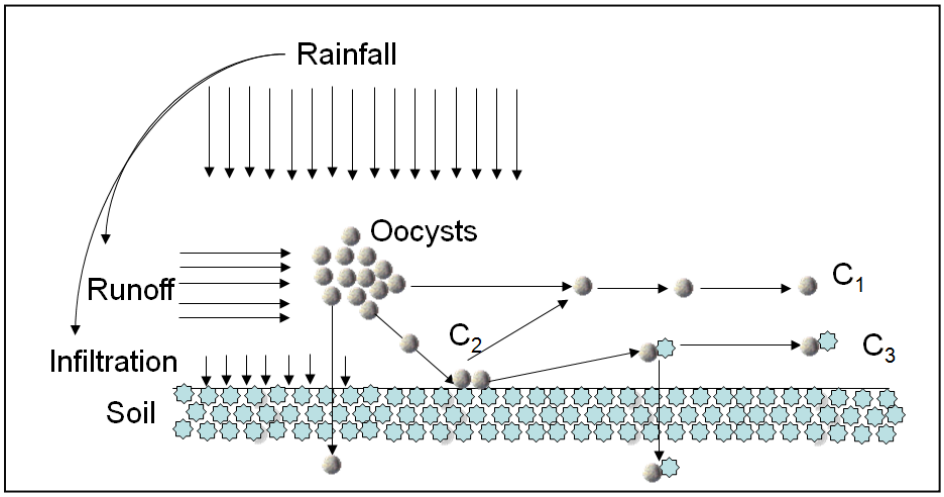

Figure 5.3 Schematic showing different processes considered in pathogen transport model framework.

Concentrations of free pathogens in water (C_1), attached to immobile soil particles (C_2), attached to mobile soil particles (C_3) can be calculated using the set of following mass balance equations:

$$\frac{\partial C_1}{\partial t} + u\frac{\partial C_1}{\partial x} = -(K_{12} + K_d + \frac{f}{D})C_1 + K_{21}C_2 \quad (1)$$

$$\frac{\partial C_2}{\partial t} = K_{12}C_1 - K_{21}C_2 - K_{23}C_2 \quad (2)$$

$$\frac{\partial C_3}{\partial t} + u\frac{\partial C_3}{\partial x} = K_{23}C_2 - (K_d + \frac{f}{D})C_3 \quad (3)$$

The system of equation basically represents one-dimensional flow along x-direction although it also incorporates term for infiltration. The system of mass-balance equations can be solved using following initial and boundary conditions:

(a) Initial conditions: $C_1^0 = C_1(0,x)$; $C_2(0,x) = C_3(0,x) = 0$

where C_1^0 is the concentration of oocysts applied to x = 0 location

The initial conditions reflect the assumption that at time zero the pathogens are unattached and freely moving in the water.

(b) Boundary condition: $C_1(t,0) = C_2(t,0) = C_3(t,0) = 0$

The boundary condition reflect the assumption that is no continuous source of pathogens exists at x = 0.

A numerical solution to a system of PDEs similar to above is outlined by Park *et al.* (2008). The flow velocity of C_2 in Equation (2) is zero because *Cryptosporidium* oocysts and rotavirus are attached to soil particles and immobile in that state. However, C_1 and C_3 are pathogen concentrations in overland flow, thus oocysts in state 1 and 3 flow downstream with surface runoff. In this study, the surface velocity was obtained from WEPP simulation result and assumed to be constant over space. The PDEs for C_1 and C_3 resemble the form of a wave equation (hyperbolic PDE). Since the flow velocity (v) is assumed constant over the space, the grid for finite difference method can be discretized by employing the following relationship:

$$dx = v\,dt \qquad (4)$$

It showed be noted that one-way wave equation represents the prototype for all hyperbolic partial differential equations. So, the characteristics of wave equation can be explained by the following relationship:

$$\frac{\partial u}{\partial t} + a\frac{\partial u}{\partial x} = 0 \qquad (5)$$

where *t* denotes time variable, *a* is a constant, and *x* denotes the spatial variable.

The following relationship represents the solution of Eq. (5):

$$u\,(x,t) = u_0\,(x - at) \qquad (6)$$

where $u_0 = u\,(x,0)$ is the initial condition. The above relationship indicates that the solution at any time is a replication of the original function when t = 0 but shifted to the right by the amount "a t_0". So, the solution of Eq. (5) can be considered as wave propagation with speed *a* and without change of shape. Similar concept can be applied to a grid discritized for the finite difference solution of the pathogen transport model (Park *et. al.*, 2008).

If each grid component in the *(x, t)* domain is assembled in such a way that the speed of propagation *a* is the same, then *dx* and *dt* can be related as $dx = a\,dt$ for each step size. This assumption can also be applied in case of proposed pathogen transport model. The term, *dx* can be determined using the relation $dx = v\,dt$, once the step size *dt* is decided for each iteration. In this way, location *x* can adjusted based on the value of *dt*. In case of C_2, the partial differential equation can be discritized with Crank-Nicolson formulation which permits the development of an accurate second-order formula in both dx and dt. Then, $\frac{\partial C_2}{\partial t}$ can be directly approximated at x and t + ½ dt with the central difference scheme. The equation for C_1 and C_3 are more complicated because both of them involve partial derivatives with respect to *x* and *t*. The terms $\frac{\partial C_1}{\partial t}$ and $\frac{\partial C_3}{\partial t}$ can both be evaluated by replacing *dx* with *v dt* as proposed earlier. Figure 5.4 demonstrates how the scheme works. While C_2 proceeds from $C\,(x,t)$ to $C\,(x, t + dt)$, C_1 and C_3 move from $C\,(x, t)$ to $C\,(x + dx, t + dt)$ along the diagonal way.

When the surface cover is vegetated, an extra equation along with two additional terms was added to the model which could represent attachment to the vegetation with the rate with k_{14} and detachment from the vegetation with the rate k_{41}. The system of equations in case of vegetated surface is as follows:

$$\frac{\partial C_1}{\partial t} + u\frac{\partial C_1}{\partial x} = -(K_{12} + K_{14} + K_d + \frac{f}{D})C_1 + K_{21}C_2 + K_{41}C_4 \quad (7)$$

$$\frac{\partial C_2}{\partial t} = K_{12}C_1 - (K_{23} + K_{21})C_2 \quad (8)$$

$$\frac{\partial C_3}{\partial t} + u\frac{\partial C_3}{\partial x} = K_{23}C_2 - (K_d + \frac{f}{D})C_3 \quad (9)$$

$$\frac{\partial C_4}{\partial t} = K_{14}C_1 - K_{41}C_4 \quad (10)$$

5.1 Model parameter identification

For the pathogen transport study, a 40-minute single storm simulation on a laboratory tilting bed was performed. The input for this simulation included: climate data including date of the storm, the storm amount, and the storm duration; hillslope profile including shape, area, and inclination of the hillslope; field operation and crop conditions; soil parameters, etc.

The WEPP simulations provided: (1) effective rainfall intensity; (2) effective saturated conductivity, which is the same as the infiltration rate when some 95% of the total pore space is filled with water; (3) average flow depth and average flow rate, which can be derived from the Chezy coefficient and the peak runoff rate; (4) average soil loss per detachment area; (5) the soil particle fraction exiting in flow.

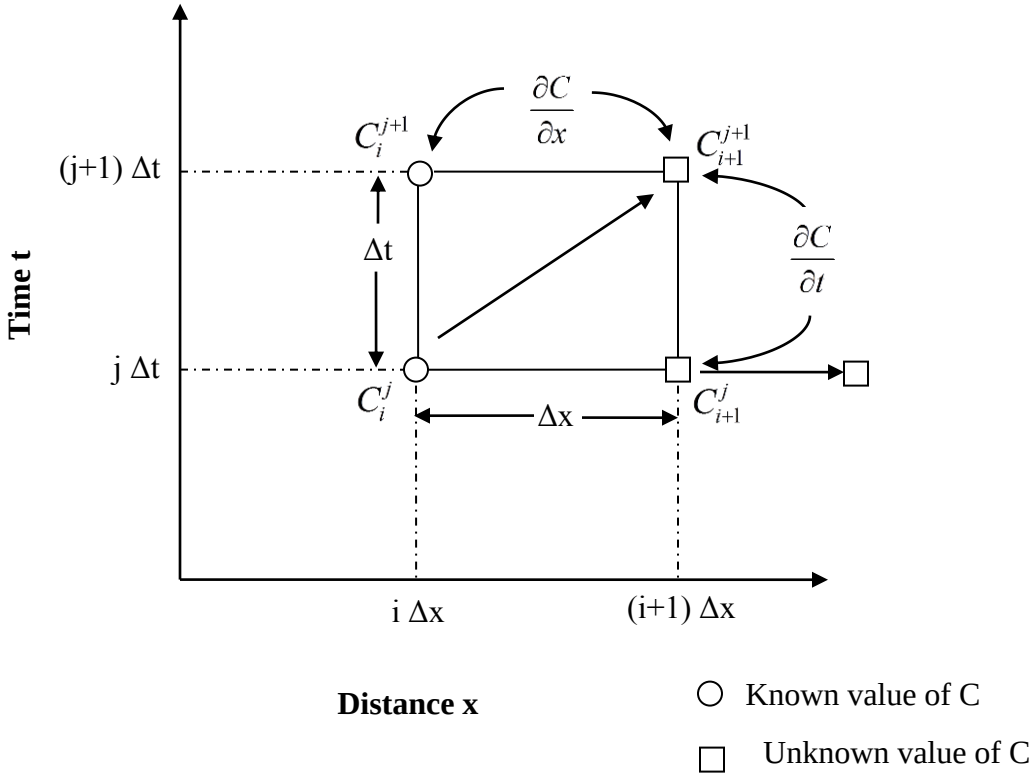

Figure 5.4 Grid discritized for the finite difference solution (Chow *et al.*, 1988).

Microorganisms and soil particles can be thought of as chemical substances that react with each other producing the third substance: microorganism-soil particle aggregates for modeling purposes (Yeghiazarian *et al.*, 2006). The strength of attachment of microorganisms to soil particles is determined by the chemical characteristics of soils which are highly correlated with the particle size. For example, the study by McLaughlin (2003) reported that *C. parvum* oocysts strongly adsorb to clay particles compared to silt or sand particles. The physical, and hence, the mathematical representation of inter-particle interactions may be further simplified by considering that the amount of soil particles participating in "reactions" is either infinite (number of soil particles on the soil surface), or can be obtained experimentally or from an erosion model

(suspended sediment). The particle size class distribution of sediment in the suspended sediment is predicted by the WEPP model. As the microorganism transport model uses WEPP output as its input, the transport model was coupled with WEPP model externally.

Initial approximation for K_{12} is obtained from Ling *et al.* (2003). They came up with an approximation for partitioning coefficient (K_d) for bacteria with the long centrifuge experiment. They found K_d to be a function of the clay content in soil as:

$$K_d = A\,(CLAY)^B \qquad (11)$$

where *CLAY* = the percentage of clay particles <0.002mm in soil (the relationship was developed for $2 < CLAY\ \% < 50$), A = the slope of the regression in log-log coordinates ($10^{-1.6 \pm 0.9}$), B = the intercept of the regression in log-log coordinates (1.98 ± 0.7).

Parameter K_{23} is the rate of microorganism-soil particle aggregate removal from the soil surface. Parameters involving free microorganism/aggregate removal from the soil surface are obtained by analogy with soil erosion processes. Soil erosion mainly occurs via two mechanisms: a) raindrop impact, and b) erosion caused by flowing water due to the effect of shear stress acting at the interface between flowing water and the soil surface. The effect of these mechanisms is additive. Hence, initial approximation for K_{23} is computed as sum of raindrop erosion and erosion induced by flow velocity as $(d_{23}\,P + e_{23}\,vS)$. Here, $d_{23}\,(=1/D)$ is detachability coefficient, P is the rainfall intensity obtained from the erosion model, e_{23} is the coefficient of micro-aggregate entrainment by the flow, v is the flow velocity and S is the slope (Yeghiazarian *et al.*, 2006).

Both vegetation related parameters K_{14} and K_{41} were treated as calibration parameters in the absence of reliable parameter estimate in the literatures.

CHAPTER 6: RESULTS AND DISCUSSION

This section provides the details of laboratory experiment and model simulation results. The model simulated results were compared with the following experimental data sets:

1. Large scale laboratory experiment: Flow and *C. parvum* recovery from two soil types (Catlin and Newberry), two rainfall conditions (2.54 and 6.35 cm/hr) and three bed slope conditions (1.5, 3.0 and 4.5%) for bare and vegetated (Brome grass) conditions
2. Small scale experiment:

   (a) Flow, *C. parvum* and rotavirus recovery from three soil type (Alvin, Catlin and Darwin), three surface conditions (bare, Brome grass and Fescue) with 2.5% bed slope subjected 6.35 cm/hr rainfall

   (b) Flow and *C. parvum* recovery from Catlin soil bed with 2.5% slope subjected 6.35 cm/hr rainfall and 3.0% slope subjected to 9.0 cm/hr rainfall intensity for bare and vegetated (Brome grass) conditions
3. Laboratory experiment on runoff induced erosion: Flow and sediment

6.1 Results from large-scale laboratory experiment

As mentioned earlier, a series of laboratory experiments were conducted by Trask (2002) using three slopes (1.5, 3.0, and 4.5%), two rainfall intensities (2.54 and 6.35 cm/hr), one vegetation type (Brome) and two soil types (Catlin and Newberry). *C. parvum* oocysts were detected in both surface runoff and near-surface flow for both bare-ground and vegetated conditions for each slope (1.5, 3.0, and 4.5%) under low rainfall intensity (2.54 cm/hr) conditions following the initial application of pathogens. For the high intensity rainfall (6.35 cm/hr), *C. parvum* oocysts

were detected in surface runoff from bare-ground and vegetated conditions while near-surface flow contained detectable oocysts from the vegetated conditions with zero flow from the bare-ground conditions from all slope conditions.

6.1.1 Runoff volume

As observed by Trask (2002), the volumes of surface runoff obtained from the bare-ground conditions were consistently higher than those from vegetated conditions. This trend was observed for all slope conditions, both rainfall intensities and soil types. These findings were expected because reduced runoff volumes from the VFS were associated with more resistance to overland flow and longer contact times allowing a higher infiltration of water into the soil profile. The collected runoff volumes for the 1.5, 3.0, and 4.5% slopes are presented in Table 6.1 for Catlin soil and in Table 6.2 for Newberry soil respectively as reported by Trask (2002).

Table 6.1 Volumes of surface runoff and near-surface flow (in liters) at three different slopes for 2.54 and 6.35-cm/hr rainfall intensities for Catlin soil.

Collection Type	Volumes in Liters					
	2.54-cm/hr Rainfall			6.35-cm/hr Rainfall		
	Slope 1.5%	Slope 3.0%	Slope 4.5%	Slope 1.5%	Slope 3.0%	Slope 4.5%
Bare-ground surface runoff	31.0	39.2	34.4	111.8	109.0	104.7
Vegetative surface runoff	17.5	27.3	24.5	56.5	68.7	76.4
Bare-ground near-surface flow	3.1	1.8	0.6	0.0	0.0	0.0
Vegetative near-surface flow	10.1	8.6	5.2	9.0	13.9	11.5

Table 6.2 Volumes of surface runoff and near-surface flow (in liters) at three different slopes for 2.54 and 6.35-cm/hr rainfall intensities for Newberry soil.

Collection Type	Volumes in Liters					
	2.54-cm/hr Rainfall			6.35-cm/hr Rainfall		
	Slope 1.5%	Slope 3.0%	Slope 4.5%	Slope 1.5%	Slope 3.0%	Slope 4.5%
Bare-ground surface runoff	35.2	45.3	50.5	116.6	115.9	118.8
Vegetative surface runoff	23.5	26.5	27.9	60.4	65.6	71.6
Bare-ground near-surface flow	3.8	2.9	3.1	0.0	0.0	0.0
Vegetative near-surface flow	10.8	8.2	4.7	12.1	11.2	9.5

6.1.2 *C. parvum* oocyst recovery

As reported by Trask (2002), the oocyst recovery rates in surface runoff for both 2.54 and 6.35 cm/hr rainfall intensities for different slopes varied. For light intensity rainfall event (2.54-cm/hr), there was a greater recovery of oocysts from the 1.5% slope as compared to those from the 3.0 and 4.5% slopes as shown in Tables 6.3 and 6.4.

Table 6.3 Total percent recovery of applied oocysts for surface and near-surface flow for bare ground and vegetated condition for Catlin soil.

Surface condition	Recovery in %					
	2.54-cm/hr Rainfall			6.35-cm/hr Rainfall		
	Slope 1.5%	Slope 3.0%	Slope 4.5%	Slope 1.5%	Slope 3.0%	Slope 4.5%
Bare-ground surface	13.77	9.53	3.35	2.53	5.32	52.45
Bare-ground near-surface	0.04	0.02	0.00	0.00	0.00	0.00
Vegetated surface	1.65	0.84	0.34	0.80	0.39	20.34
Vegetated near-surface	1.25	0.04	0.01	0.08	0.18	1.62

Table 6.4 Total percent recovery of applied oocysts for surface and near-surface flow for bare ground and vegetated condition for Newberry soil.

Surface condition	Recovery in %					
	2.54 cm/hr Rainfall			6.35 cm/hr Rainfall		
	Slope 1.5%	Slope 3.0%	Slope 4.5%	Slope 1.5%	Slope 3.0%	Slope 4.5%
Bare-ground surface	20.08	4.17	9.30	17.16	79.69	98.50
Bare-ground near-surface	0.03	0.01	0.00	0.00	0.00	0.00
Vegetated surface	6.88	0.51	0.64	1.57	2.93	8.27
Vegetated near-surface	0.65	0.03	0.01	0.00	0.10	0.65

6.2 Results from small-scale laboratory experiment

A series of laboratory experiments were conducted at the University of Illinois at Urbana-Champaign from 2007-2009. The experiments conducted by Koch (2009) included two sets of slope and intensity conditions (2.5% slope and 6.35 cm/hr intensity along with 3.0% slope and 9.0 cm/hr rainfall intensity), Catlin soil bed with and without vegetation (Brome grass). Experiments conducted by Davidson (2010) used three types of soil beds (a moderately drained Catlin silt-loam, Alvin fine sandy-loam, Darwin silty-clay soil) set at 2.5% slope under simulated rainfall intensity 6.35 cm/hr with three surface conditions: bare, Brome grass and Fescue.

6.2.1 Runoff Volume and oocyst recovery

Table 6.5 summarizes the runoff volume and oocysts recovery from a Catlin soil bed with and without vegetation under different slopes (2.5 and 3.0%) and rainfall intensities (6.35 and 9.0 cm/hr) as reported by Koch (2009).

Table 6.5 Runoff volumes and oocysts recovery from a small-scale Catlin soil bed.

Sampling Location	Surface Condition	Bed Slope %	Rainfall Intensity cm/hr	Total Runoff (mL)	Oocyst recovery (%)
Surface	Bare	2.5	6.5	1847.0	14.6
Surface	Vegetated	2.5	6.5	1633.0	7.1
Near-Surface	Bare	2.5	6.5	0.0	0.0
Near-Surface	Vegetated	2.5	6.5	9.5	0.0
Surface	Bare	3.0	9.0	2645.0	2.45
Surface	Vegetated	3.0	9.0	1950.0	1.47
Near-Surface	Bare	3.0	9.0	0.0	0.0
Near-Surface	Vegetated	3.0	9.0	43.0	0.0

Similarly, Table 6.6 and 6.7 summarize the runoff volume and pathogen recovery from a three types of soil bed with and without vegetation with 2.5% slope and 65 mm/hr rainfall intensity for three different cover conditions: bare, Brome grass and Fescue, in surface flow as reported by Davidson (2010).

Table 6.6 Runoff volumes and *C. parvum* recovery from a small-scale different soil beds.

Pathogen Type	Surface Condition	Soil type	Total Runoff (mL)	Pathogen recovery (%)
C. parvum	Bare	Catlin	4384.0	33.38
C. parvum	Vegetated (Brome)	Catlin	2387.0	14.91
C. parvum	Vegetated (Fescue)	Catlin	284.0	22.07
C. parvum	Bare	Darwin	3189.0	38.58
C. parvum	Vegetated (Brome)	Darwin	2711.0	8.81
C. parvum	Vegetated (Fescue)	Darwin	467.0	0.00
C. parvum	Bare	Alvin	3140.0	1.17
C. parvum	Vegetated (Brome)	Alvin	2139.0	1.10
C. parvum	Vegetated (Fescue)	Alvin	1301.0	0.06

Table 6.7 Runoff volumes and rotavirus recovery from a small-scale different soil beds.

Pathogen Type	Surface Condition	Soil type	Total Runoff (mL)	Pathogen recovery (%)
Rotavirus	Bare	Catlin	4384.0	34.92
Rotavirus	Vegetated (Brome)	Catlin	2387.0	9.87
Rotavirus	Vegetated (Fescue)	Catlin	2894.0	14.23
Rotavirus	Bare	Darwin	3189.0	26.56
Rotavirus	Vegetated (Brome)	Darwin	2711.0	16.91
Rotavirus	Vegetated (Fescue)	Darwin	467.0	0.08
Rotavirus	Bare	Alvin	3140.0	8.28
Rotavirus	Vegetated (Brome)	Alvin	2139.0	0.67
Rotavirus	Vegetated (Fescue)	Alvin	1301.0	1.83

6.3 Modeling result

The simulations were carried out a system identical to the large-scale experimental setup described by Trask (2002). For WEPP model simulation, many input parameters were obtained from the experimental setup such as soil plot length of 3.6 m, rainfall intensity of 2.54 and 6.35 mm/hr applied for 40 minutes and two different soil types (Catlin and Newberry). Similarly, the simulations were carried out two smaller systems identical to the experimental setup described Davidson (2010) and by Koch (2009). The model results are compared with experimental data.

6.3.1 Comparison of simulated runoff with the observations from large scale experiment

For bare ground simulations, initial saturation level (antecedent moisture content) for the soil and hydraulic conductivity were used as the calibration parameters. The parameter was calibrated in such a way that Nash-Sutcliffe efficiency index (EI) and coefficient of determination (R^2) between observed and simulated runoff rate were maximized. The Nash–Sutcliffe efficiency

index (EI) has been widely used to assess the predictive power of hydrological models and is defined as:

$$E = 1 - \frac{\sum_{t=1}^{T} (Q_o^t - Q_m^t)^2}{\sum_{t=1}^{T} \left(Q_o^t - \overline{Q_o}\right)^2} \quad (12)$$

where Q_o is observed discharge, Q_m^t is modeled discharge, Q_o^t is observed discharge at time *t*, and $\overline{Q_o}$ is average of observed discharge (Nash and Sutcliffe, 1970). The values for EI can range from $-\infty$ to 1. An EI value of 1 corresponds to a perfect match of modeled discharge to the observed data, whereas an EI value of 0 indicates that the model predictions are as accurate as the mean of the observed data. EI value of less than zero indicates that the observed mean is a better predictor than the model. In other words, when the residual variance (described by the nominator in the expression above) is larger than the data variance (described by the denominator), EI value will be less than zero. Since simulated discharge hydrograph had more points compared to observation, the simulated discharge value corresponding to observation at that particular time stamp was used to compute EI and R^2. In the absence of sediment data, WEPP model was calibrated using runoff only.

Comparison of simulated WEPP model result with observations is presented in Figures 6.1-6.20 below. Although total runoff volume and oocyst recovery data was available, runoff hydrograph and oocysts break-through curve data was not available for low intensity rainfall experiments (2.54 cm/hr) with Catlin soil bed. So, WEPP simulations were carried out for Catlin soil beds with three different slope conditions subjected to high intensity of simulated rainfall (6.35 cm/hr). Figures 6.1, 6.2 and 6.3 show the comparison of the observation with WEPP simulation result for surface runoff for bare ground condition, 6.35 cm/hr rainfall applied for 40

minutes at 1.5, 3 and 4.5% slope conditions, respectively for Catlin soil. In all three cases, WEPP model results were in good agreement with the observations as shown below which is also demonstrated by statistical analysis. Computed R^2 values for 1.5, 3.0 and 4.5% slope conditions were 0.81, 0.64 and 0.83, respectively. Similarly, computed EI value between observed and simulated flow were for 1.5, 3.0 and 4.5% slope condition were 0.26, 0.42 and 0.66, respectively.

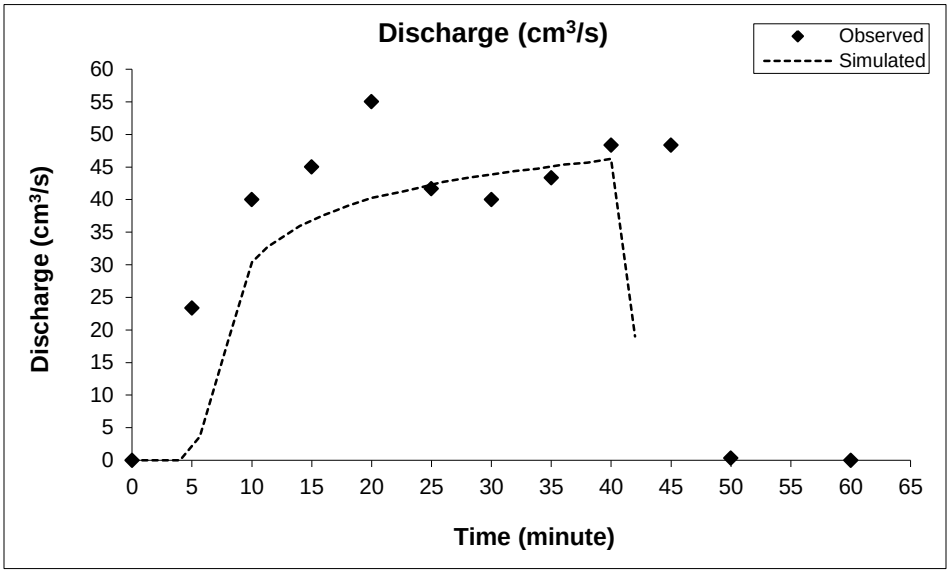

Figure 6.1 WEPP simulation result for surface runoff for bare ground condition, 6.35 cm/hr rainfall applied for 40 minutes at 1.5% slope conditions for Catlin soil.

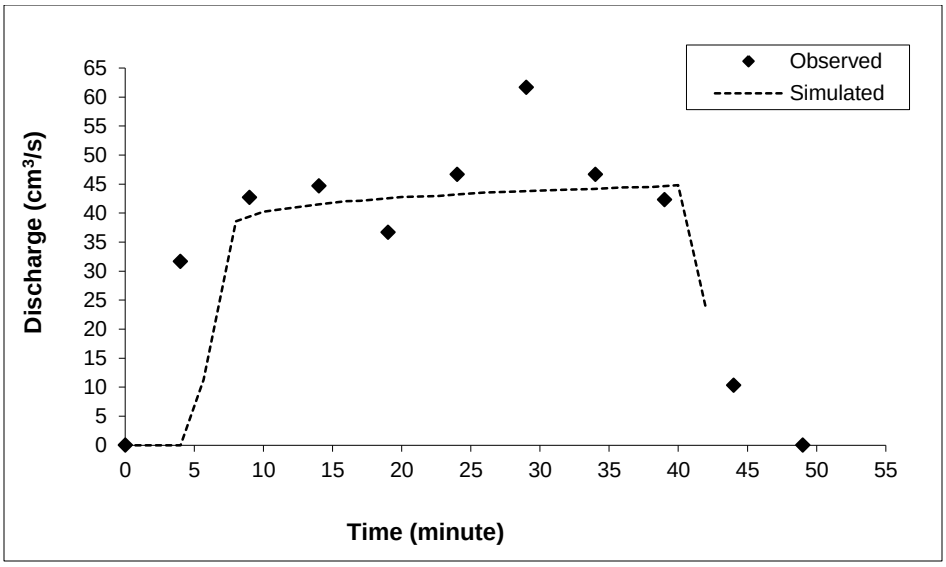

Figure 6.2 WEPP simulation result for surface runoff for bare ground condition, 6.35 cm/hr rainfall applied for 40 minutes at 3.0% slope conditions for Catlin soil.

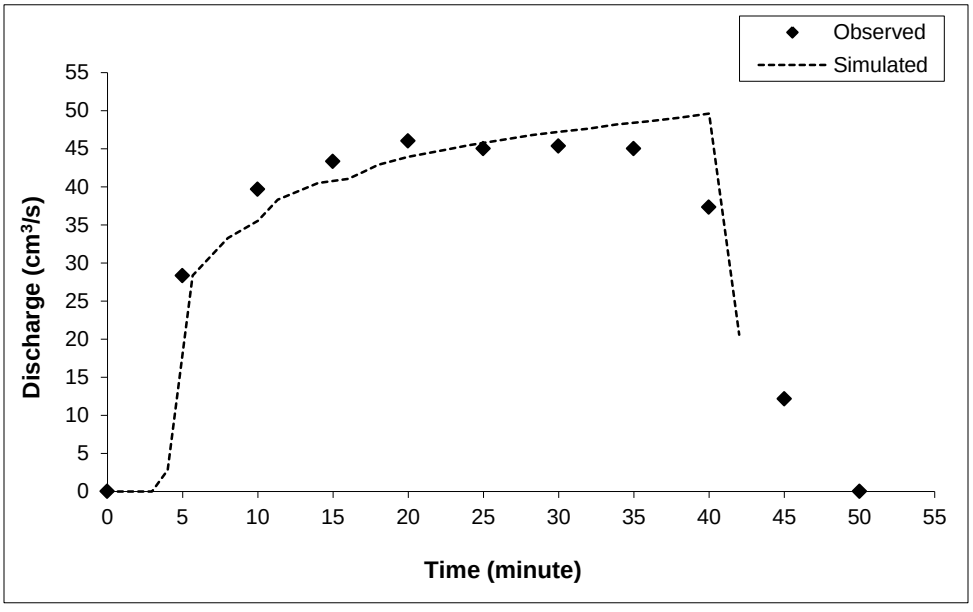

Figure 6.3 WEPP simulation result for surface runoff for bare ground condition, 6.35 cm/hr rainfall applied for 40 minutes at 4.5% slope conditions for Catlin soil.

Figures 6.4, 6.5 and 6.6 show the comparison of the observation with WEPP simulation result for surface runoff for bare ground condition, 2.54 cm/hr rainfall applied for 40 minutes at

1.5, 3 and 4.5% slope conditions, respectively for Newberry soil. As in case of Catlin soil, initial saturation level (antecedent moisture content) and hydraulic conductivity were the calibration parameters for WEPP simulation for Newberry soil bare ground condition. It was noted that antecedent moisture content affected when runoff started while hydraulic conductivity governed the peak runoff rate and total runoff volume. In all three cases, WEPP model results were in good agreement with the observations as shown below which is also substantiated by statistical analysis of observed and simulated runoff. Computed R^2 values for 1.5, 3.0 and 4.5% slope conditions were 0.63, 0.84 and 0.46, respectively. Similarly, computed EI values for 1.5, 3.0 and 4.5% slope condition were 0.25, 0.28 and -1.35, respectively. Negative value of EI indicates that the residual variance is larger than the data variance.

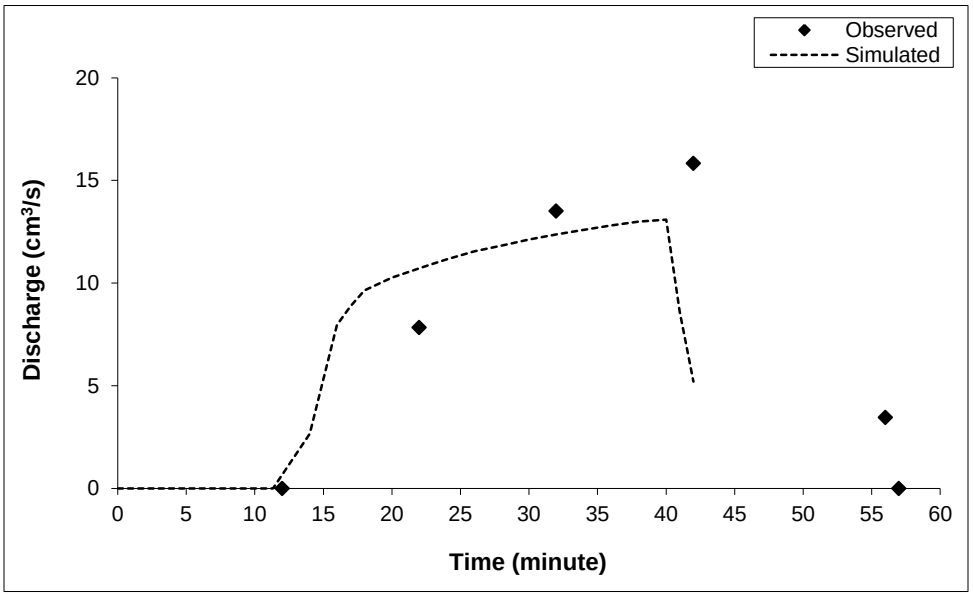

Figure 6.4 WEPP simulation results for surface runoff for bare ground condition, 2.54 cm/hr rainfall applied for 40 minutes at 1.5% slope conditions for Newberry soil.

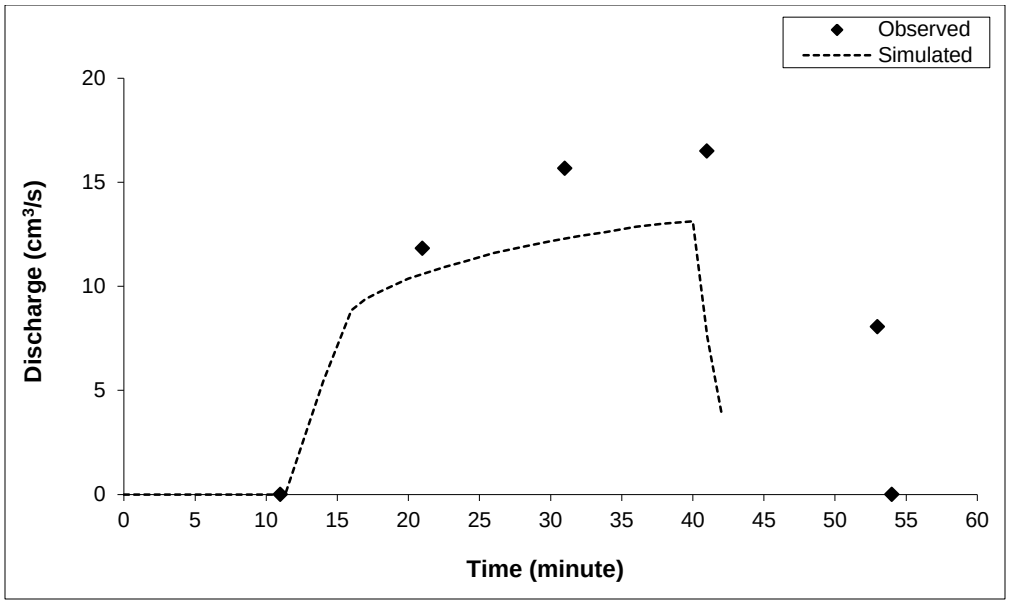

Figure 6.5 WEPP simulation result for surface runoff for bare ground condition, 2.54 cm/hr rainfall applied for 40 minutes at 3.0% slope conditions for Newberry soil.

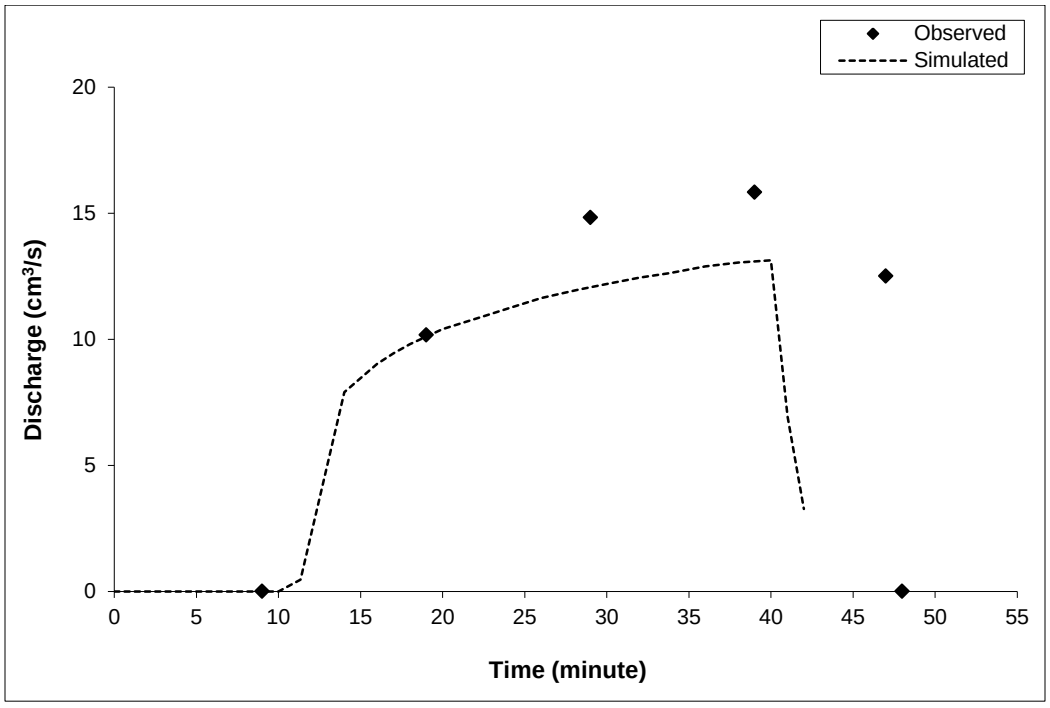

Figure 6.6 WEPP simulation result for surface runoff for bare ground condition, 2.54 cm/hr rainfall applied for 40 minutes at 4.5% slope conditions for Newberry soil.

Figures 6.7, 6.8 and 6.9 show the comparison of the observed hydrograph with WEPP simulation result for bare ground condition, 6.35 cm/hr rainfall applied for 40 minutes at 1.5, 3 and 4.5% slope conditions, respectively for Newberry soil. For all slope conditions, WEPP model results were in good agreement with the observations as shown below which is also substantiated by statistical analysis of observed and simulated runoff. Computed R^2 values for 1.5, 3.0 and 4.5% slope conditions were 0.89, 0.86 and 0.94, respectively. Similarly, computed EI value between observed and simulated flow were for 1.5, 3.0 and 4.5% slope condition were 0.85, 0.82 and 0.79, respectively.

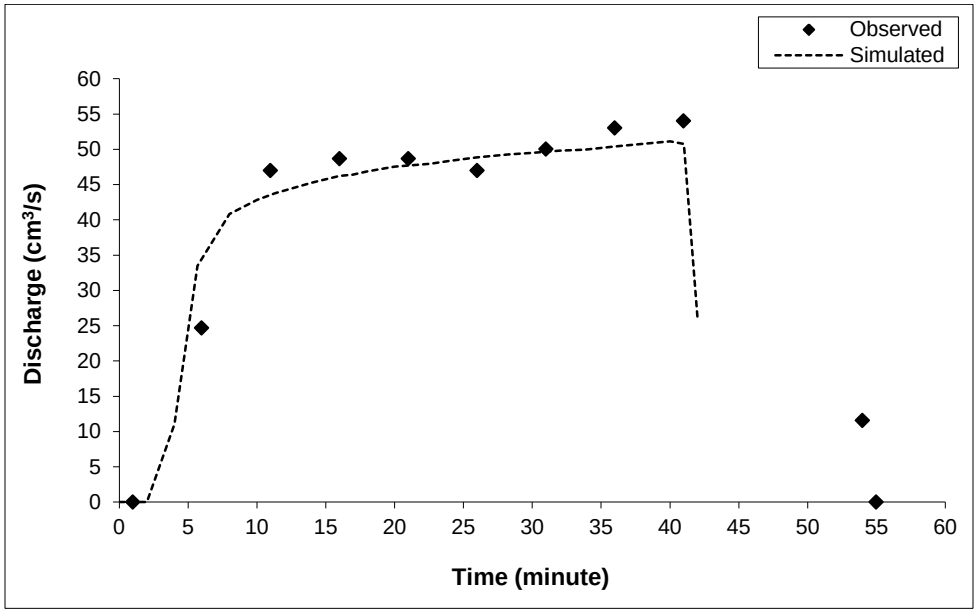

Figure 6.7 WEPP simulation results for surface runoff for bare ground condition, 6.35 cm/hr rainfall applied for 40 minutes at 1.5% slope conditions for Newberry soil.

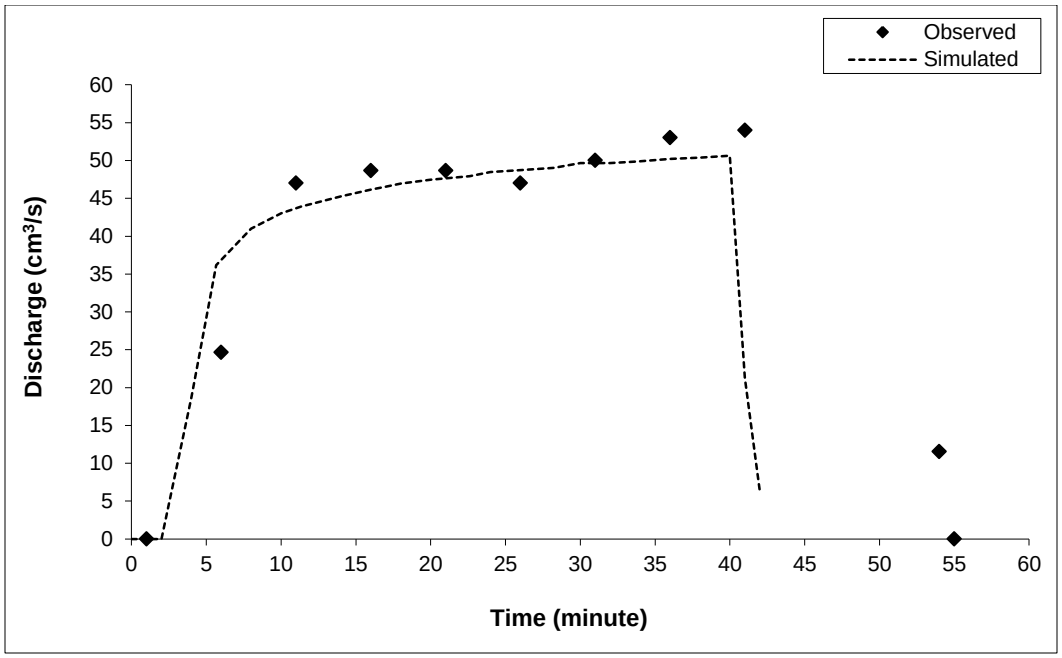

Figure 6.8 WEPP simulation results for surface runoff for bare ground condition, 6.35 cm/hr rainfall applied for 40 minutes at 3.0% slope conditions for Newberry soil.

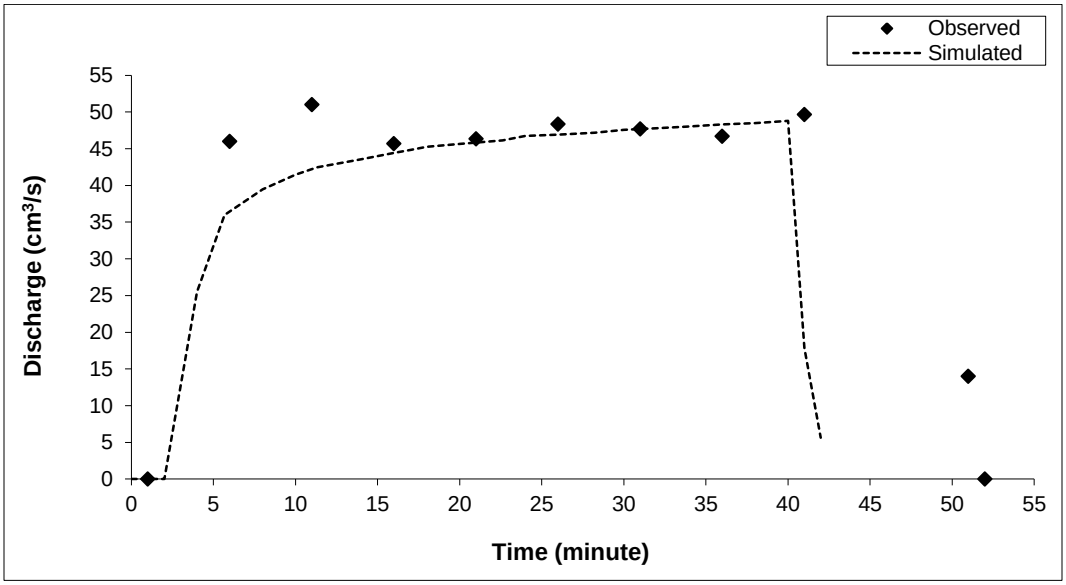

Figure 6.9 WEPP simulation results for surface runoff for bare ground condition, 6.35 cm/hr rainfall applied for 40 minutes at 4.5% slope conditions for Newberry soil.

In case of vegetated condition, soil parameters (initial saturation level and hydraulic conductivity) along with vegetation parameters (canopy, interrill and rill cover, roughness after tillage) were WEPP model calibration parameters. Comparison of observed hydrograph with WEPP simulated result for vegetated condition, 6.35 cm/hr rainfall applied for 40 minutes at 1.5, 3.0 and 4.5% slope conditions for Catlin soil are presented in Figures 6.10 - 6.12. Since the moisture holding capacity of bare ground and vegetated surface is different, the soil parameters were calibrated separately for those two conditions. As the moisture condition in the laboratory varied for each set of run, separate parameters were calibrated for different rainfall intensities and slope conditions. WEPP model could replicate observed runoff pattern fairy well for all three slope conditions results as demonstrated statistical analysis. Computed R^2 values for 1.5, 3.0 and 4.5% slope conditions were 0.60, 0.71 and 0.57, respectively. Similarly, computed EI value between observed and simulated flow were for 1.5, 3.0 and 4.5% slope condition were 0.51, 0.67 and -0.05, respectively. Negative value of EI for 4.5% slope condition indicates that the residual variance is larger than the (observed) data variance.

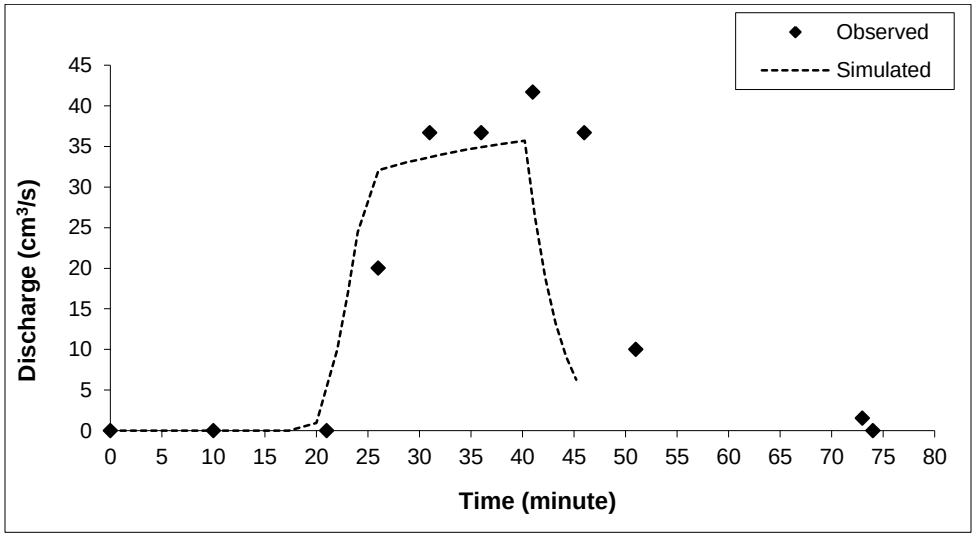

Figure 6.10 WEPP simulation results for surface runoff for vegetated condition, 6.35 cm/hr rainfall applied for 40 minutes at 1.5% slope conditions for Catlin soil.

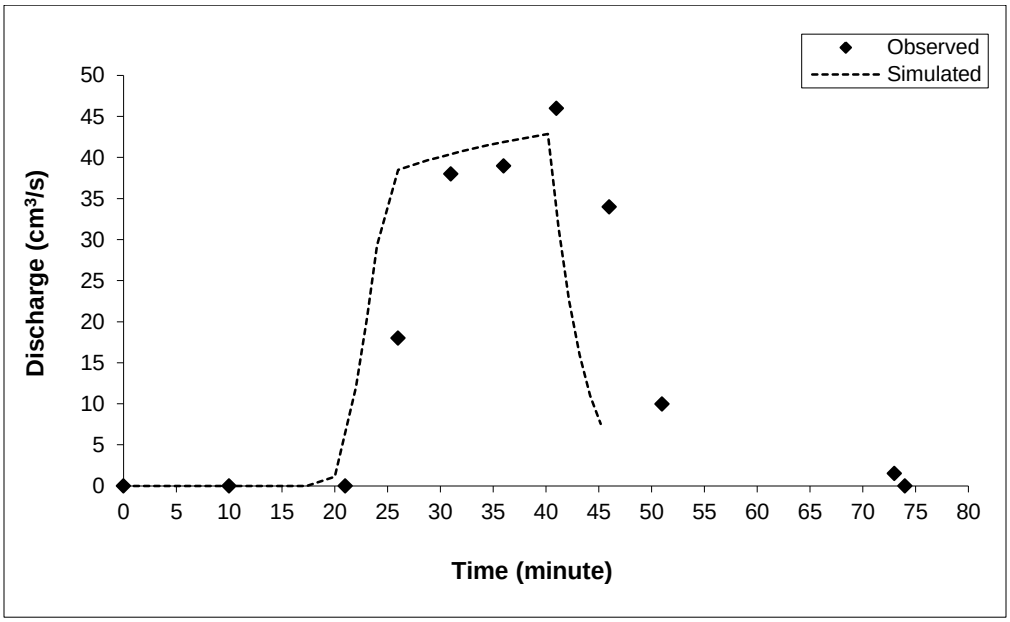

Figure 6.11 WEPP simulation results for surface runoff for vegetated condition, 6.35 cm/hr rainfall applied for 40 minutes at 3.0% slope conditions for Catlin soil.

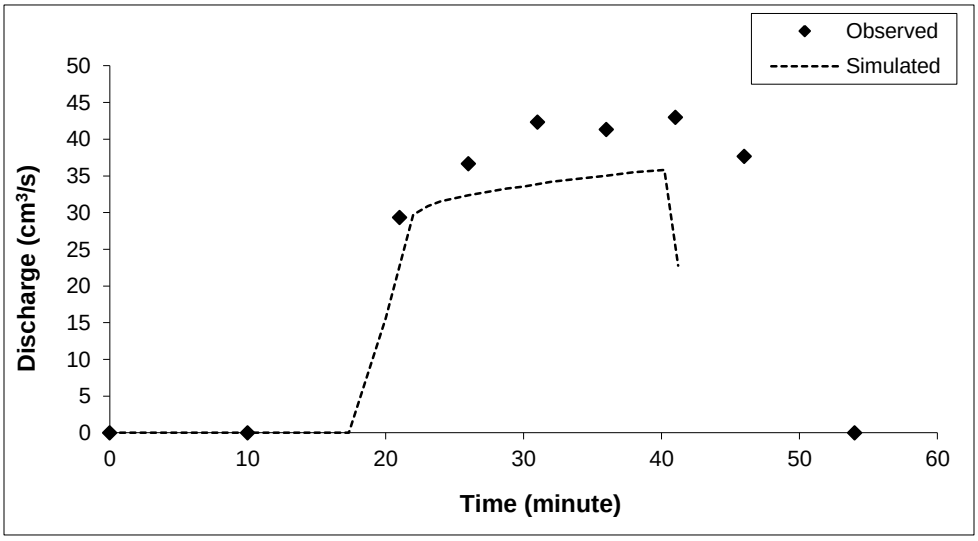

Figure 6.12 WEPP simulation results for surface runoff for vegetated condition, 6.35 cm/hr rainfall applied for 40 minutes at 4.5% slope conditions for Catlin soil.

For Newberry soil with vegetated surface, both soil parameters (initial saturation level and hydraulic conductivity) along with the vegetation parameters (canopy, interrill and rill cover,

roughness after tillage) were used as calibration parameters for WEPP model to simulate surface runoff. Comparisons of observed hydrograph with WEPP simulation results for vegetated condition, 2.54 cm/hr rainfall applied for 40 minutes at 1.5, 3 and 4.5% slope conditions respectively for Newberry soil are presented in Figures 6.13, 6.14 and 6.15. Compared to earlier simulation results, WEPP model could not replicate observed hydrograph fairy well in these three conditions. Computed R^2 values (for observed and simulated runoff values) for 1.5, 3.0 and 4.5% slope conditions were 0.39, 0.79 and 0.58, respectively. Similarly, computed EI value between observed and simulated flow were for 1.5, 3.0 and 4.5% slope condition were -0.03, 0.20 and -0.11, respectively.

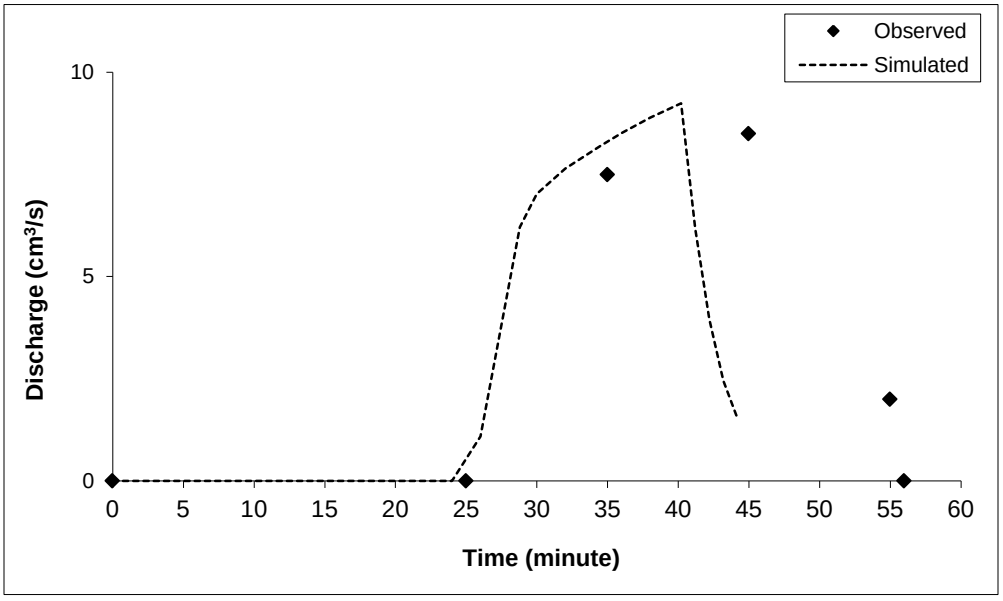

Figure 6.13 WEPP simulation results for surface runoff for vegetated condition, 2.54 cm/hr rainfall applied for 40 minutes at 1.5% slope conditions for Newberry soil.

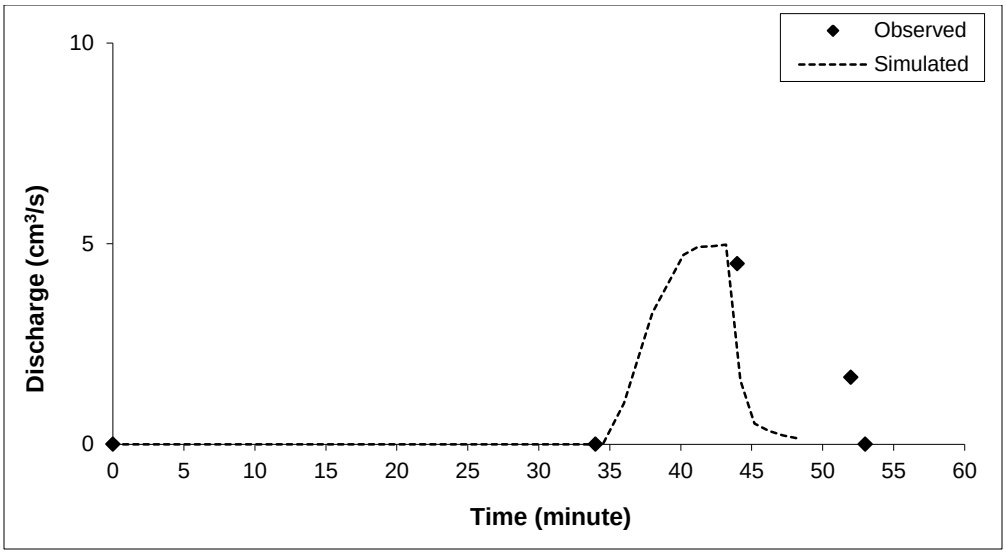

Figure 6.14 WEPP simulation results for surface runoff for vegetated condition, 2.54 cm/hr rainfall applied for 40 minutes at 3.0% slope conditions for Newberry soil.

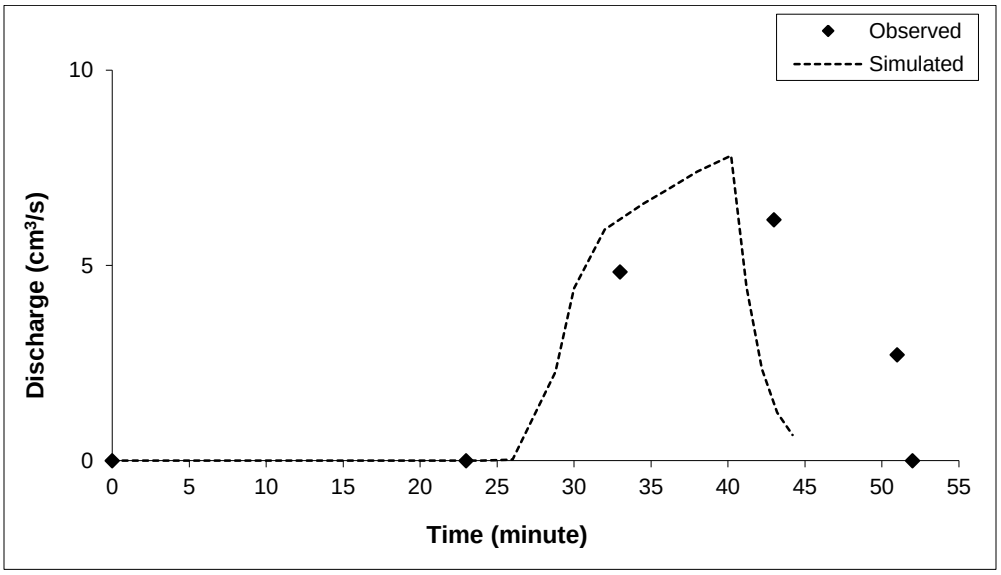

Figure 6.15 WEPP simulation results for surface runoff for vegetated condition, 2.54 cm/hr rainfall applied for 40 minutes at 4.5% slope conditions for Newberry soil.

Comparisons of observed hydrograph with WEPP simulation results for vegetated condition, 6.35 cm/hr rainfall applied for 40 minutes at 1.5, 3 and 4.5% slope conditions respectively for Newberry soil are presented in Figures 6.16 - 6.18. In case of 1.5% slope

condition, multiple peaks were detected in observed hydrograph. Those multiple peaks could not be replicated by WEPP simulation result which is evident by low R^2 (0.18) and negative EI value (-0.23). In case of 3.0 and 4.5% bed slope conditions, WEPP model could replicate the pattern of observed hydrograph as demonstrated by statistical analysis. Computed R^2 values (for observed and simulated runoff values) for 3.0 and 4.5% slope conditions were 0.74 and 0.75, respectively. Similarly, computed EI values for 3.0 and 4.5% slope conditions were 0.66 and 0.74, respectively.

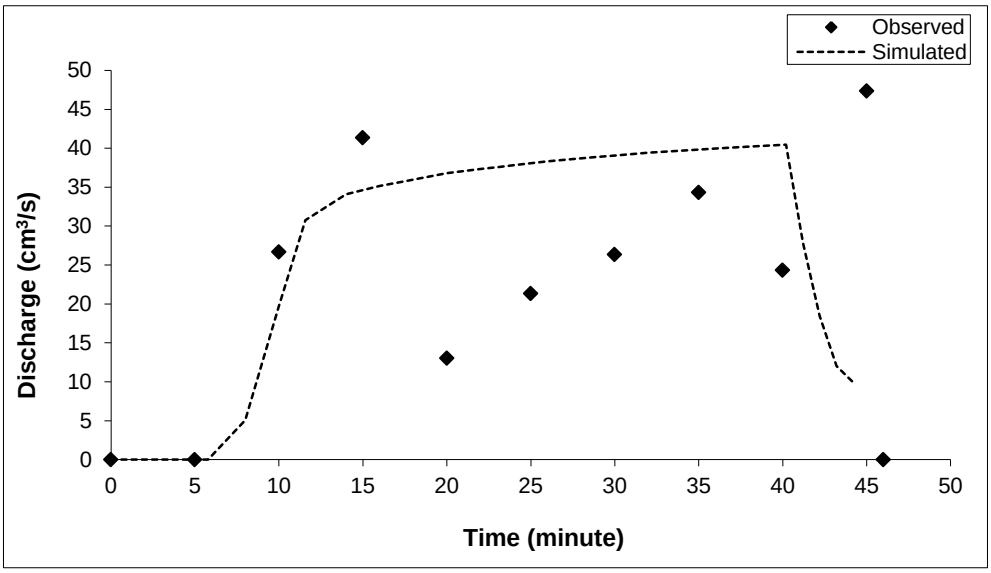

Figure 6.16 WEPP simulation results for surface runoff for vegetated condition, 6.35 cm/hr rainfall applied for 40 minutes at 1.5% slope conditions for Newberry soil.

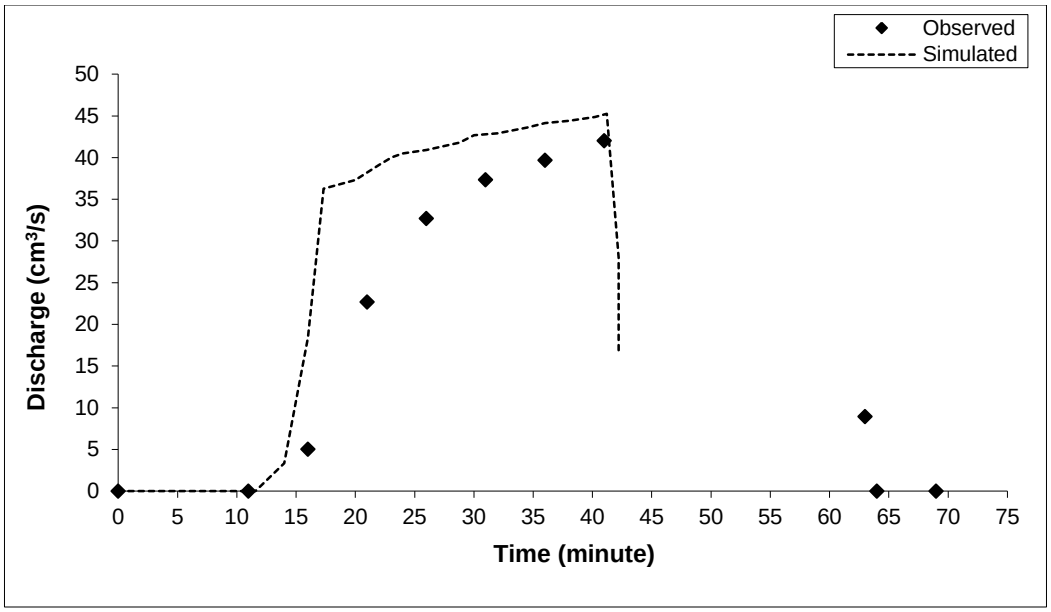

Figure 6.17 WEPP simulation results for surface runoff for vegetated condition, 6.35 cm/hr rainfall applied for 40 minutes at 3.0% slope conditions for Newberry soil.

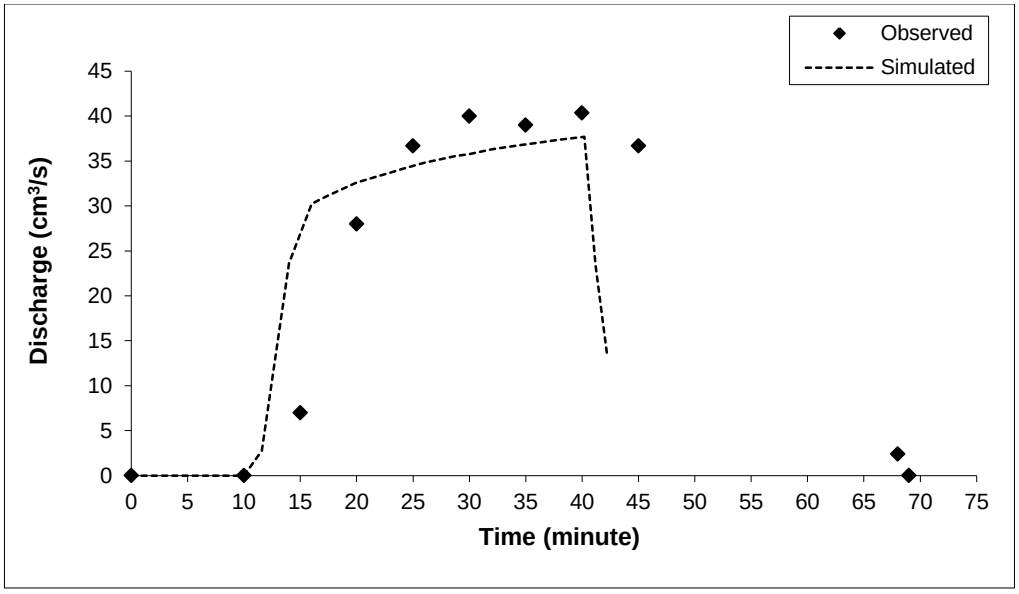

Figure 6.18 WEPP simulation results for surface runoff for vegetated condition, 6.35 cm/hr rainfall applied for 40 minutes at 4.5% slope conditions for Newberry soil.

Figures 6.19 and 6.20 show the comparison of simulated results from WEPP for total runoff volume with observation for all surface cover, slope and rainfall conditions. In case of Catlin soil, the results obtained from WEPP simulation for total runoff volume result were similar to those from laboratory experiment as shown in Figure 6.19. Similarly, observed and simulated total runoff volume in different rainfall, slope and cover condition for Newberry soil also showed a good agreement as presented in Figure 6.20. These results indicate that WEPP model can predict surface runoff rate and total volume fairly well in case of small scale laboratory experiments.

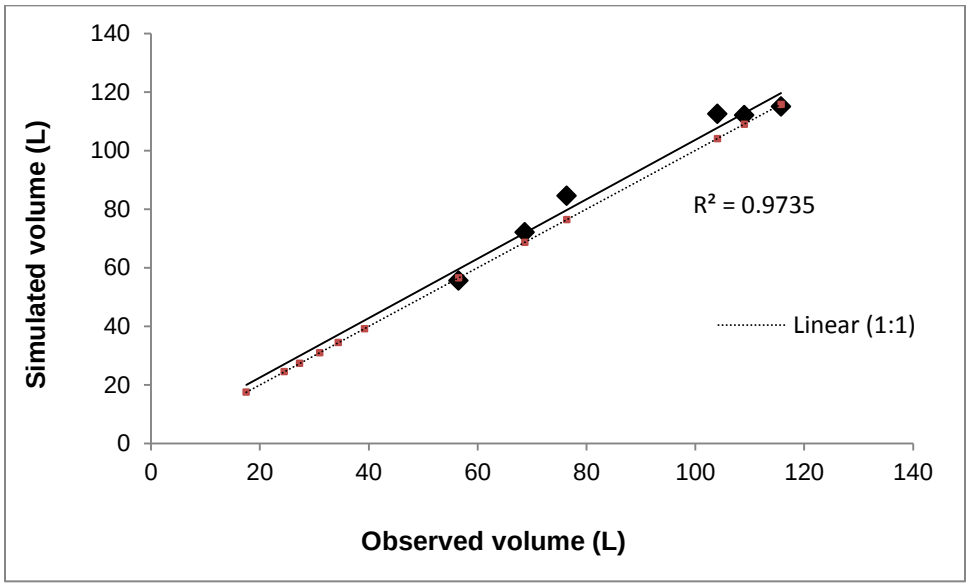

Figure 6.19 Comparison of WEPP simulation results with observations for surface runoff volume for different slopes, rainfall and surface cover conditions for Catlin soil.

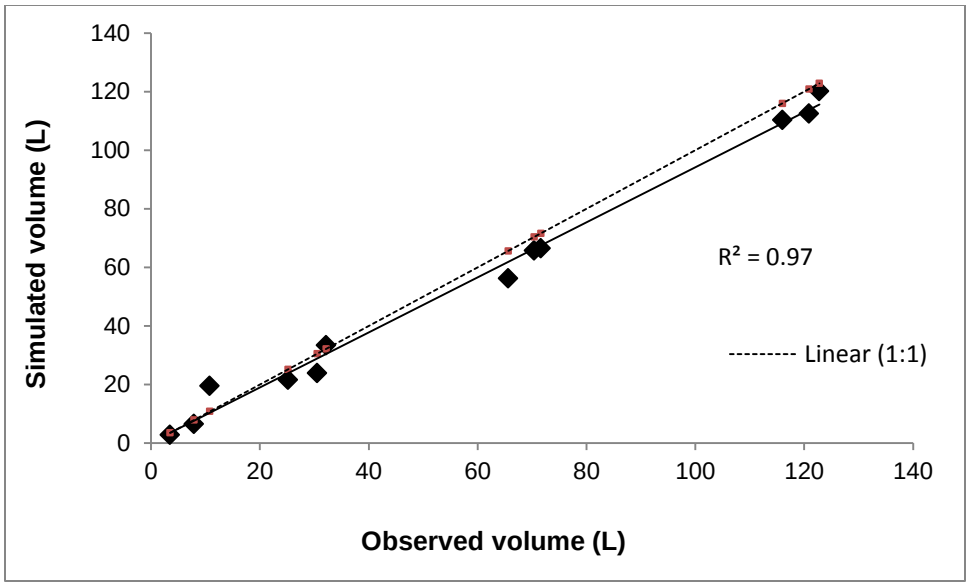

Figure 6.20 Comparison of WEPP simulation results with observations for surface runoff volume for different slopes, rainfall and surface cover conditions for Newberry soil.

6.3.2 Comparison of simulated runoff with the observations from small scale experiments

WEPP simulations were carried out for Alvin, Catlin and Darwin soil beds with 2.5% slope with three different cover conditions: bare, Brome and Fescue grasses replicating the experimental conditions of Davidson (2010). The soil beds were subjected a simulated rainfall intensity of 6.35 cm/hr applied for 20 minutes. These soil beds were 0.61 m (2 ft) long, 0.305 m (1 ft) wide and 0.015 m (0.5 ft) thick. Figures 6.21, 6.22 and 6.23 show the comparison of the observation with WEPP simulation result for surface runoff for bare ground and two vegetated conditions for Alvin soil. In all three cases, WEPP model produced reasonable results as compared with the observations as shown below, which is also demonstrated by statistical analysis. Computed R^2 values for bare, Brome and Fescue cover conditions were 0.62, 0.37 and 0.48, respectively. Similarly, computed EI value between observed and simulated flow for bare, Brome and Fescue cover conditions were 0.56, -0.63 and -0.12, respectively.

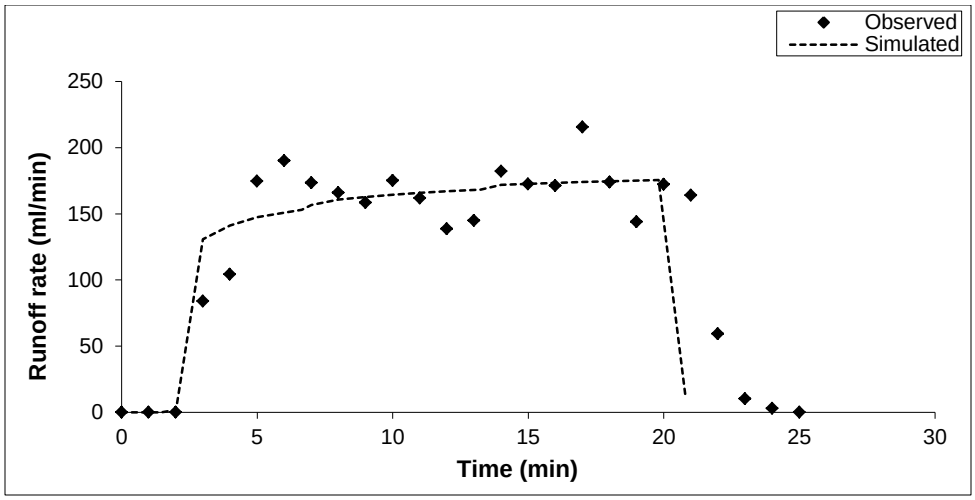

Figure 6.21 WEPP simulation results for surface runoff for bare Alvin soil bed subjected to 6.35 cm/hr rainfall applied for 20 minutes at 2.5% slope.

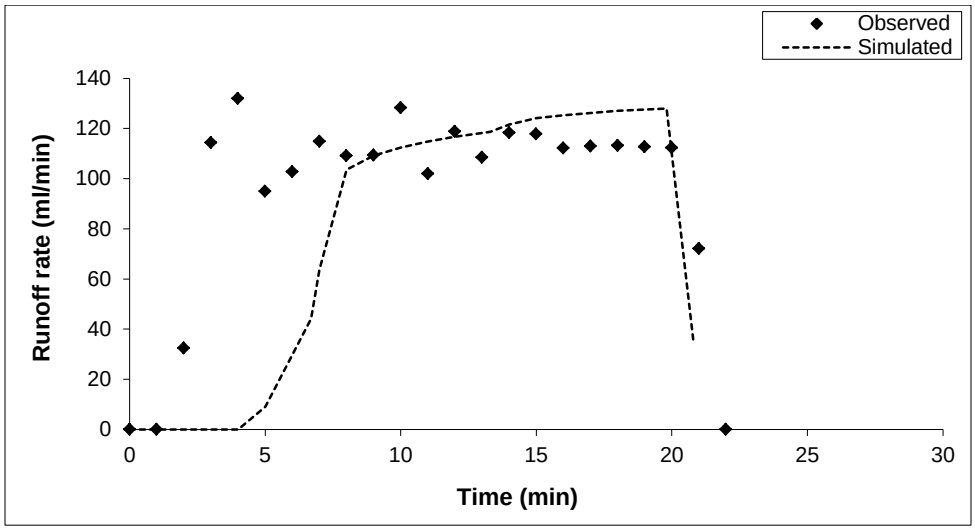

Figure 6.22 WEPP simulation results for surface runoff for Alvin soil bed with Brome grass cover subjected to 6.35 cm/hr rainfall applied for 20 minutes at 2.5% slope.

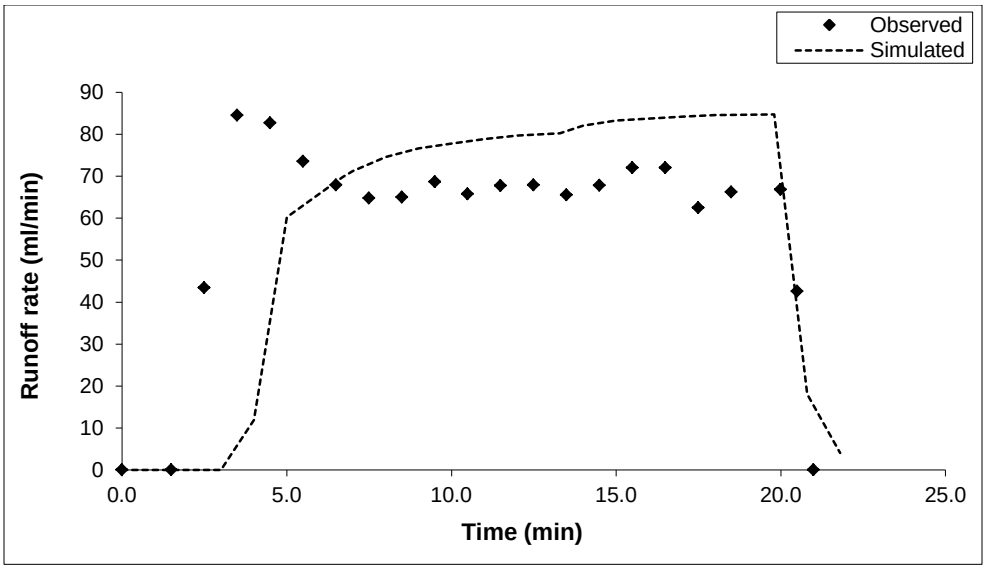

Figure 6.23 WEPP simulation results for surface runoff for Alvin soil bed with Fescue cover subjected to 6.35 cm/hr rainfall applied for 20 minutes at 2.5% slope.

Figures 6.24, 6.25 and 6.26 show the comparison of the experimental data with WEPP simulation result for surface runoff for bare ground and two vegetated conditions for Catlin soil. WEPP model results were in a good agreement with the experimental data as shown below which is also demonstrated by statistical analysis. Computed R^2 values for bare, Brome and Fescue cover conditions were 0.65, 0.41 and 0.81, respectively. Similarly, computed EI value between observed and simulated flow for bare, Brome and Fescue cover conditions were 0.93, 0.86 and 0.65, respectively.

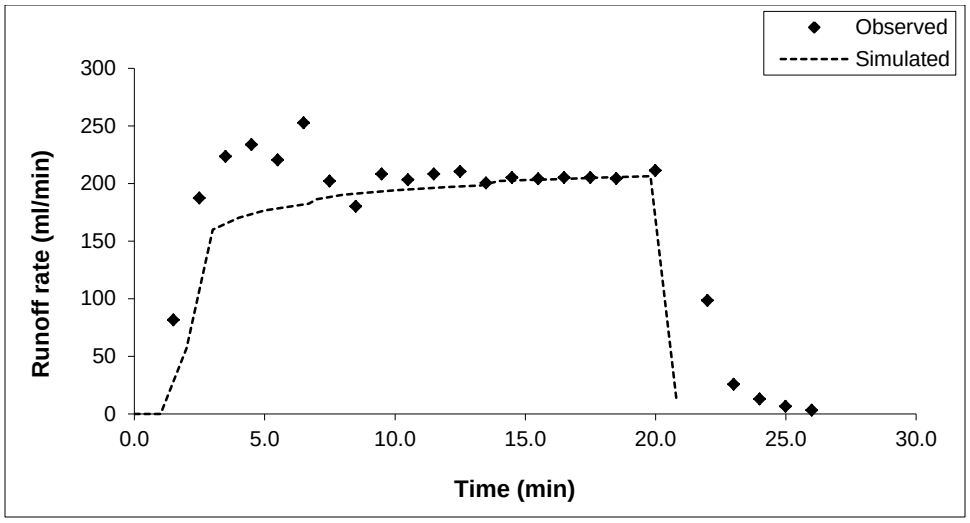

Figure 6.24 WEPP simulation results for surface runoff for bare Catlin soil bed subjected to 6.35 cm/hr rainfall applied for 20 minutes at 2.5% slope.

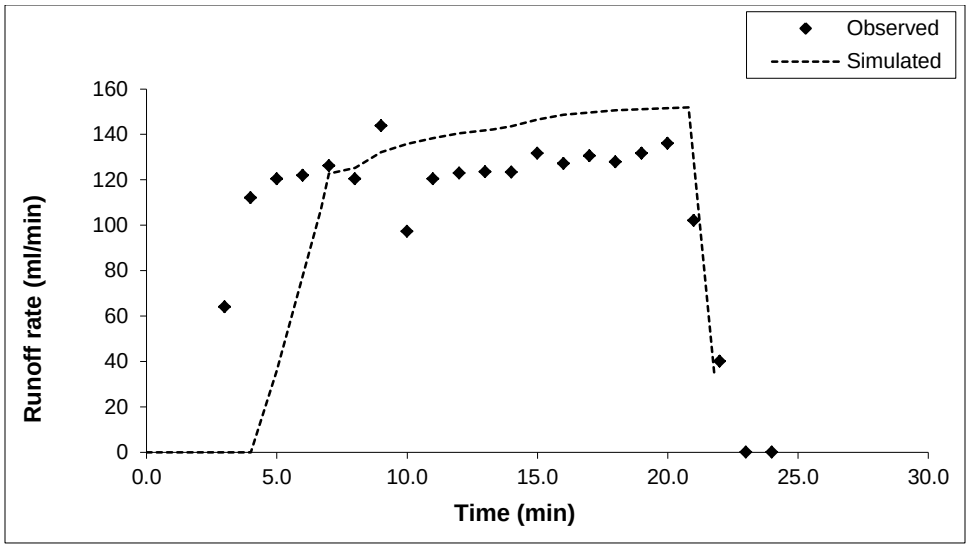

Figure 6.25 WEPP simulation results for surface runoff for Catlin soil bed with Brome grass vegetation subjected to 6.35 cm/hr rainfall applied for 20 minutes at 2.5% slope.

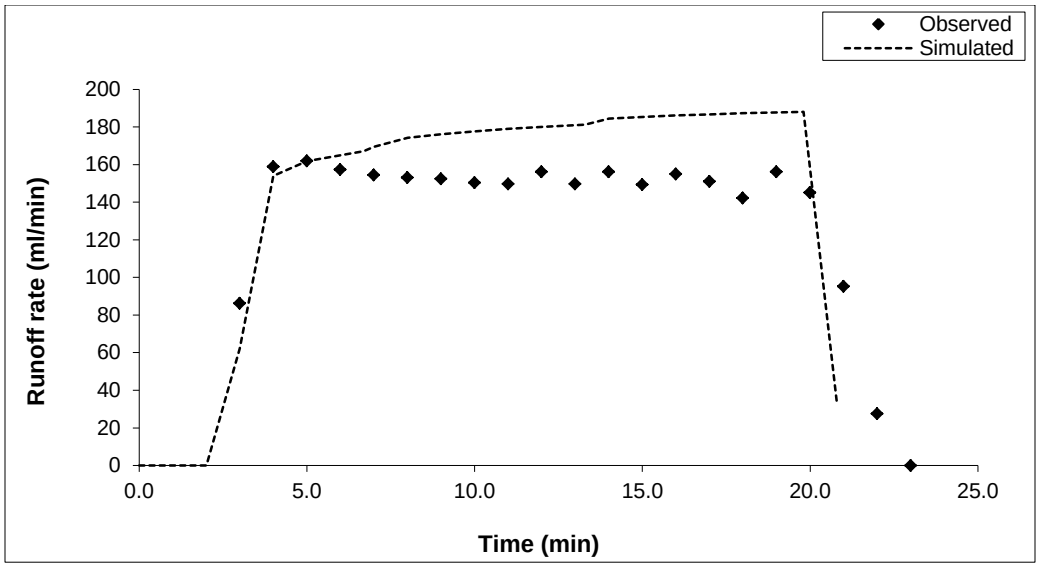

Figure 6.26 WEPP simulation results for surface runoff for Catlin soil bed with Fescue vegetation subjected to 6.35 cm/hr rainfall applied for 20 minutes at 2.5% slope.

The comparison of the experimental data with WEPP simulation result for surface runoff for bare ground and two vegetated conditions for Darwin soil is presented in Figures 6.27, 6.28 and 6.29 below. WEPP model results showed a good agreement with the experimental data which is also demonstrated by statistical analysis. Computed R^2 values for bare, Brome and Fescue cover conditions were 0.78, 0.83 and 0.72, respectively. Similarly, computed EI value between observed and simulated flow for bare, Brome and Fescue cover conditions were 0.64, 0.71 and -4.27, respectively. Observed surface runoff rate for Darwin soil bed with Fescue vegetation was much less compared to runoff data for Brome grass cover condition for the similar condition. The difference in factors like root zone depth, surface cover and leaf area index between Brome grass and Fescue may be attributed to the decrease in surface runoff rate. This might have resulted the over estimation of WEPP simulation result compared to experimental data for this particular condition as observed in Figure 6.29.

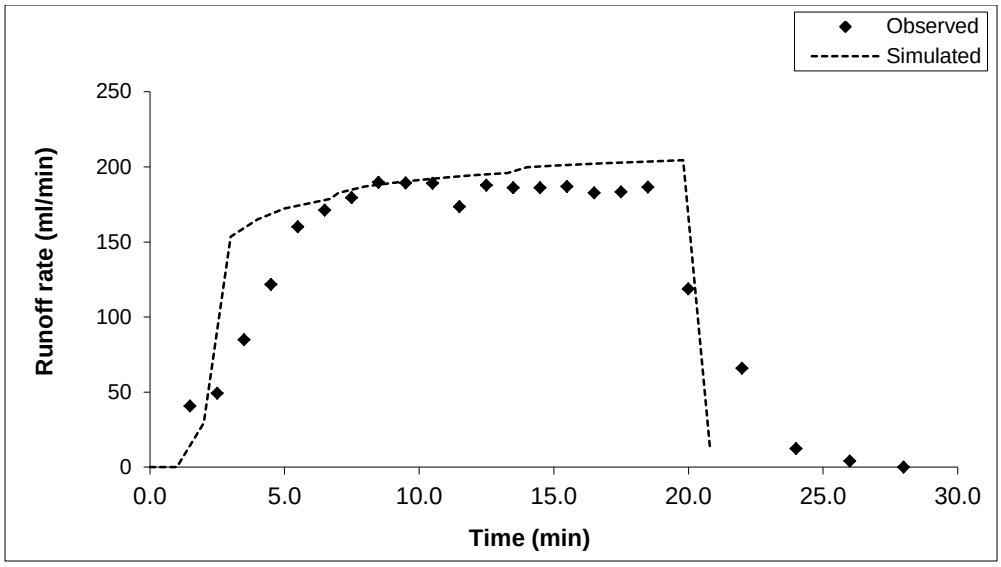

Figure 6.27 WEPP simulation results for surface runoff for bare Darwin soil bed subjected to 6.35 cm/hr rainfall applied for 20 minutes at 2.5% slope.

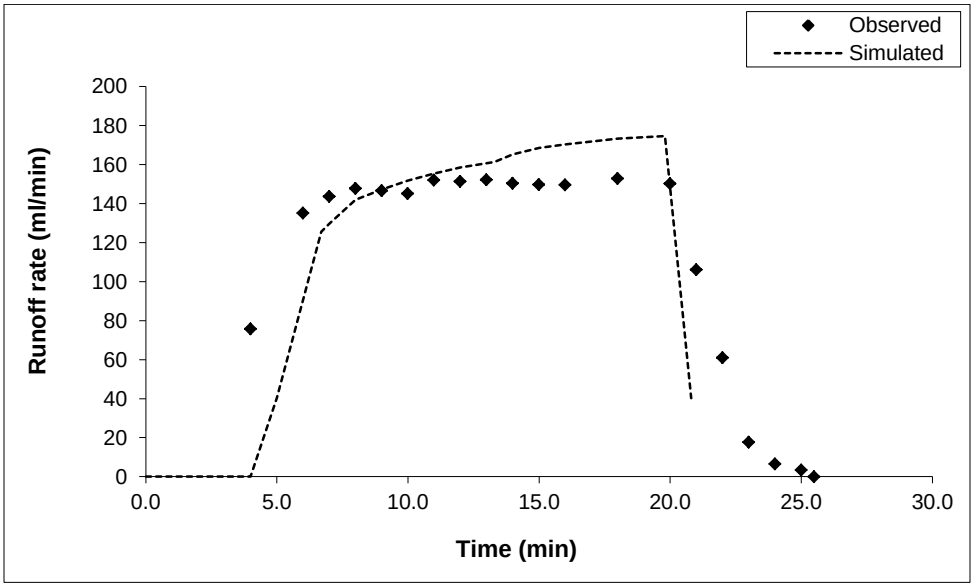

Figure 6.28 WEPP simulation results for surface runoff for Darwin soil bed with Brome grass vegetation subjected to 6.35 cm/hr rainfall applied for 20 minutes at 2.5% slope.

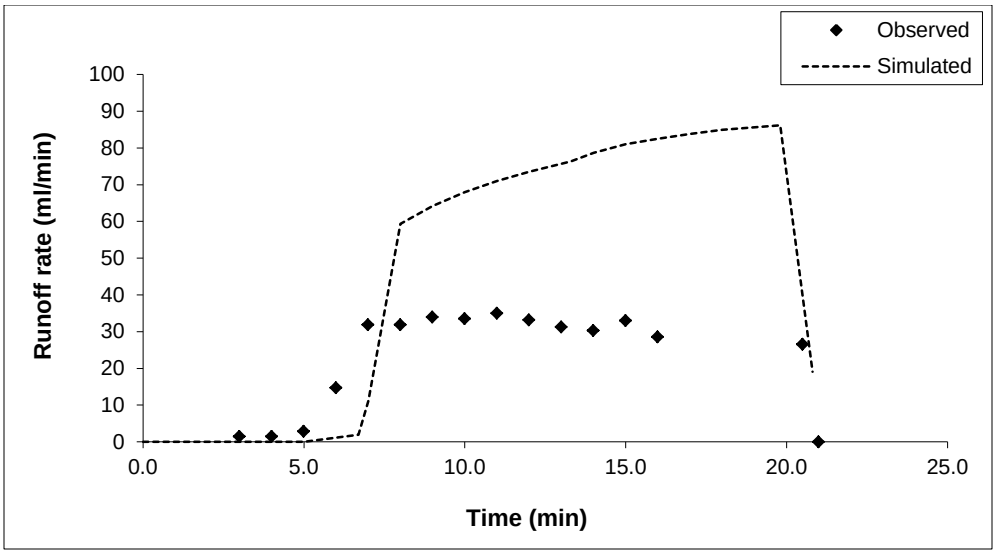

Figure 6.29 WEPP simulation results for surface runoff for Darwin soil bed with Fescue vegetation subjected to 6.35 cm/hr rainfall applied for 20 minutes at 2.5% slope.

Koch (2009) carried out laboratory experiments using small scale bare and vegetated Catlin soil beds with 2.5% slope subjected to 6.35 cm/hr (2.5 in/hr) rainfall applied for 10 minutes. Similarly, he also carried out another set of experiments using small scale bare and vegetated Catlin soil beds with 3.0% slope subjected to 8.9 cm/hr (3.5 cm/hr) rainfall applied for 10 minutes. WEPP simulations were carried out to replicate these four conditions. Figures 6.30 and 6.31 show the comparison of the observation with WEPP simulation result for surface runoff for bare ground and vegetated conditions. In both cases, WEPP model produced reasonable results as compared with the observations as shown below which is also demonstrated by statistical analysis. Computed R^2 values for bare, Brome grass cover conditions were 0.75 and 0.82, respectively. Similarly, computed EI value between observed and simulated flow for bare and Brome grass cover conditions were 0.42 and 0.66, respectively.

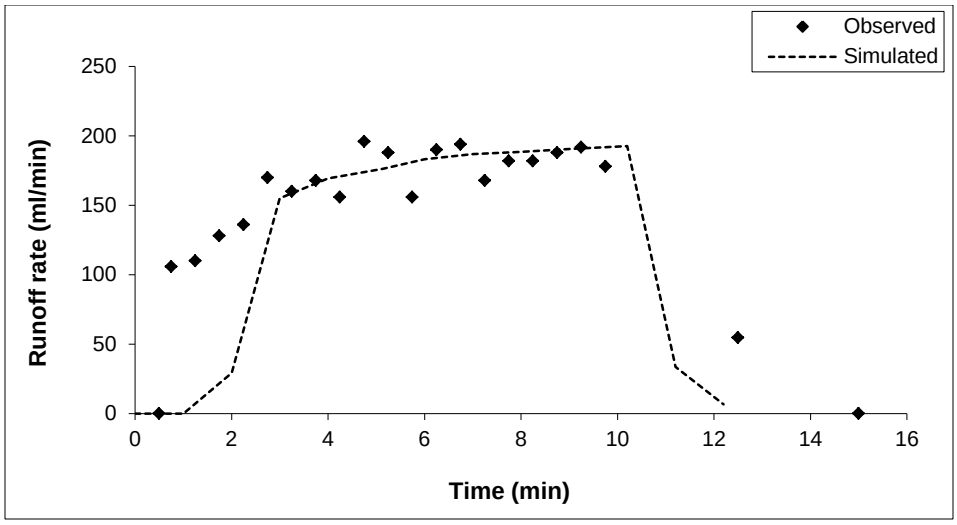

Figure 6.30 WEPP simulation results for surface runoff for bare Catlin soil bed with 2.5% slope subjected to 6.35 cm/hr rainfall applied for 10 minutes.

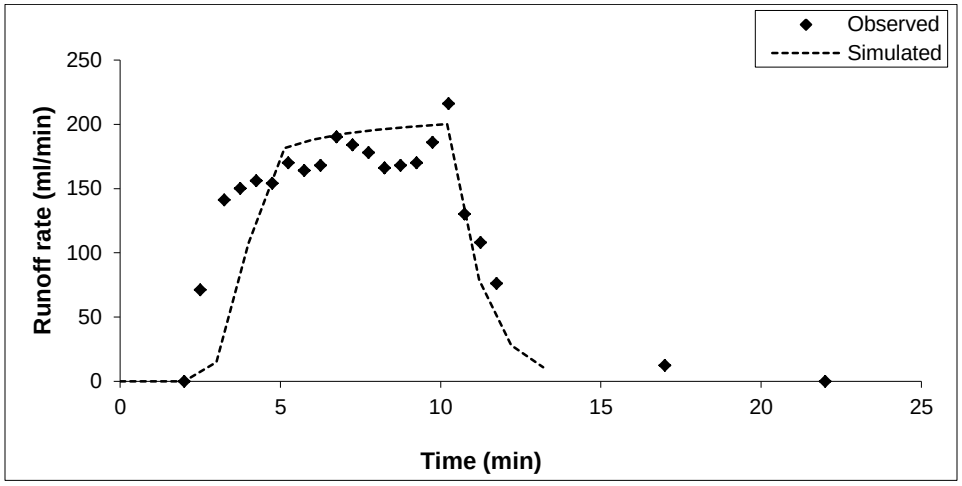

Figure 6.31WEPP simulation results for surface runoff for Catlin soil bed with at 2.5% slope and Brome grass vegetation subjected to 6.35 cm/hr rainfall applied for 10 minutes.

Figures 6.32 and 6.33 show the comparison of the observation with WEPP simulation result for surface runoff for bare ground and vegetated conditions for 3.0% Catlin soil beds. In both cases, WEPP model produced reasonable results as compared with the observations as shown below which is also demonstrated by statistical analysis. Computed R^2 values for bare, Brome grass cover conditions were 0.66 and 0.74, respectively. Similarly, computed EI value

between observed and simulated flow for bare and Brome grass cover conditions were 0.34 and 0.41, respectively.

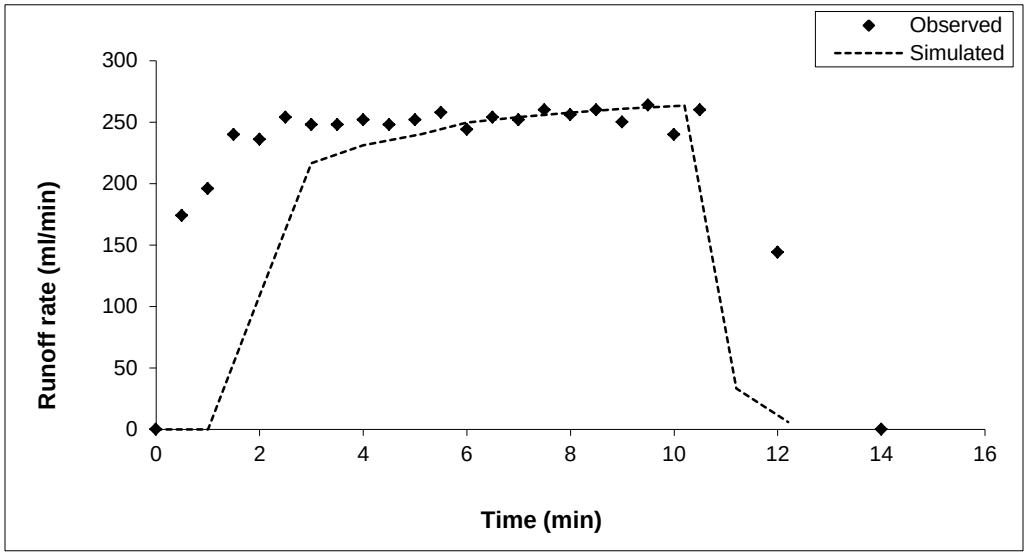

Figure 6.32 WEPP simulation results for surface runoff for bare Catlin soil bed with 3.0% slope subjected to 9.0 cm/hr rainfall applied for 10 minutes.

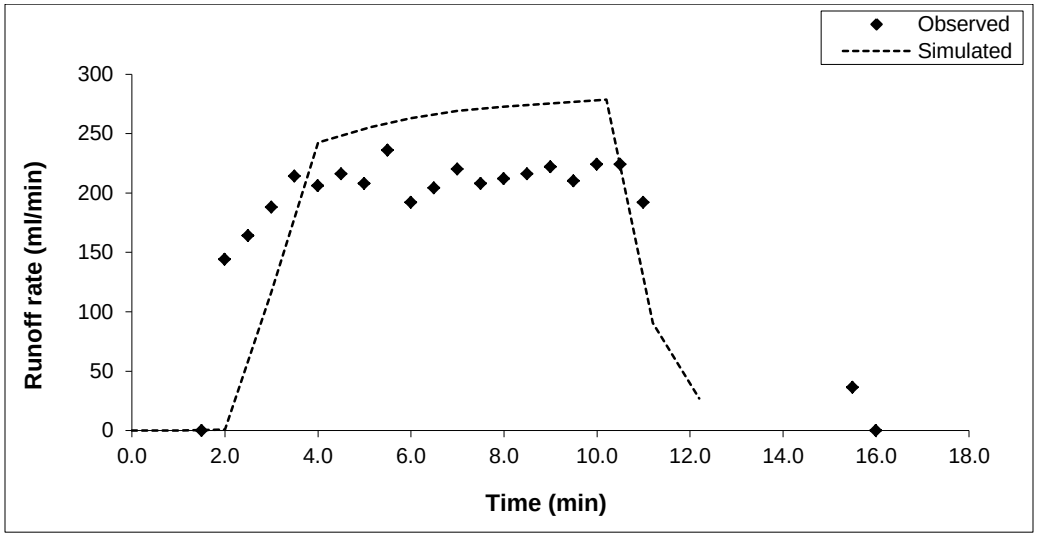

Figure 6.33 WEPP simulation results for surface runoff for Catlin soil bed with 3.0% slope and Brome grass cover subjected to 9.0 cm/hr rainfall applied for 10 minutes.

Figure 6.34 shows the comparison of simulated results from WEPP for total runoff volume with experimental result from small scale experiments for all surface cover, slope and rainfall conditions. The comparison graph indicates that that WEPP model can predict surface runoff rate and total volume fairly well in case of small scale laboratory experiments ($R^2 = 0.96$).

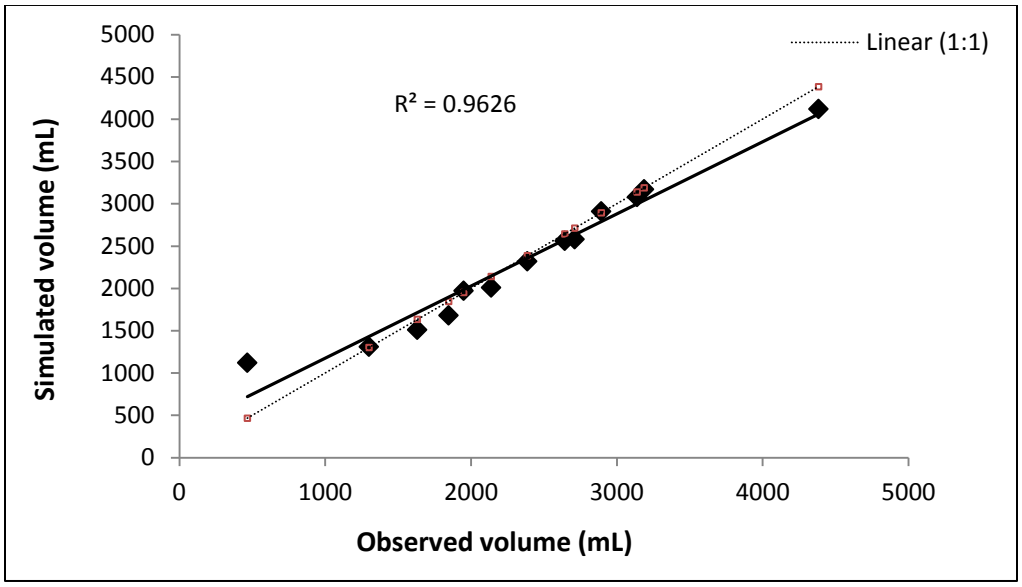

Figure 6.34 Comparison of WEPP simulation results with observations for surface runoff volume for different slopes, rainfall and surface cover conditions for Alvin, Catlin and Darwin soils.

6.3.3 Oocyst transport model simulation with large scale experiment data

After calibrating WEPP model successfully, the output from simulated WEPP model was used to drive oocysts transport model. WEPP model simulations provided input parameters: bed slope, rainfall intensity, flow velocity, flow depth, saturated hydraulic conductivity and soil loss for oocysts transport model. During calibration process, break-through curve from the oocysts

transport model was compared with the laboratory experiments to estimate different attachment factors K_{12}, $K_{23,}$ K_{21}.

Figures 6.35, 6.36 and 6.37 show the comparison of break-through curve obtained from oocysts transport model with experimental data for 1.5, 3.0 and 4.50% slope condition with 6.35 cm/hr rainfall for Catlin soil. In case of 1.5% slope, the model could replicate observed oocysts pattern fairly well ($R^2 = 0.88$).

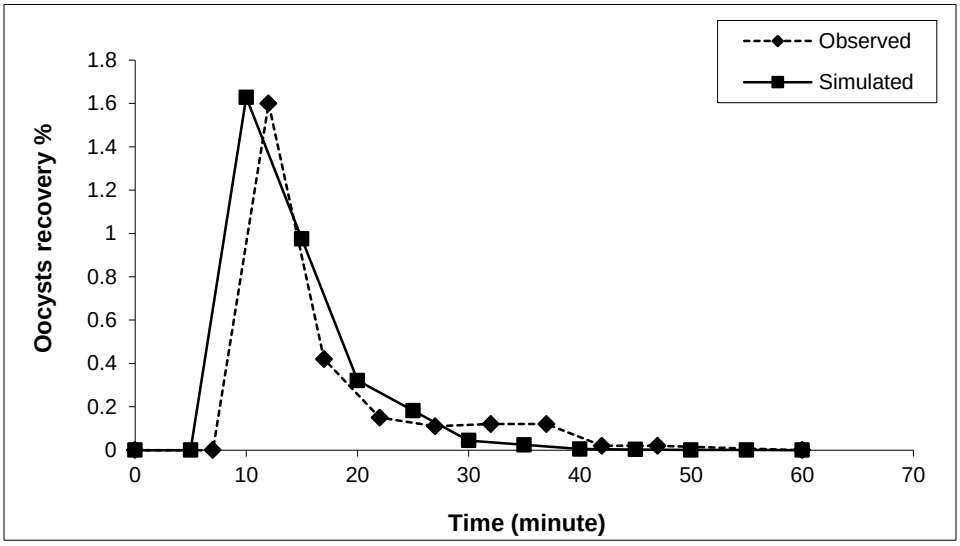

Figure 6.35 Comparison of oocyst transport simulation result with observations for bare ground condition, 6.35 cm/hr rainfall applied for 40 minutes at 1.5% slope for Catlin soil.

For 3.0 and 4.5% slope conditions, the model could reproduce the first oocysts peak observed during the experiment fairy well but recovery pattern was different from the observations. As seen in Figure 6.36, experimental data showed a small jump in oocyst recovery after 30 minutes and the model simulation could not match that jump. Similarly, second peak was observed around 40 minutes in case of 4.5% slope condition which could not be matched by simulated model results. Even though the simulated results could match the very first peak

observed during experiments in most cases, the model could not reproduce multiple peaks obtained from experimental results and under-predicted total oocysts recovery in few similar cases. Computed R^2 values (for observed and simulated oocysts break-through curve values) for 3.0 and 4.5% slope conditions were 0.48 and 0.11, respectively.

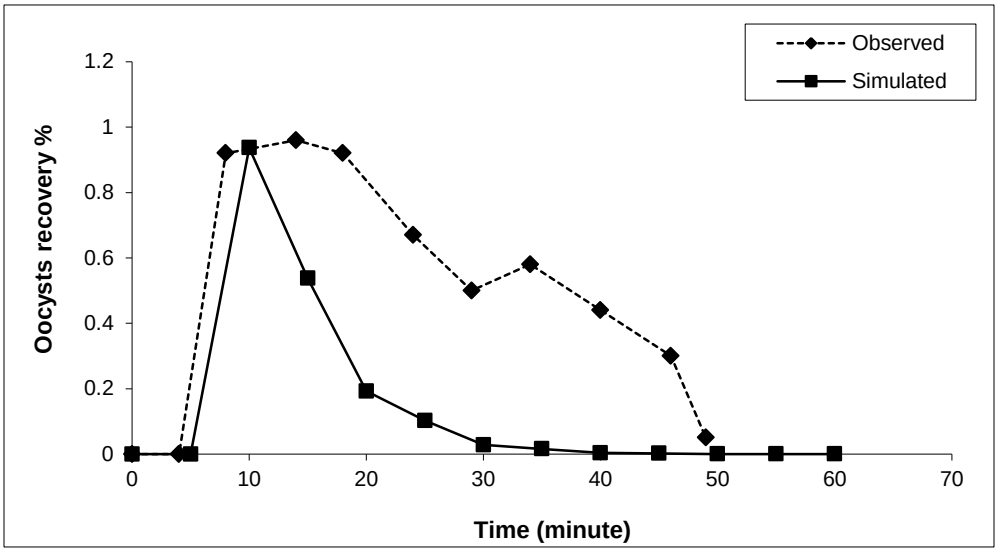

Figure 6.36 Comparison of oocyst transport simulation result with observations for bare ground condition, 6.35 cm/hr rainfall applied for 40 minutes at 3.0% slope for Catlin soil.

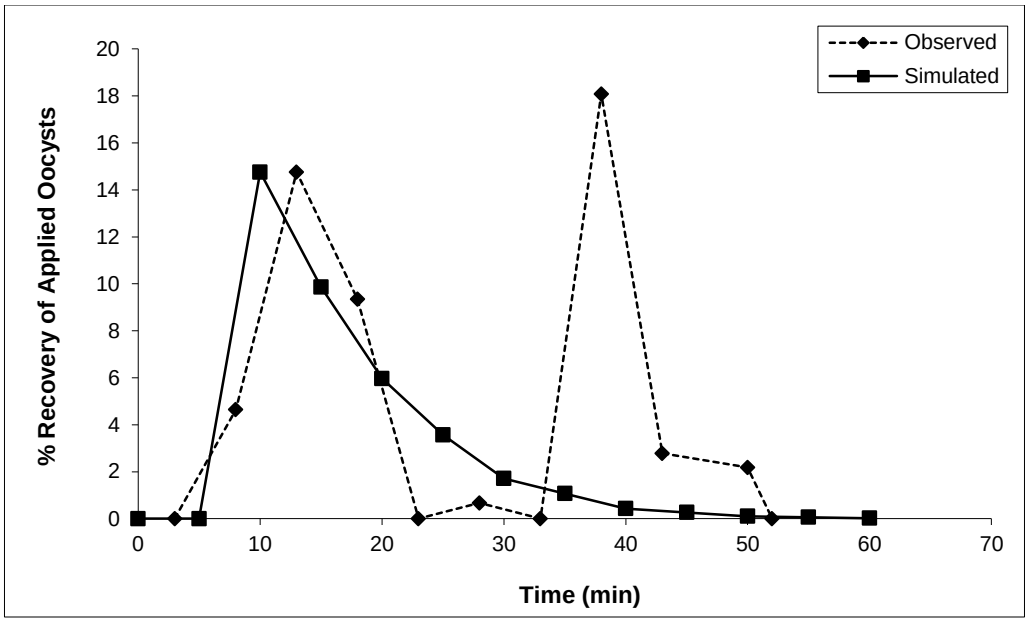

Figure 6.37 Comparison of oocyst transport simulation result with observations for bare ground condition, 6.35 cm/hr rainfall applied for 40 minutes at 4.5% slope for Catlin soil.

Figures 6.38 – 6.40 show the comparison of break-through curve obtained from oocysts transport model with experimental data for 1.5, 3.0 and 4.5% slope condition with 2.54 cm/hr rainfall for Newberry soil with no cover. The model simulation results are pretty consistent with experiment data for these singled peak observations as evident by high R^2 values (0.64, 0.87 and 0.65 for 1.5, 3.0 and 4.5% bed slope conditions, respectively).

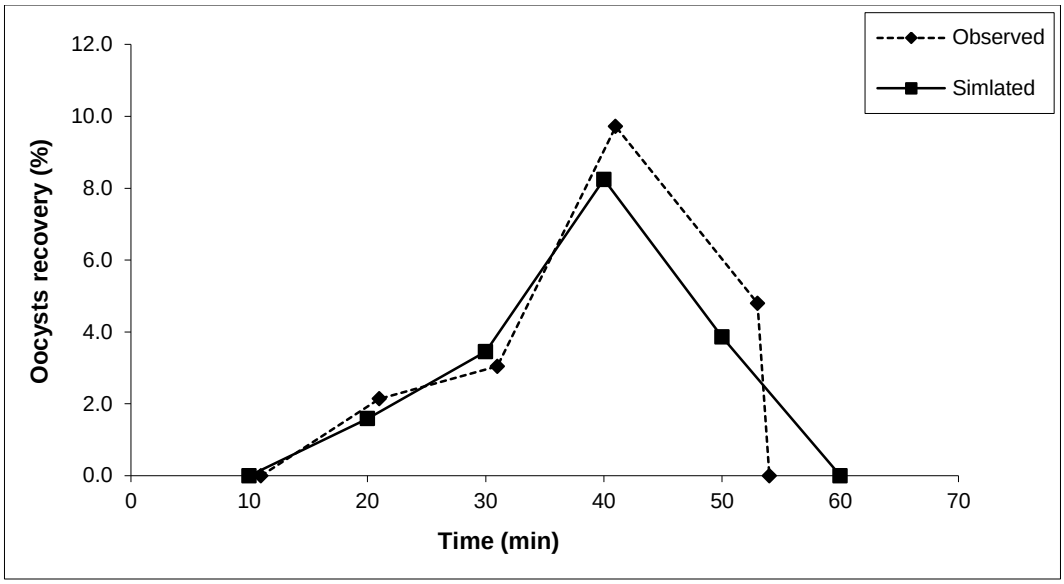

Figure 6.38 Oocyst transport simulation result for surface runoff for bare ground condition, 2.54 cm/hr rainfall applied for 40 minutes at 1.5% slope for Newberry soil.

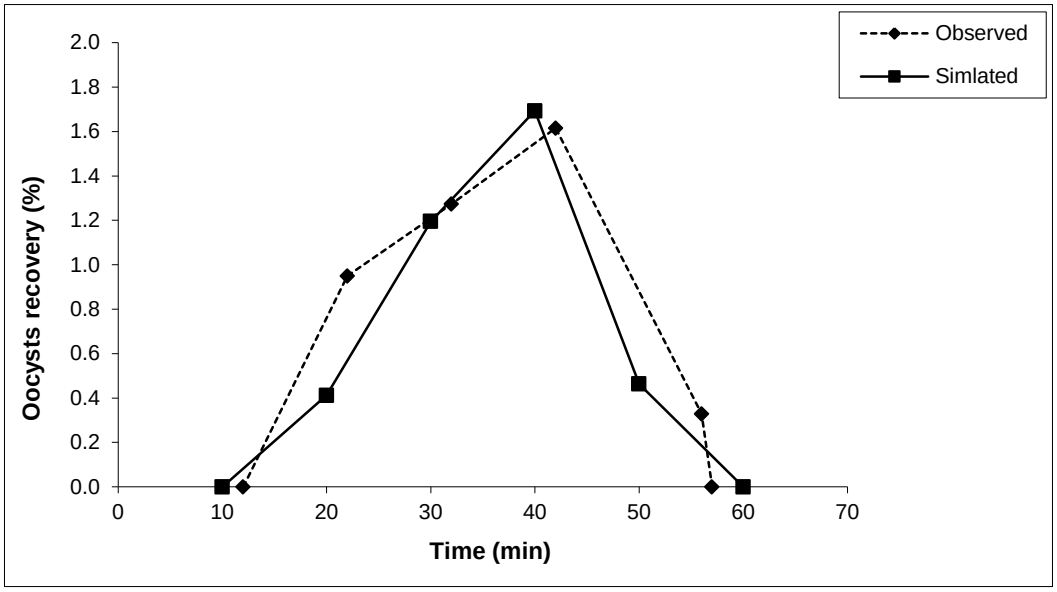

Figure 6.39 Oocyst transport simulation result for surface runoff for bare ground condition, 2.54 cm/hr rainfall applied for 40 minutes at 3.0% slope for Newberry soil.

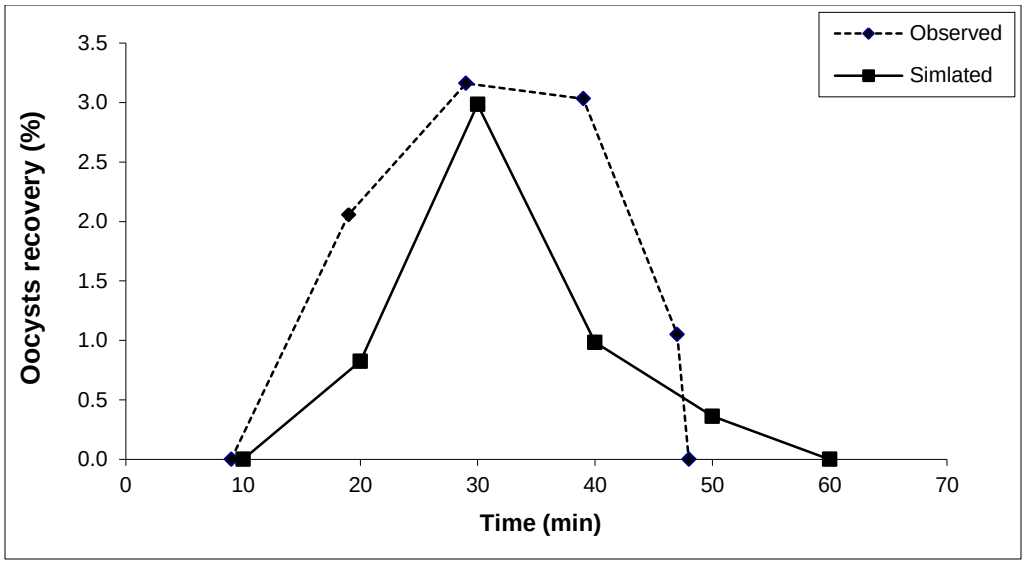

Figure 6.40 Oocyst transport simulation result for surface runoff for bare ground condition, 2.54 cm/hr rainfall applied for 40 minutes at 4.5% slope for Newberry soil.

Figures 6.41, 6.42 and 6.43 show the comparison of break-through curve obtained from oocysts transport model with experimental data for 1.5, 3.0 and 4.5% slope condition with 6.35 cm/hr rainfall for Newberry soil with no cover. For all three cases, the model could reproduce the first oocysts peak observed during the experiment fairy well but could not capture the second peak in the observed data. So, the model simulation results were not consistent with experiment data for these multiple peak observations. Computed R^2 values (for observed and simulated oocysts break-through curve values) for 1.5, 3.0 and 4.5% slope conditions were 0.68, 0.01 and 0.49, respectively.

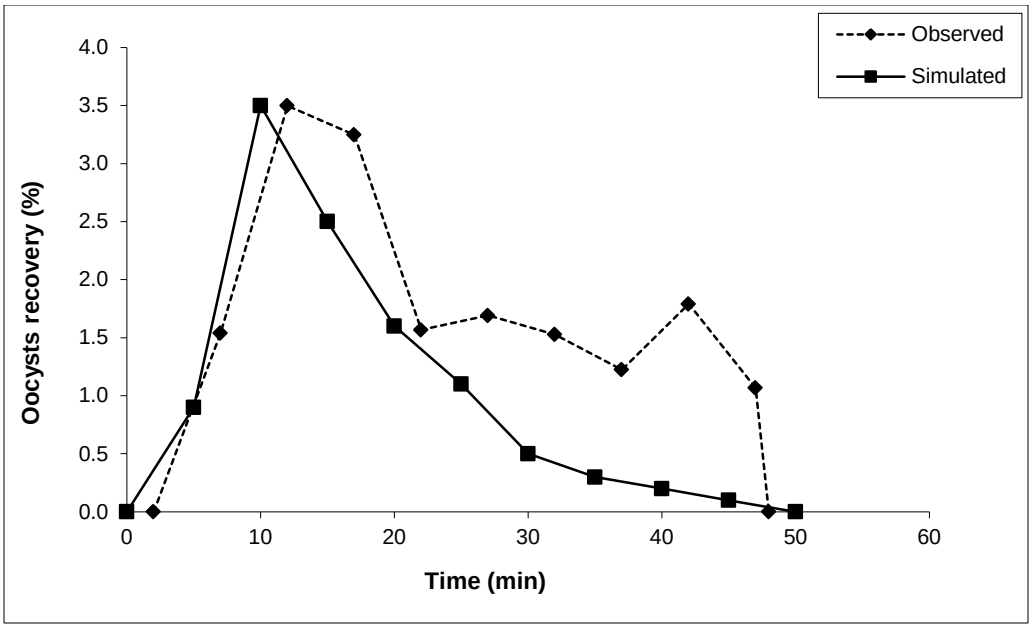

Figure 6.41 Oocyst transport simulation result for surface runoff for bare ground condition, 6.35 cm/hr rainfall applied for 40 minutes at 1.5% slope for Newberry soil.

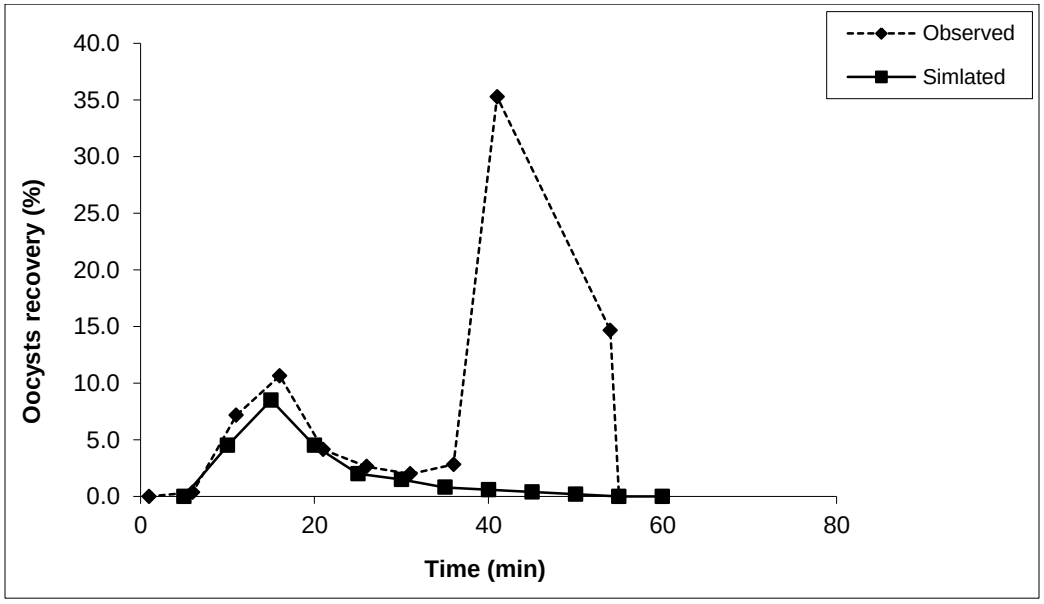

Figure 6.42 Oocyst transport simulation result for surface runoff for bare ground condition, 6.35 cm/hr rainfall applied for 40 minutes at 3.0% slope for Newberry soil.

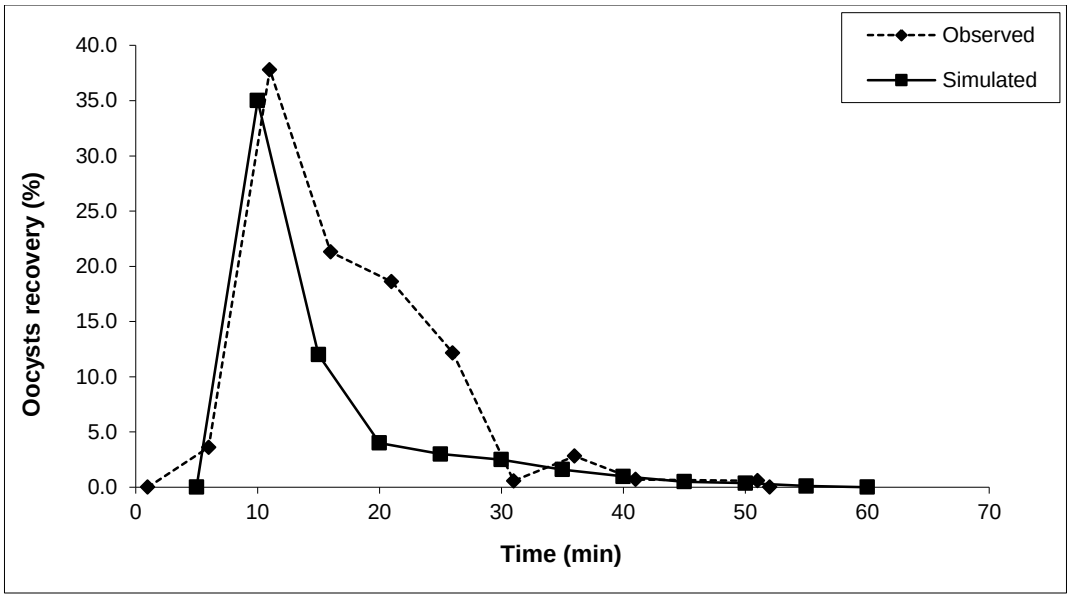

Figure 6.43 Oocyst transport simulation result for surface runoff for bare ground condition, 6.35 cm/hr rainfall applied for 40 minutes at 4.5% slope for Newberry soil.

Figures 6.44, 6.45 and 6.46 show the comparison of break-through curve obtained from oocysts transport model with experimental data for 1.5, 3.0 and 4.5% slope condition with 6.35 cm/hr rainfall for Catlin soil with vegetation. In case of 1.5% slope, the model could replicate single-peaked break-through curve fairly well while the model could not capture second peak in break-through curve in observed data in case of 3 and 4.5 % slope conditions. Computed R^2 values (for observed and simulated oocysts break-through curve values) for 1.5, 3.0 and 4.5% slope conditions were 0.82, 0.60 and 0.41, respectively.

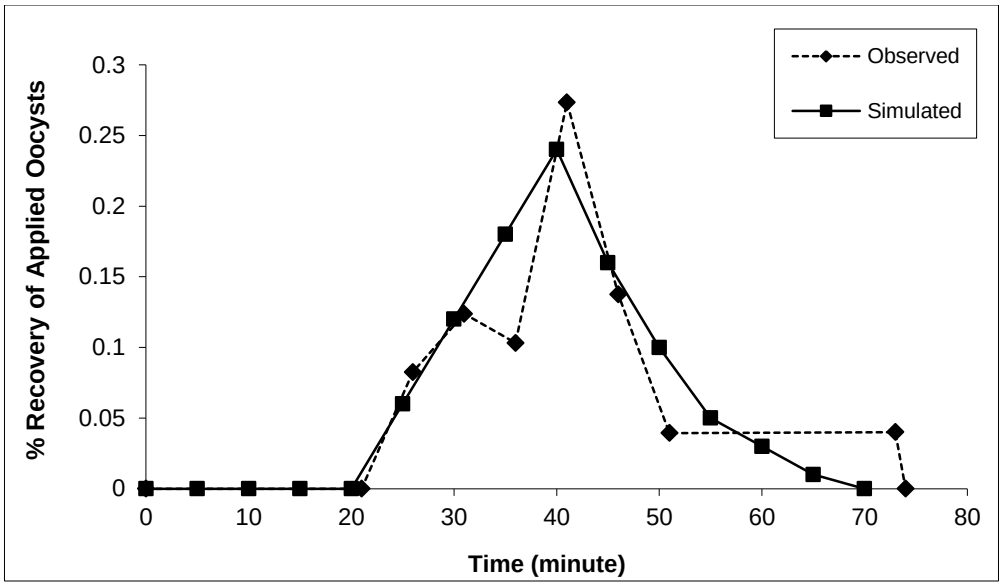

Figure 6.44 Comparison of oocyst transport simulation result with observations for vegetated Catlin soil bed with 1.5% slope subjected to 6.35 cm/hr rainfall for 40 minutes.

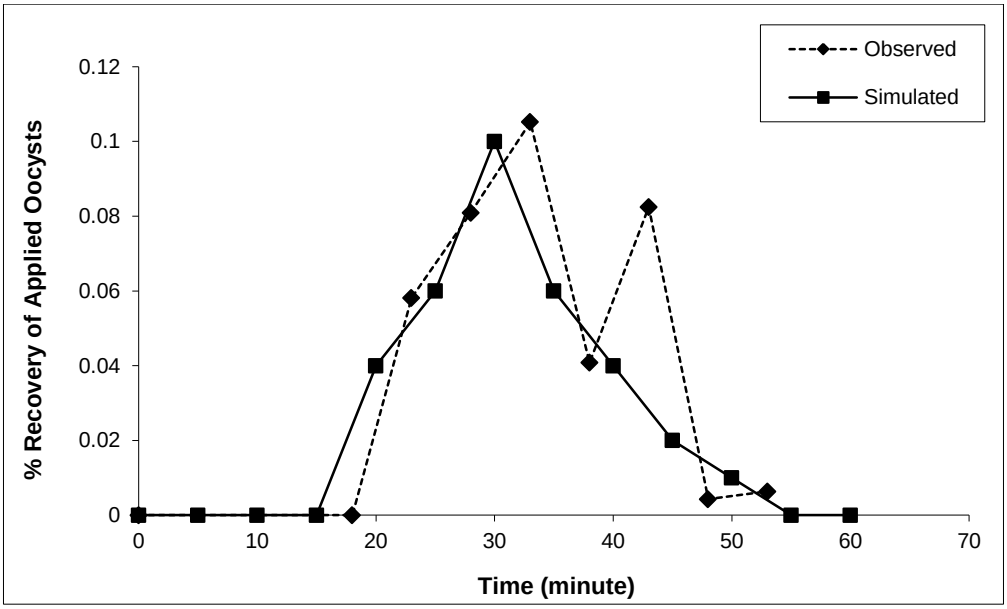

Figure 6.45 Comparison of oocyst transport simulation result with observations for vegetated Catlin soil bed with 3% slope subjected to 6.35 cm/hr rainfall for 40 minutes.

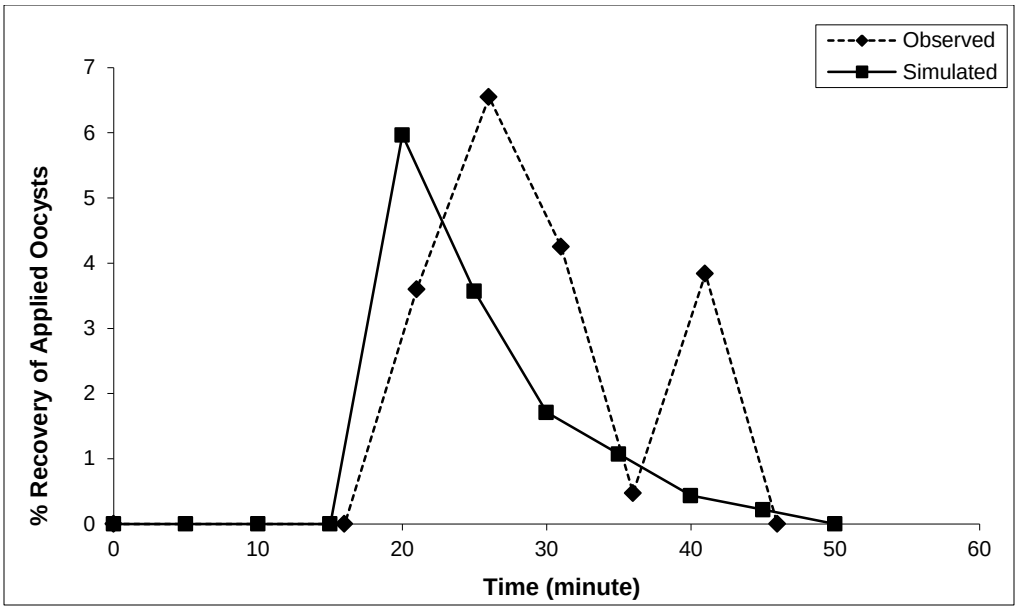

Figure 6.46 Comparison of oocyst transport simulation result with observations for vegetated Catlin soil bed with 4.5% slope subjected to 6.35 cm/hr rainfall for 40 minutes.

Figures 6.47 – 6.49 show the comparison of break-through curve obtained from oocysts transport model with experimental data for 1.5, 3.0 and 4.5% slope condition with 2.54 cm/hr rainfall for Newberry soil with vegetation. The model simulation results are pretty consistent with experiment data for these singled peak observations as shown in Figures 6.47, 6.48 and 6.4. Computed R^2 values (for observed and simulated oocysts break-through curve values) for 1.5, 3.0 and 4.5% slope conditions were 0.63, 0.90 and 0.50, respectively.

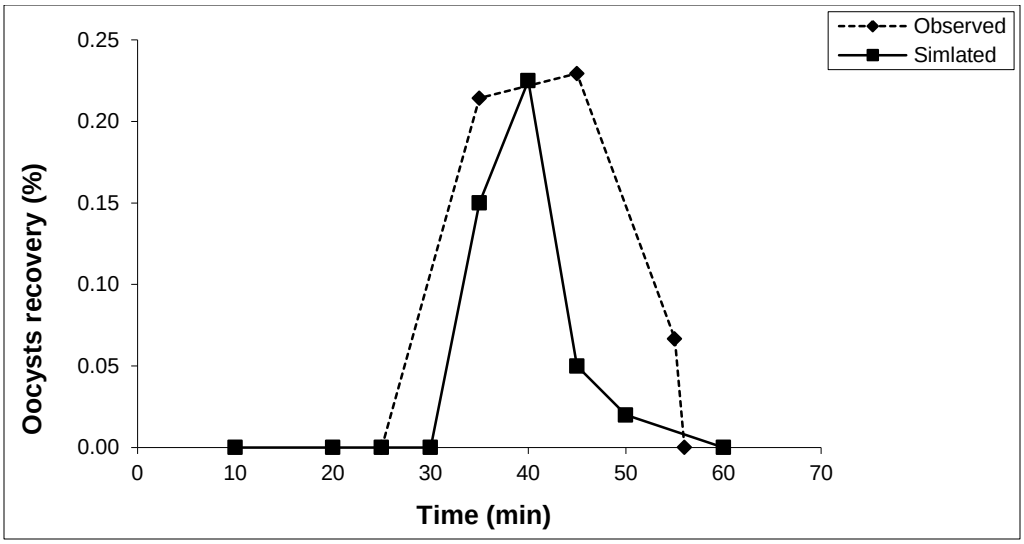

Figure 6.47 Oocysts transport simulation result for surface runoff for vegetated condition, 2.54 cm/hr rainfall applied for 40 minutes at 1.5% slope for Newberry soil.

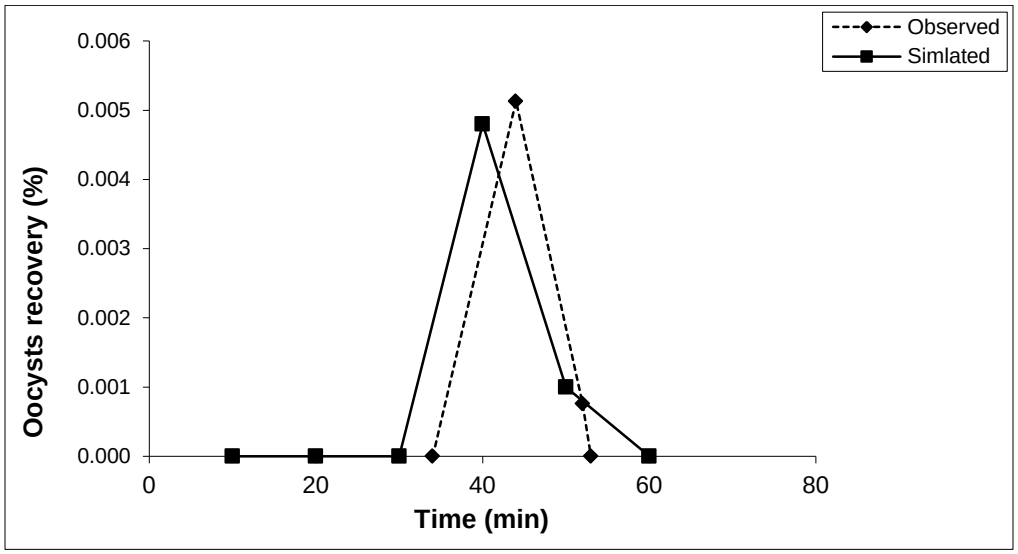

Figure 6.48 Oocyst transport simulation result for surface runoff for vegetated condition, 2.54 cm/hr rainfall applied for 40 minutes at 3.0% slope for Newberry soil.

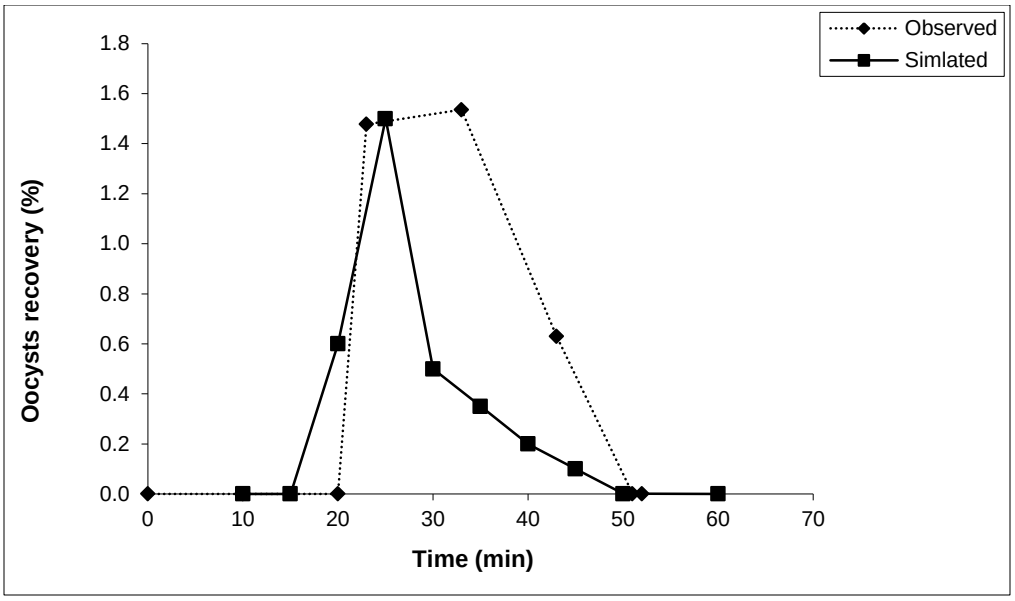

Figure 6.49 Oocyst transport simulation result for surface runoff for vegetated condition, 2.54 cm/hr rainfall applied for 40 minutes at 4.5% slope for Newberry soil.

Figures 6.50, 6.51 and 6.52 show the comparison of break-through curve obtained from oocysts transport model with the experimental data for 1.5, 3.0 and 4.5% slope condition with 6.35 cm/hr rainfall for Newberry soil with vegetation. For 1.5 and 3.0% slope conditions, the model could reproduce the observed first peak in break-through curve observed in experiment data but the model could not reproduce second peak in experimental data. Computed R^2 values (for observed and simulated oocyst break-through curve values) for 1.5 and 3.0 % slope conditions were 0.28 and 0.04, respectively. The model could replicate the oocyst break-through pattern in case of 4.5% slope condition which is evident by high R^2 value (0.90).

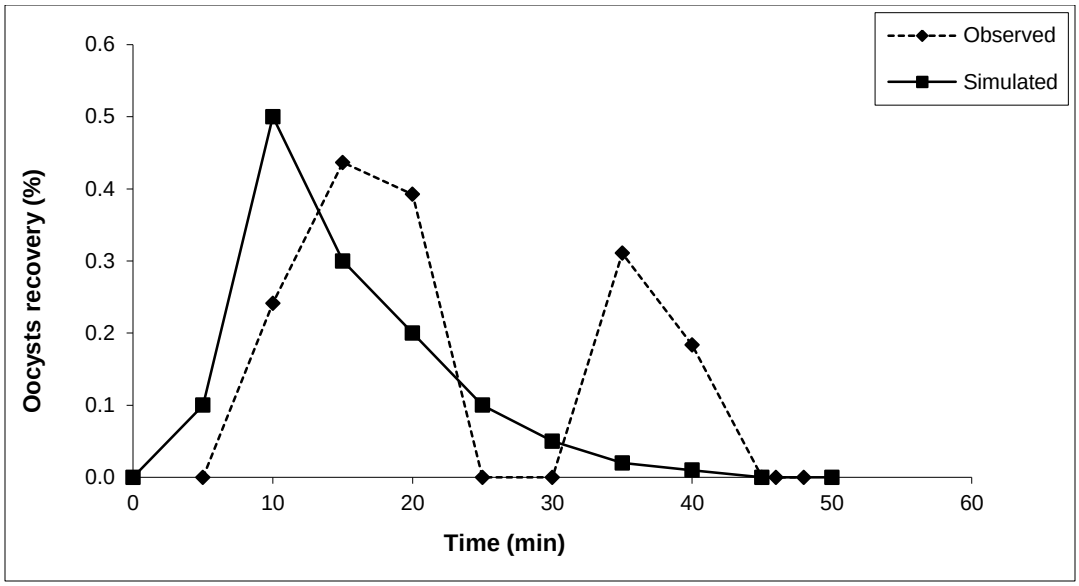

Figure 6.50 Oocyst transport simulation result for surface runoff for vegetated condition, 6.35 cm/hr rainfall applied for 40 minutes at 1.5% slope for Newberry soil.

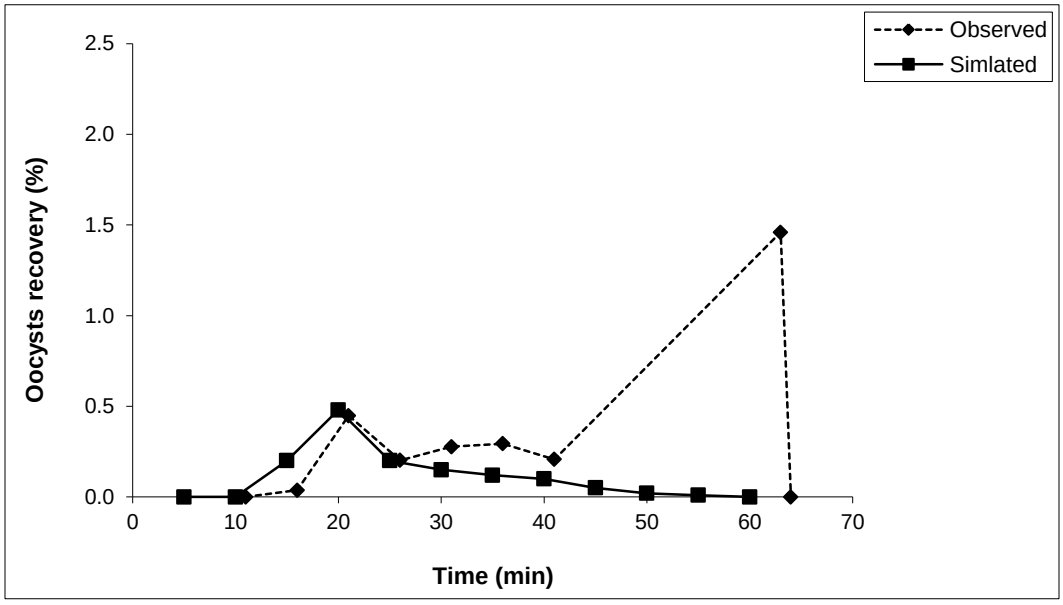

Figure 6.51 Oocyst transport simulation result for surface runoff for vegetated condition, 6.35 cm/hr rainfall applied for 40 minutes at 3.0% slope for Newberry soil.

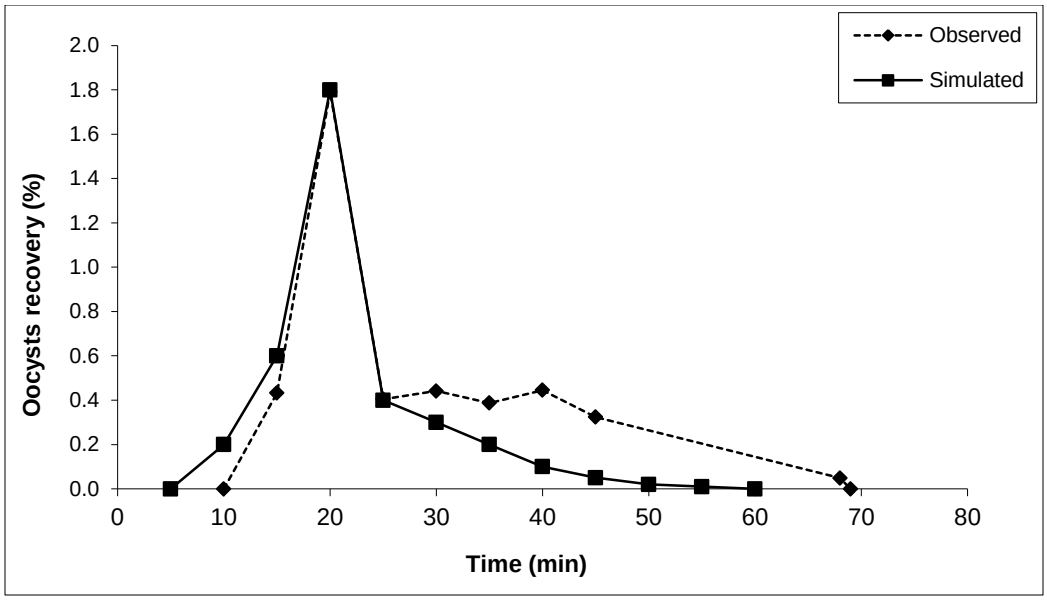

Figure 6.52 Oocyst transport simulation result for surface runoff for vegetated condition, 6.35 cm/hr rainfall applied for 40 minutes at 4.5% slope for Newberry soil.

Figures 6.53 and 6.54 show the comparison of total oocysts recovery obtained from oocysts transport model with the experimental results different slope, cover and rainfall conditions for Catlin and Newberry soils, respectively. The simulated results showed that recovery % was higher for Newberry soil compared to Catlin soil confirming the findings from experimental results. The model simulation result produced similar oocysts recovery rate for most of the conditions, and demonstrated by reasonably higher value of R^2 (0.90 for Catlin soil and 0.91 for Newberry soil) for both soil types.

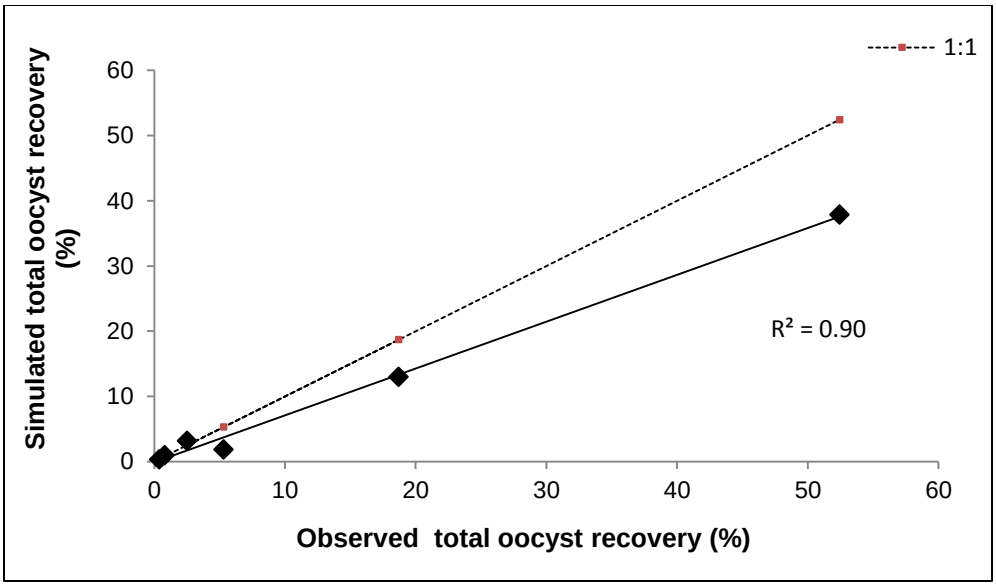

Figure 6.53 Comparison of oocysts transport model simulation result with observations for total oocysts recovery for different slopes, rainfall and surface cover conditions for Catlin soil.

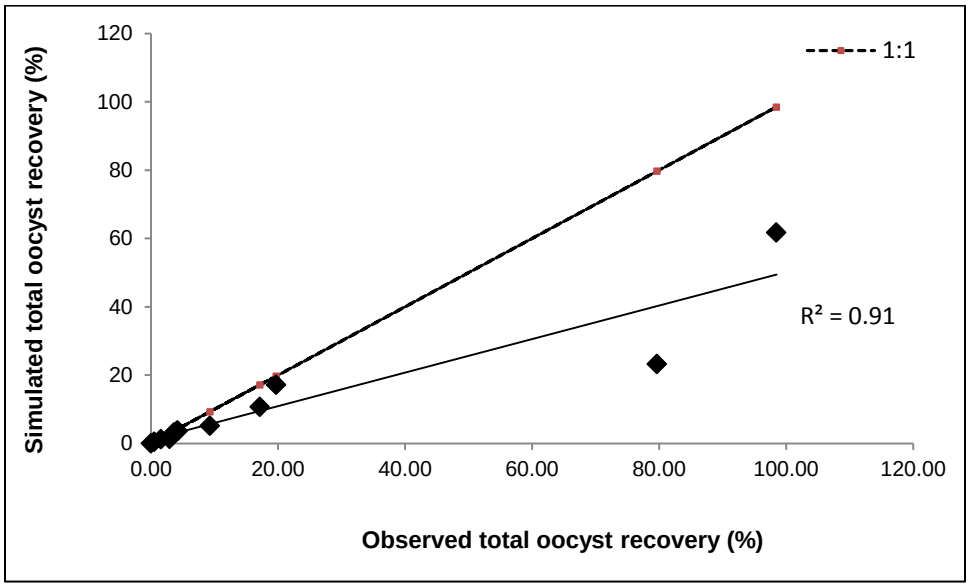

Figure 6.54 Comparison of oocysts transport model simulation result with observations for total oocysts recovery for different slopes, rainfall and surface cover conditions for Newberry soil.

6.3.4 Oocyst transport model simulation with small scale experiment data

Replicating the experimental condition described by of Davidson (2010), pathogen (*C. parvum* and rotavirus) transport simulations were carried out for Alvin, Catlin and Darwin soil beds with 2.5% slope with three different cover conditions: bare, Brome and Fescue grasses. The soil beds were subjected a simulated rainfall intensity of 6.35 cm/hr applied for 20 minutes. The soil bed dimensions were 0.61 m (2 ft) long, 0.305 m (1 ft) wide and 0.015 m (0.5 ft) thick. Figures 6.55, 6.56 and 6.57 show the comparison of *C. parvum* break-through experimental data with pathogen transport model simulation result for surface runoff for bare ground and vegetated (Brome grass and Fescue) conditions for Alvin soil. In case of bare ground condition, observed break-through curve showed multiple peaks as shown in Figure 6.55. The pathogen transport model could only replicate the timing and amount of recovered oocyst in the observed first peak but not the other peaks. Hence, the computed R^2 value between observed and simulated oocyst recovery was very low (0.05) in case of bare Alvin soil bed. In case of Brome grass and Fescue beds, the pathogen transport model produced reasonable results as compared with the observations as shown below which is also demonstrated by statistical analysis. Computed R^2 values for Brome grass and Fescue cover conditions were 0.95 and 0.98, respectively.

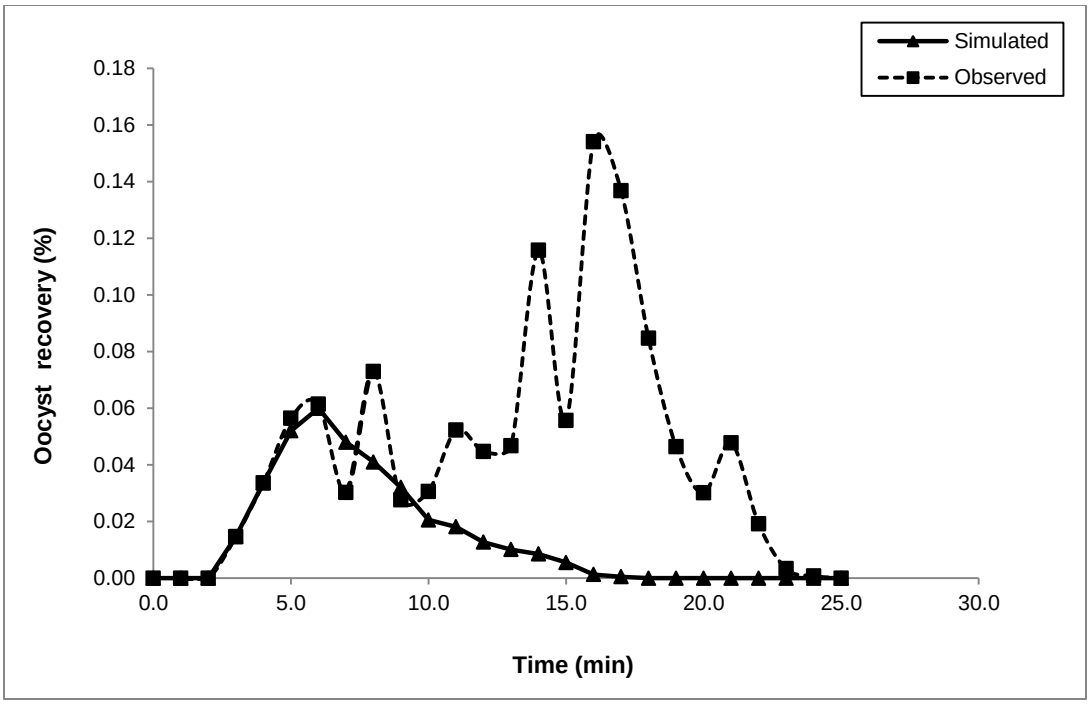

Figure 6.55 Oocyst transport in surface runoff simulation for bare Alvin soil bed subjected to 6.35 cm/hr rainfall applied for 20 minutes at 2.5% slope.

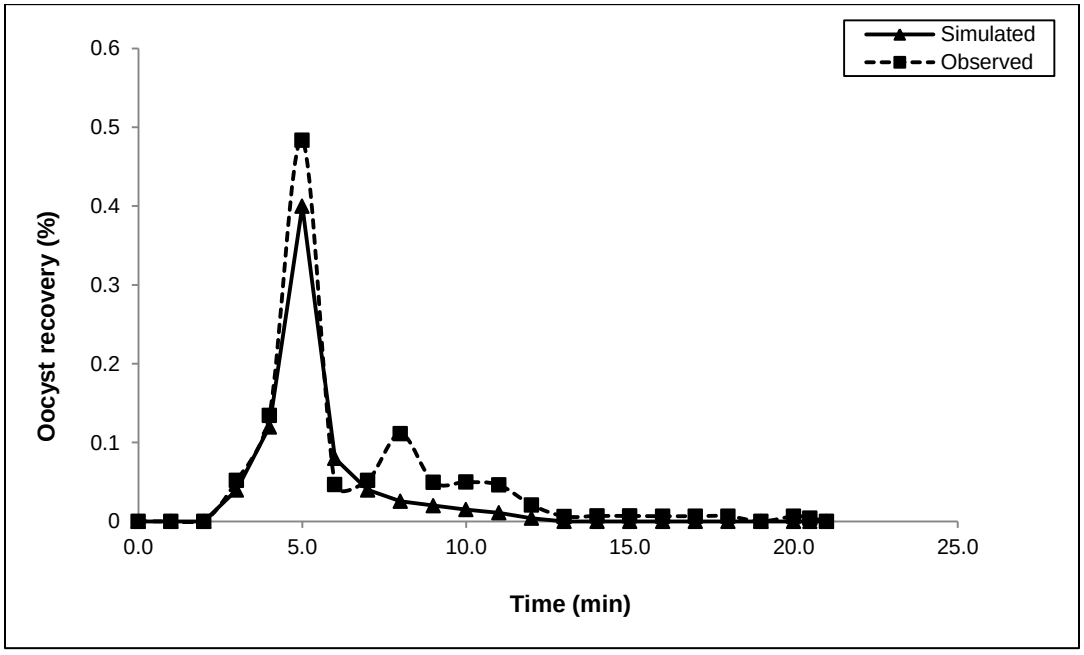

Figure 6.56 Oocyst transport in surface runoff simulation for Alvin soil bed with Brome grass vegetation subjected to 6.35 cm/hr rainfall applied for 20 minutes at 2.5% slope.

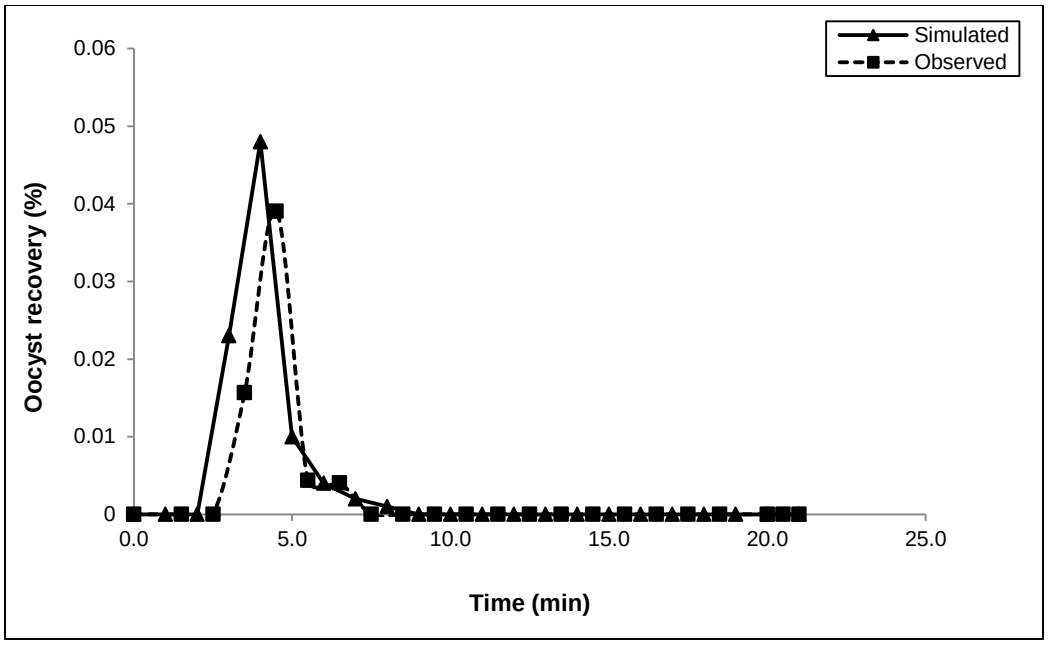

Figure 6.57 Oocyst transport in surface runoff simulation for Alvin soil bed with Fescue vegetation subjected to 6.35 cm/hr rainfall applied for 20 minutes at 2.5% slope.

The comparison of *C. parvum* break-through experimental data with pathogen transport model simulation result for surface runoff for bare ground and vegetated (Brome grass and Fescue) conditions for Catlin soil is presented in Figures 6.58, 6.59 and 6.60. The observed break-through for bare ground condition curve showed multiple peaks as shown in Figure 6.58. The pathogen transport model could only replicate the timing and amount of recovered oocyst in the observed first peak but not the other peaks. Hence, the computed R^2 value between observed and simulated oocyst recovery was low (0.46) compared to vegetated conditions. In case of Brome grass and Fescue beds, the pathogen transport model produced reasonable results as compared with the observations as shown below which is also demonstrated by statistical analysis. Computed R^2 values for Catlin soil beds with Brome grass and Fescue cover conditions were 0.95 and 0.93, respectively.

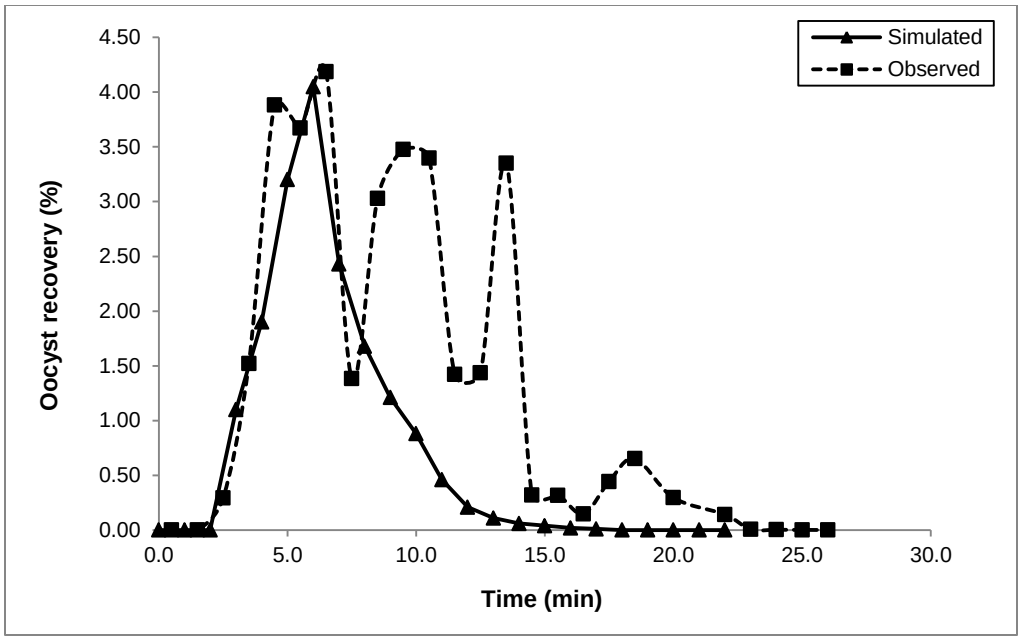

Figure 6.58 Oocyst transport in surface runoff simulation for bare Catlin soil bed subjected to 6.35 cm/hr rainfall applied for 20 minutes at 2.5% slope.

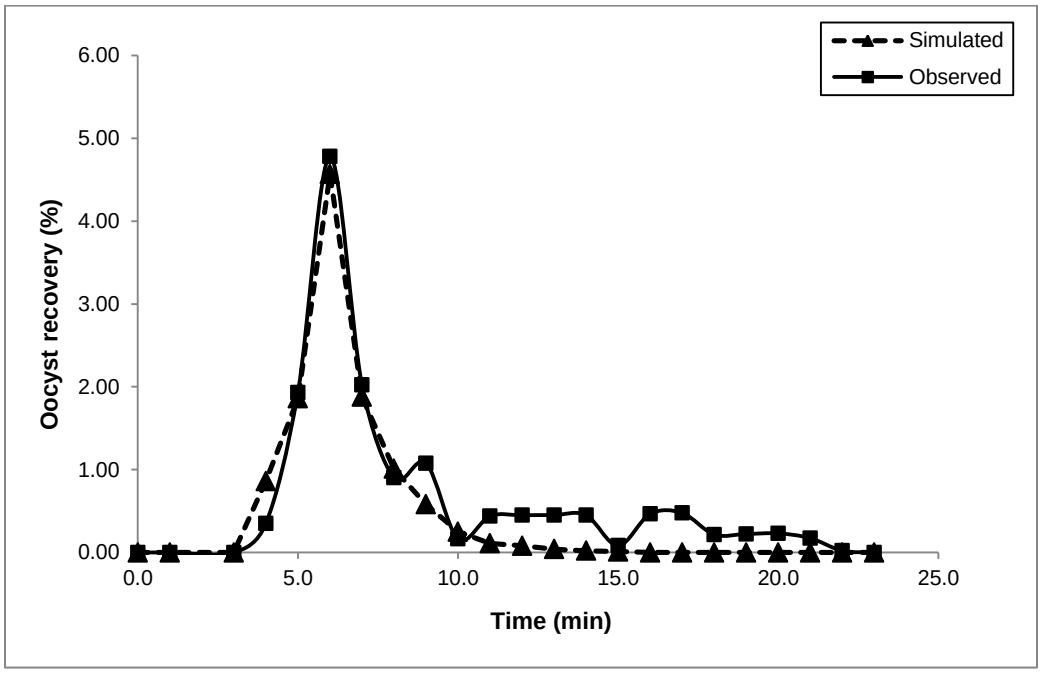

Figure 6.59 Oocyst transport in surface runoff simulation for Catlin soil bed with Brome grass vegetation subjected to 6.35 cm/hr rainfall applied for 20 minutes at 2.5% slope.

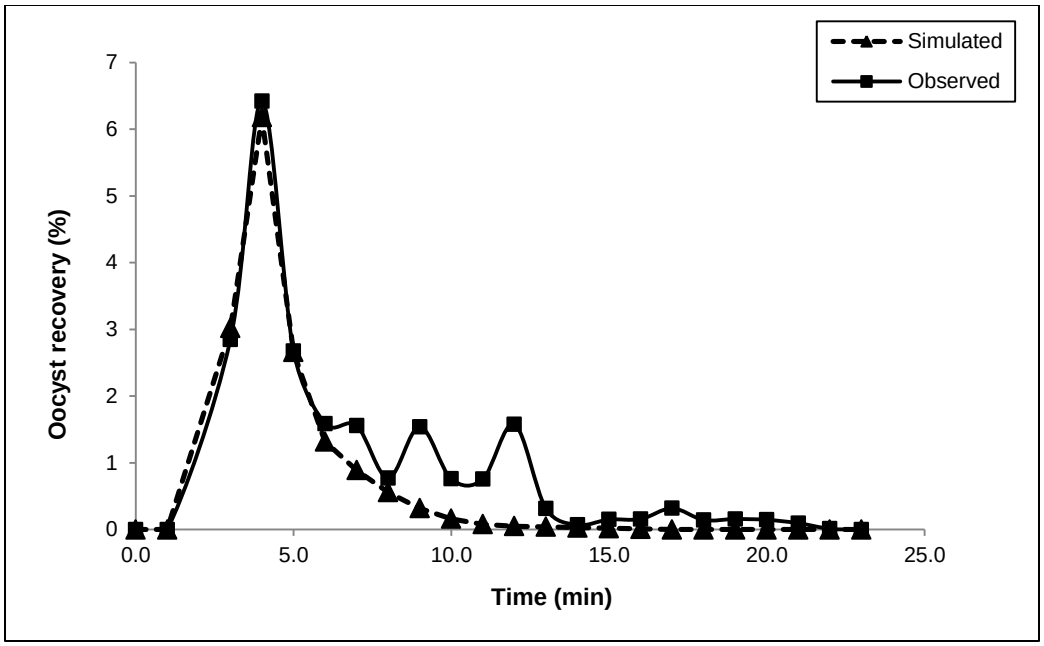

Figure 6.60 Oocyst transport in surface runoff simulation for Catlin soil bed with Fescue vegetation subjected to 6.35 cm/hr rainfall applied for 20 minutes at 2.5% slope.

The comparison of *C. parvum* break-through experimental data with the simulation result from pathogen transport model for surface runoff for bare ground and vegetated (Brome grass) conditions for Darwin soil is presented in Figures 6.61 and 6.62. In case of Fescue cover condition, the total oocyst recovered from surface runoff was zero. So, the result from pathogen transport model could not be compared with the observations due to lack of experimental data. In case bare Darwin soil bed, the pathogen transport model produced reasonable result as compared with the observations as shown below which is also demonstrated by statistical analysis (R^2 = 0.90).

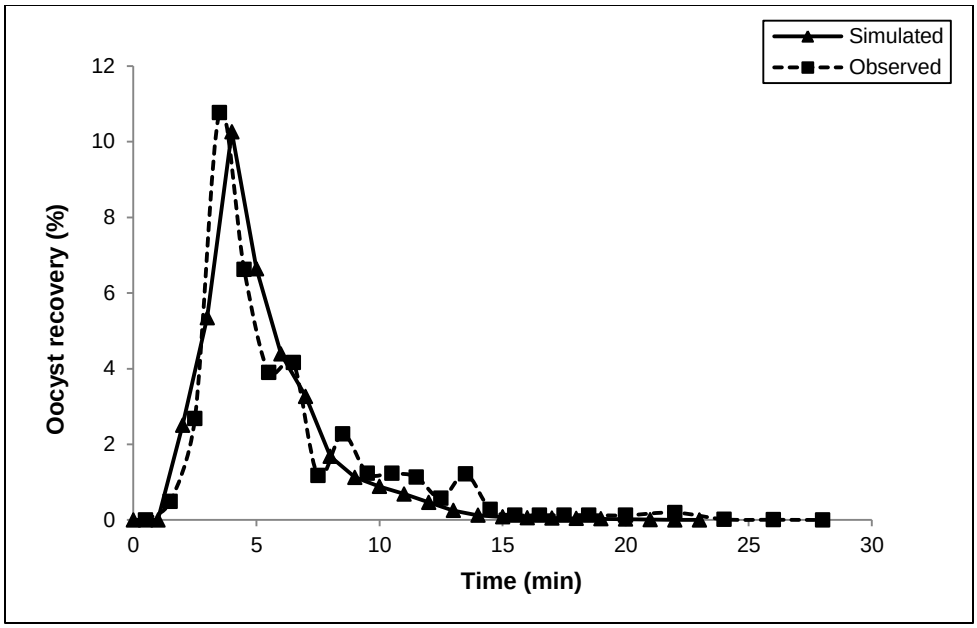

Figure 6.61 Oocyst transport in surface runoff simulation for bare Darwin soil bed subjected to 6.35 cm/hr rainfall applied for 20 minutes at 2.5% slope.

The observed break-through curve for Brome grass vegetation cover condition showed double peaks as shown in Figure 6.62. The pathogen transport model could only replicate the timing and amount of recovered oocyst in the observed first peak but not the second one. Hence, the computed R^2 value between observed and simulated oocyst recovery for Brome grass cover condition was low (0.64) compared to bare soil bed condition (0.90).

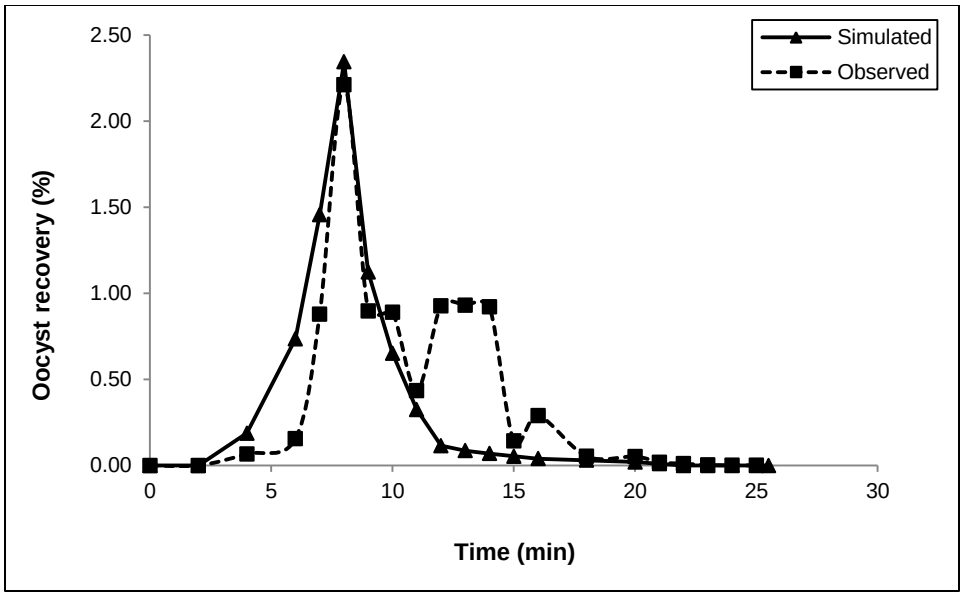

Figure 6.62 Oocyst transport in surface runoff simulation for Darwin soil bed with Brome grass vegetation subjected to 6.35 cm/hr rainfall for 20 minutes at 2.5% slope.

Replicating the experimental condition described by of Koch (2009), *C. parvum* transport simulations were carried out for Catlin soil bed with two different cover conditions: bare and Brome grass. The soil bed with 2.5% slope were subjected a simulated rainfall intensity of 6.35 cm/hr applied for 10 minutes. Similarly, the soil bed with 3.0% slope were subjected a simulated rainfall intensity of 9.0 cm/hr applied for 10 minutes. The soil bed dimensions were 0.61 m (2 ft) long, 0.305 m (1 ft) wide and 0.015 m (0.5 ft) thick. Figure 6.63 shows the comparison of *C. parvum* break-through experimental data with pathogen transport model simulation result for surface runoff for bare Catlin soil bed subjected to rainfall intensity of 6.35 cm/hr applied for 10 minutes. In case of bare Catlin soil bed, the pathogen transport model produced reasonable results compared with the observations.

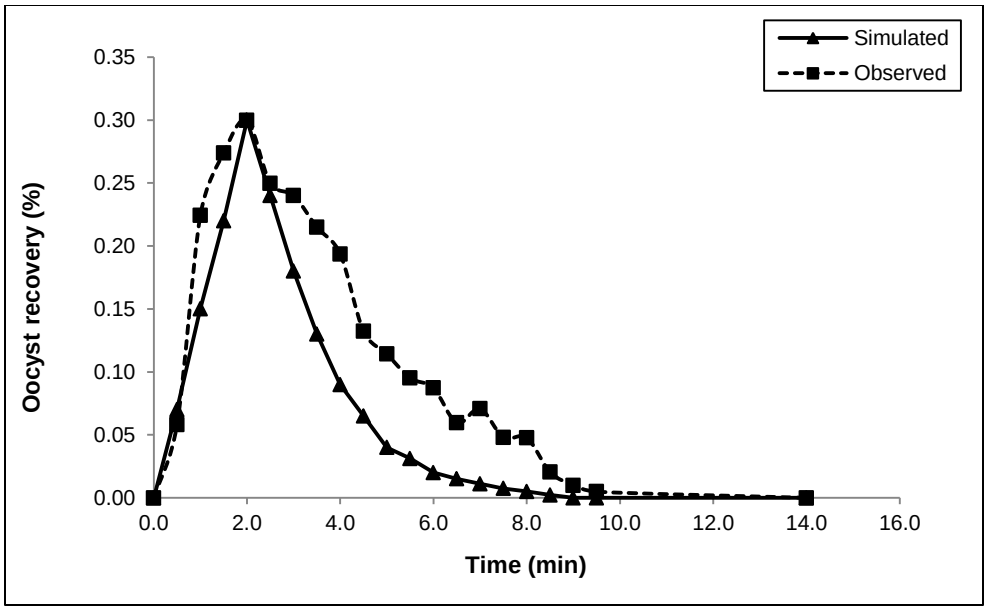

Figure 6.63 Oocyst transport in surface runoff simulation for bare Catlin soil bed subjected to 6.35 cm/hr rainfall for 10 minutes at 2.5% slope.

Figure 6.64 shows the comparison of *C. parvum* break-through experimental data with pathogen transport model simulation result for surface runoff for Catlin soil bed with Brome grass cover subjected to rainfall intensity of 6.35 cm/hr applied for 10 minutes. In case of Brome grass cover condition, observed break-through curve showed double peaks. The model could only replicate the timing and amount of recovered oocyst in the observed first peak but not the second peak. Hence, the computed R^2 value between observed and simulated oocyst recovery was lower (0.48) than R^2 value for bare condition (0.89).

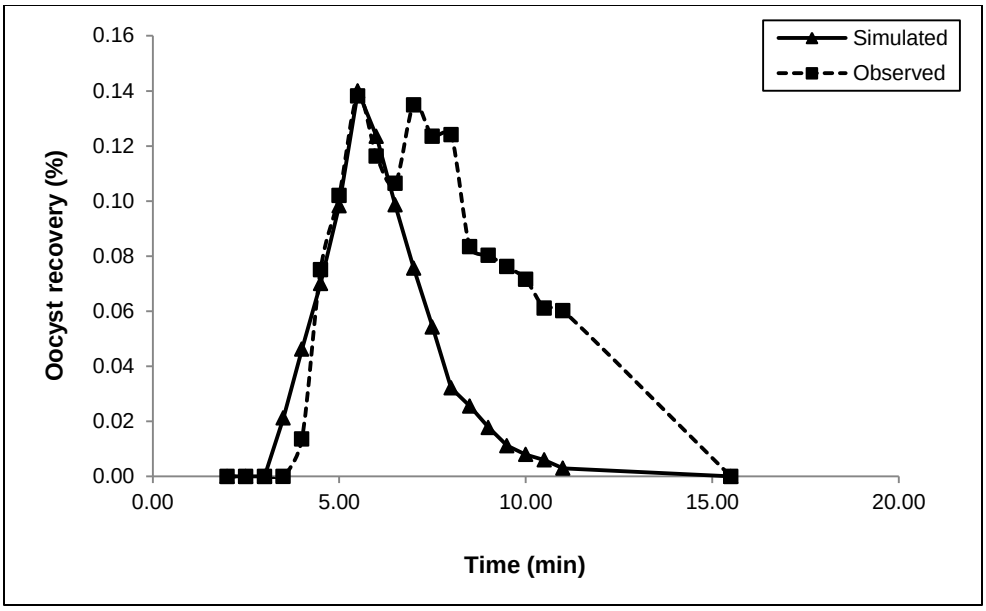

Figure 6.64 Oocyst transport in surface runoff simulation for Catlin soil bed with Brome grass vegetation subjected to 6.35 cm/hr rainfall for 10 minutes at 2.5% slope.

The comparison of *C. parvum* break-through experimental data with pathogen transport model simulation result for surface runoff for bare ground and vegetated (Brome grass) conditions for Catlin soil with high slope (3.0%) and high intensity (9.0 cm/hr) is presented in Figures 6.65 and 6.66. In case of bare Catlin bed, the pathogen transport model produced reasonable results as compared with the observations as shown below which is also demonstrated by high R^2 value (0.92). The observed break-through for vegetated condition curve showed multiple peaks as shown in Figure 6.66. The pathogen transport model could only replicate the timing and amount of recovered oocyst in the observed first peak but not the other peaks. Hence, the computed R^2 value between observed and simulated oocyst recovery was lower (0.69) compared to bare condition.

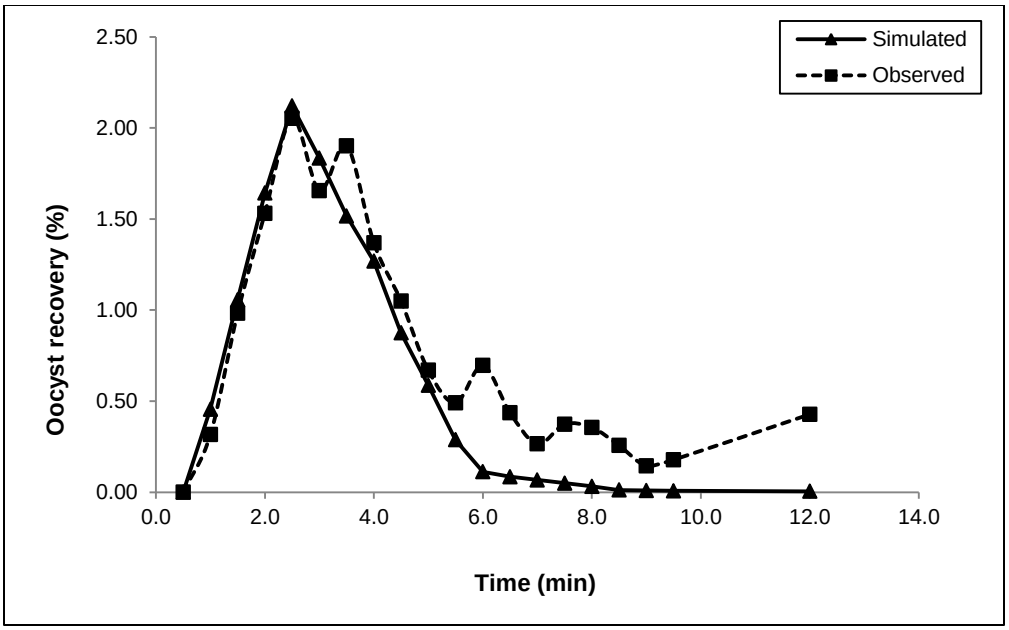

Figure 6.65 Oocyst transport in surface runoff simulation for bare Catlin soil bed subjected to 9.0 cm/hr rainfall for 10 minutes at 3.0% slope.

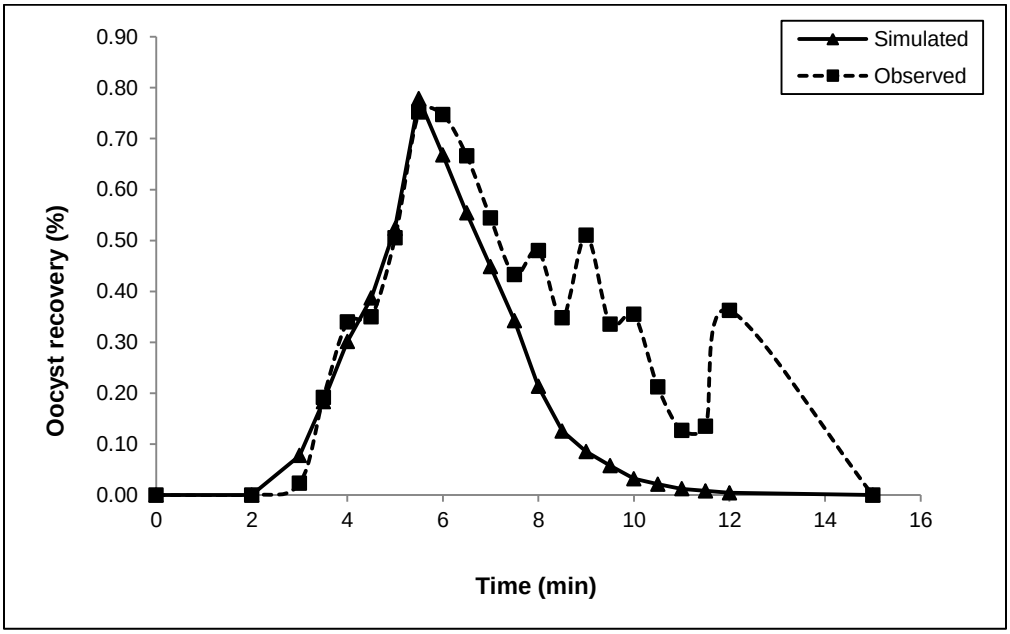

Figure 6.66 Oocyst transport in surface runoff simulation for Catlin soil bed with Brome grass vegetation subjected to 9.0 cm/hr rainfall for 10 minutes at 3.0% slope.

Figures 6.67 shows the comparison of simulated total oocyst recovery from pathogen transport model with experimental result from small scale experiments for all surface cover, slope and rainfall conditions. The comparison graph indicates that that the pathogen transport model can predict total oocyst recovery fairly well in case of small scale laboratory experiments in most cases (R^2 = 0.90).

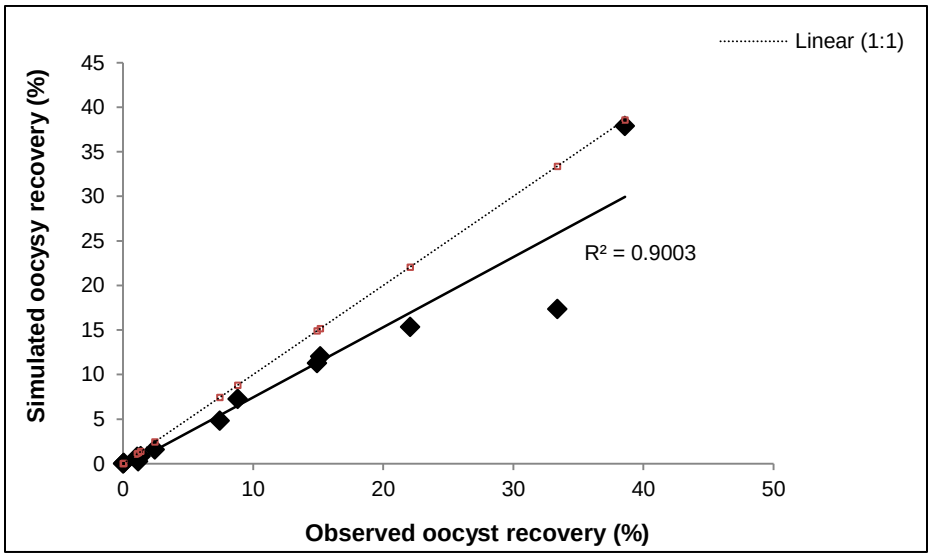

Figure 6.67 Comparison of oocysts transport model simulation result with observations for total oocysts recovery for different slopes, rainfall and surface cover conditions for Alvin, Catlin and Darwin soils.

6.3.5 Rotavirus transport simulation

Figures 6.68, 6.69 and 6.70 show the comparison of rotavirus break-through experimental data with pathogen transport model simulation result for surface runoff for bare ground and two vegetated (Brome grass and Fescue) conditions for Alvin soil. In case of bare and Fescue cover beds, the pathogen transport model produced reasonable results as compared with the observations as shown below. In case of Brome grass cover condition, observed break-through

curve showed multiple peaks as shown in Figure 6.69. The pathogen transport model could only replicate the timing and amount of recovered oocyst in the observed first peak but not the other peaks. Hence, the computed R^2 value between observed and simulated oocyst recovery was low (0.77) in case of Alvin soil bed with Brome grass. Computed R^2 values for bare and Fescue cover conditions were 0.98 and 0.92, respectively.

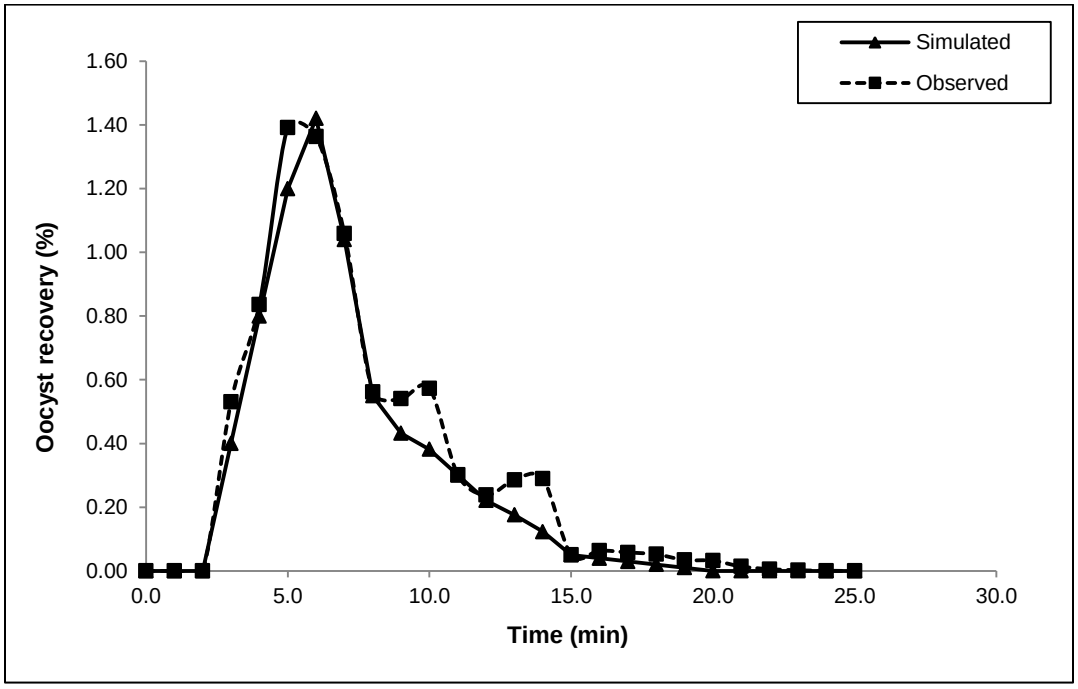

Figure 6.68 Rotavirus transport in surface runoff simulation for bare Alvin soil bed subjected to 6.35 cm/hr rainfall applied for 20 minutes at 2.5% slope.

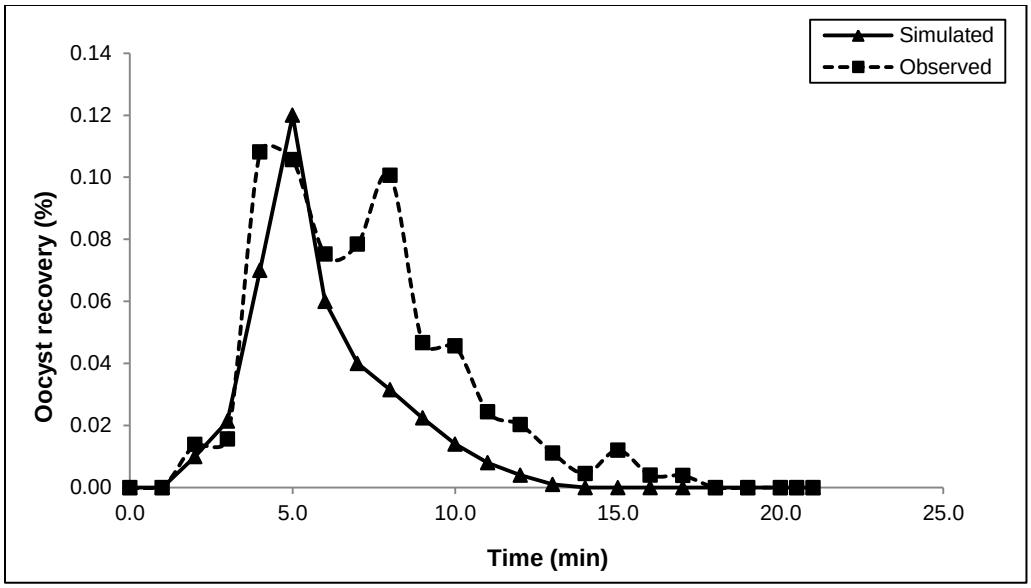

Figure 6.69 Rotavirus transport in surface runoff simulation for Alvin soil bed with Brome grass vegetation subjected to 6.35 cm/hr rainfall for 20 minutes at 2.5% slope.

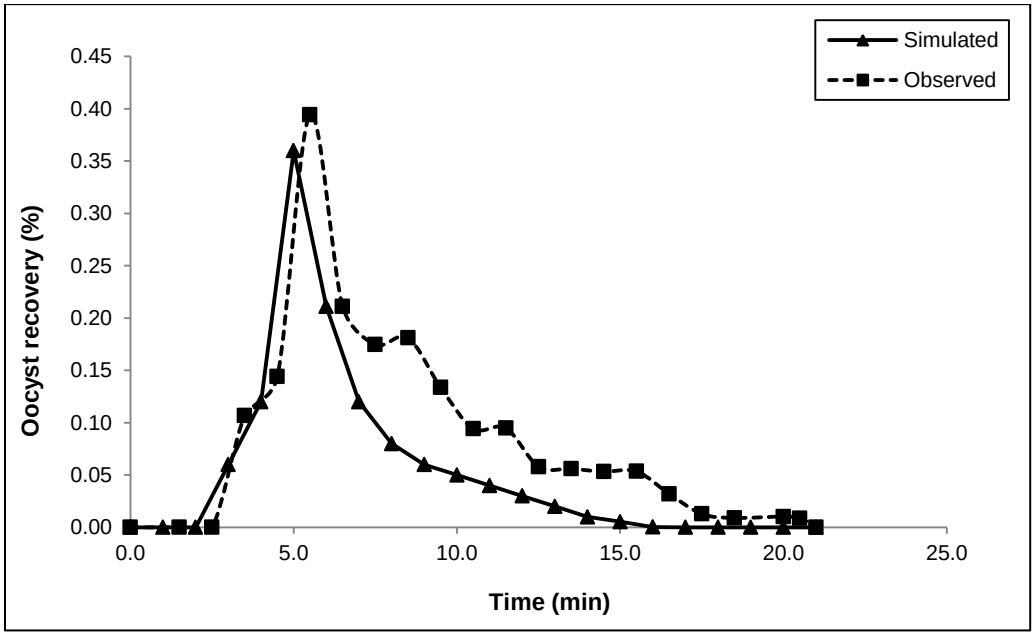

Figure 6.70 Rotavirus transport in surface runoff simulation for Alvin soil bed with Fescue vegetation subjected to 6.35 cm/hr rainfall applied for 20 minutes at 2.5% slope.

Figures 6.71, 6.72 and 6.73 show the comparison of rotavirus break-through experimental data with pathogen transport model simulation result for surface runoff for bare ground and two vegetated (Brome grass and Fescue) conditions for Catlin soil. In all three cases of bare and vegetated cover beds, the pathogen transport model produced reasonable results as compared with the observations as shown below. Computed R^2 values for bare, Brome grass and Fescue cover conditions were 0.60, 0.77 and 0.71, respectively.

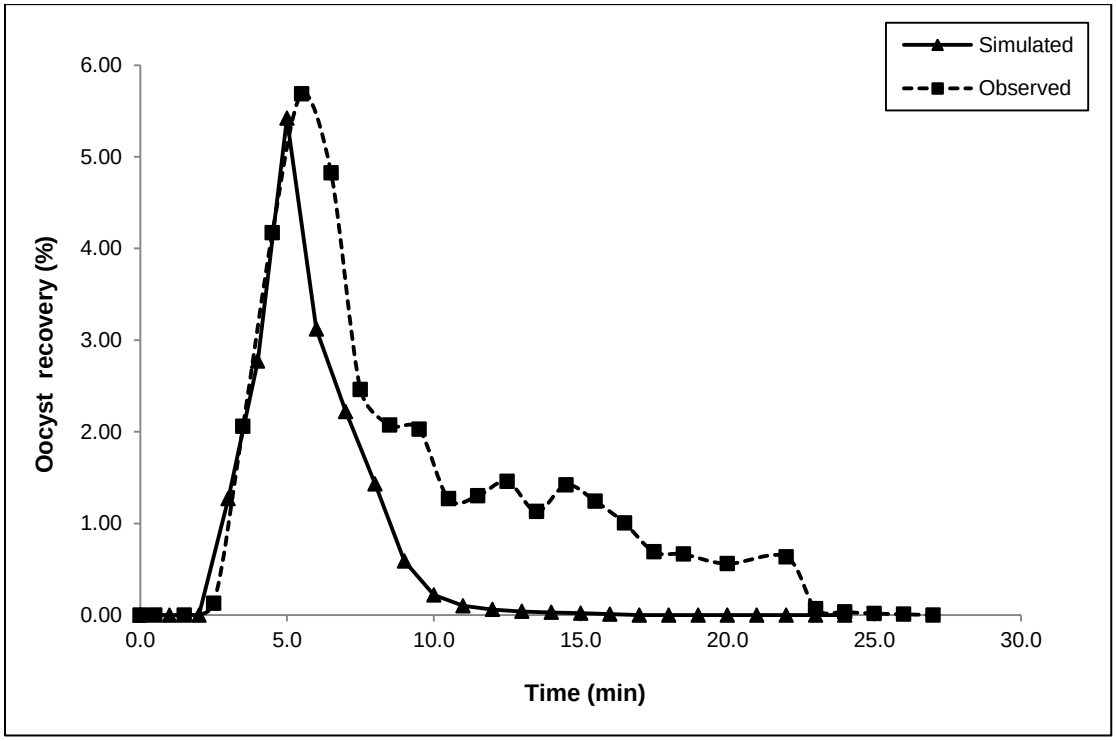

Figure 6.71 Rotavirus transport in surface runoff simulation for bare Catlin soil bed with subjected to 6.35 cm/hr rainfall applied for 20 minutes at 2.5% slope.

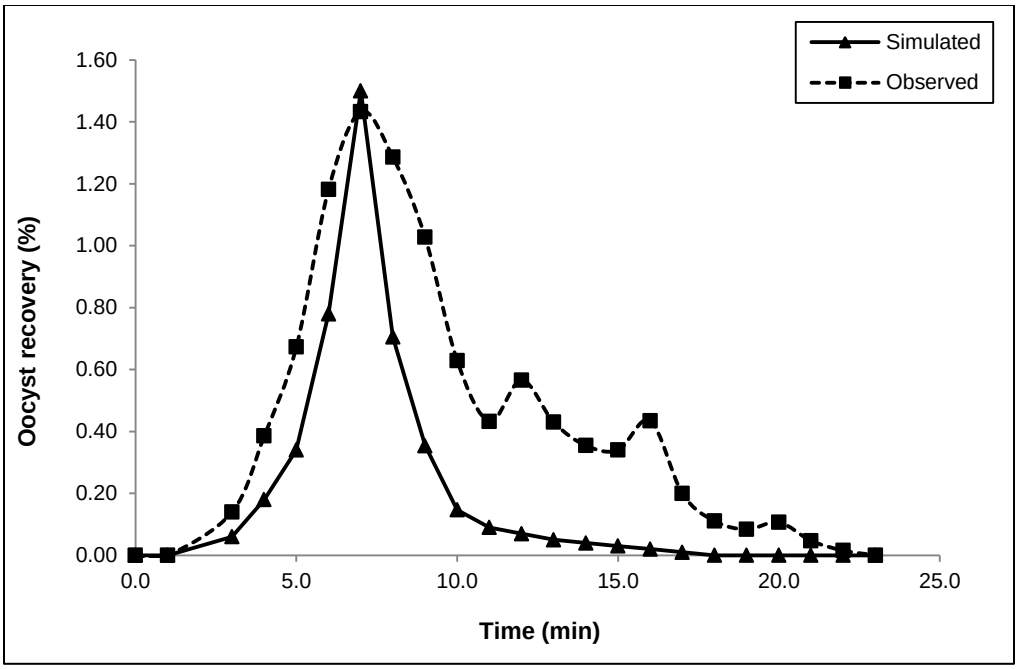

Figure 6.72 Rotavirus transport in surface runoff simulation for Catlin soil bed with Brome grass vegetation subjected to 6.35 cm/hr rainfall for 20 minutes at 2.5% slope.

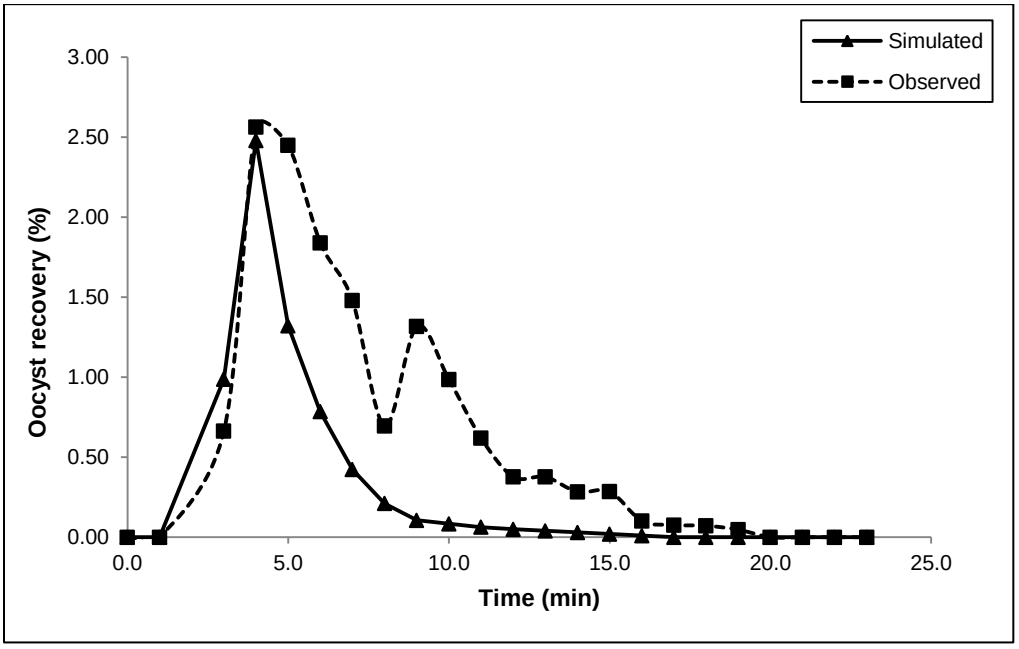

Figure 6.73 Rotavirus transport in surface runoff simulation for Catlin soil bed with Fescue vegetation subjected to 6.35 cm/hr rainfall applied for 20 minutes at 2.5% slope.

Figures 6.74, 6.75 and 6.76 show the comparison of rotavirus break-through experimental data with pathogen transport model simulation result for surface runoff for bare ground and two vegetated (Brome grass and Fescue) conditions for Darwin soil. In all three cases of bare and vegetated cover beds, the experimental data showed more than one peak. Although pathogen transport model reproduced the first peak, it could not replicate remaining peaks observed in experimental data, resulting in low R^2 values. Computed R^2 values for bare, Brome grass and Fescue cover conditions were 0.61, 0.26 and 0.75, respectively.

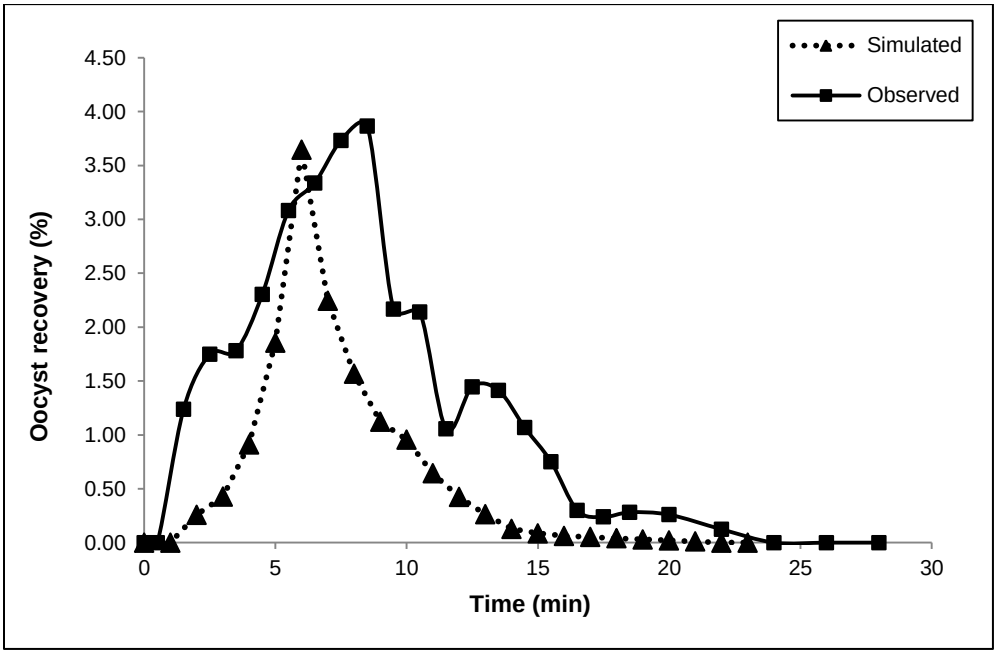

Figure 6.74 Rotavirus transport in surface runoff simulation for bare Darwin soil bed subjected to 6.35 cm/hr rainfall applied for 20 minutes at 2.5% slope.

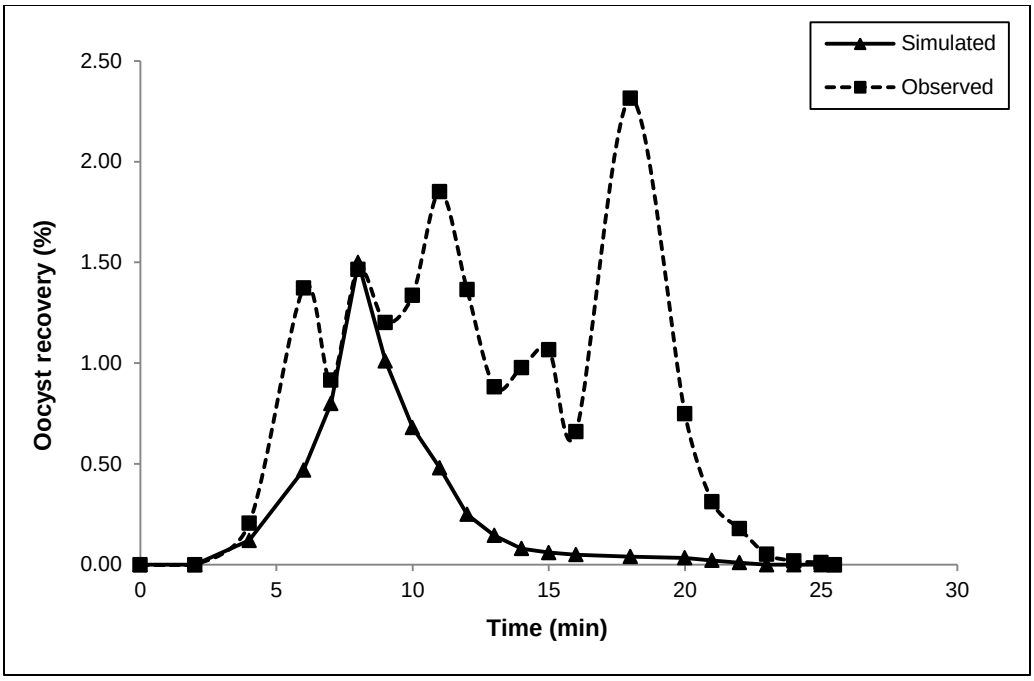

Figure 6.75 Rotavirus transport in surface runoff simulation for Darwin soil bed with Brome grass vegetation subjected to 6.35 cm/hr rainfall for 20 minutes at 2.5% slope.

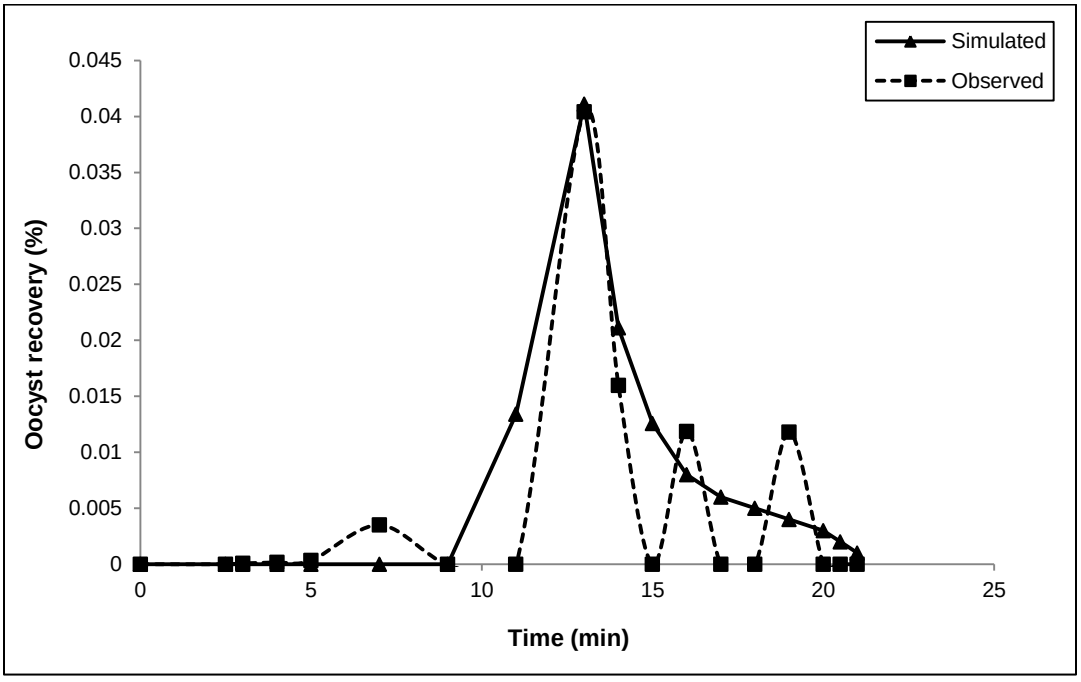

Figure 6.76 Rotavirus transport in surface runoff simulation for Darwin soil bed with Fescue vegetation subjected to 6.35 cm/hr rainfall applied for 20 minutes at 2.5% slope.

Figures 6.77 shows the comparison of simulated total rotavirus recovery from pathogen transport model with experimental result from small scale experiments for all surface cover, slope and rainfall conditions. The comparison graph indicates that that the pathogen transport model can predict total rotavirus recovery fairly well in case of small scale laboratory experiments in most cases ($R^2 = 0.93$).

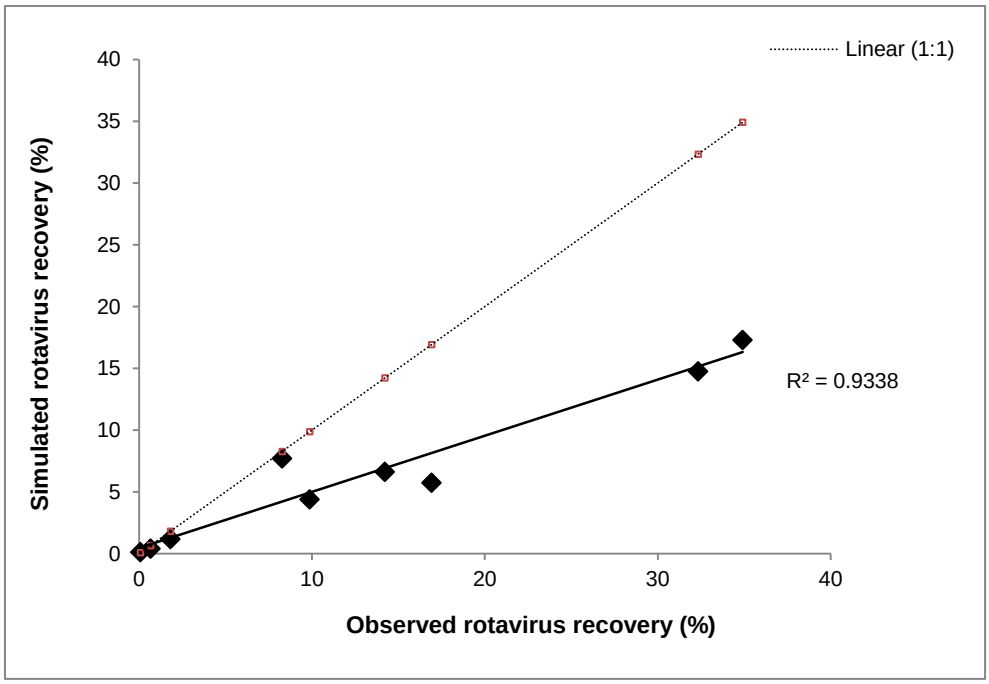

Figure 6.77 Comparison of rotavirus transport model simulation result with observations for total rotavirus recovery for different slopes, rainfall and surface cover conditions for Alvin, Catlin and Darwin soils.

Although the relationship provided by Ling *et al.* (2003) gave an initial parameter to drive the model, the one parameter approach for all slope, cover and rainfall conditions didn't result satisfactory result in this study. In absence of a reliable approach that can incorporate the effect of variability in rainfall intensity (or its surrogates like flow depth and velocity), slope and

soil types in a partitioning coefficient, the parameter K_{12} had to be calibrated for each case by comparing model results with the experimental data. The different values of attachment rate parameter k_{12} for bare and vegetated surface were used during simulation process to replicate the result obtained from the experiments. These simulation results indicate that one portioning parameter for varying environmental and topographic condition may not work for *C. parvum* oocysts and similar microorganisms and future modeling attempts have to include the dynamic nature of environmental and topographic conditions for formulating portioning parameter.

Table 6.8 shows calibrated *C. parvum* oocysts partition coefficients for three slopes, two rainfall intensities, bare and vegetated surface condition for both Catlin and Newberry soils. In case of bare soil simulations, it was observed that the parameters K_{12} and K_{21} were more sensitive compared to the parameter K_{23}. It should be noted that the effect of the parameter K_{23} could not be accessed effectively in this exercise due to the absence of measured data on oocyst and soil aggregate. Parameter K_{12} affected the peak of pathogen recovery curve while the parameter K_{21} dictated the shape of the curve. Parameter K_{23} governed the formation of oocysts and soil particle aggregate which was not quantified in this study. In case of vegetated surface, parameters K_{12} and K_{14} were two sensitive parameters, which governed how many oocysts got attached to soil surface and vegetation, respectively. Parameters K_{21} and K_{41} were another set of sensitive parameters which governed how many oocysts got released from soil surface and vegetation, respectively.

Table 6.8 Calibrated model coefficients for different slope, rainfall intensity, cover condition and soil.

Soil Type	Rainfall intensity	Slope	Cover condition	Parameters				
				K_{12}	K_{21}	K_{23}	K_{14}	K_{41}
Catlin	6.35 in/hr	1.5%	Bare	0.254	0.074	0.05		
		3.0%	Bare	0.235	0.116	0.05		
		4.5%	Bare	0.127	0.194	0.03		
Newberry	2.54 in/hr	1.5%	Bare	0.155	0.183	0.05		
		3.0%	Bare	0.224	0.103	0.05		
		4.5%	Bare	0.208	0.126	0.05		
Newberry	6.35 in/hr	1.5%	Bare	0.155	0.165	0.05		
		3.0%	Bare	0.106	0.208	0.02		
		4.5%	Bare	0.088	0.245	0.01		
Catlin	6.35 in/hr	1.5%	Vegetated	0.256	0.070	0.05	0.135	0.128
		3.0%	Vegetated	0.238	0.111	0.05	0.282	0.021
		4.5%	Vegetated	0.129	0.191	0.05	0.118	0.187
Newberry	2.54 in/hr	1.5%	Vegetated	0.225	0.054	0.05	0.285	0.024
		3.0%	Vegetated	0.328	0.028	0.05	0.365	0.035
		4.5%	Vegetated	0.236	0.089	0.05	0.105	0.165
Newberry	6.35 in/hr	1.5%	Vegetated	0.266	0.078	0.05	0.128	0.135
		3.0%	Vegetated	0.225	0.084	0.05	0.108	0.146
		4.5%	Vegetated	0.185	0.105	0.05	0.095	0.158

Table 6.9 shows calibrated *C. parvum* oocysts and rotavirus partition coefficients for bare and vegetated surface conditions for Alvin, Catlin and Darwin soils. It was observed that the parameters K_{12} and K_{21} were more sensitive compared to the parameter K_{23}. As in case of large scale experiment simulation, parameter K_{12} affected the peak of pathogen recovery curve while the parameter K_{21} dictated the shape of the curve. Parameter K_{23} governed the formation of pathogen and soil particle aggregate which was not quantified in this study. In case of vegetated surface, parameters K_{12} and K_{14} were two sensitive parameters, which governed how many pathogens got attached to soil surface and vegetation, respectively. Parameters K_{21} and K_{41} were another set of sensitive parameters which governed how many pathogens got released from soil surface and vegetation, respectively.

Table 6.9 Calibrated model coefficients for different cover conditions and soil types for *C. parvum* and Rotavirus.

Soil Type	Pathogen	Cover condition	Parameters				
			K_{12}	K_{21}	K_{23}	K_{14}	K_{41}
Alvin	*C. parvum*	Bare	0.654	0.081	0.05		
		Vegetated (Brome)	0.335	0.048	0.05	0.305	0.098
		Vegetated (Fescue)	0.368	0.014	0.03	0.417	0.021
Catlin	*C. parvum*	Bare	0.154	0.184	0.05		
		Vegetated (Brome)	0.104	0.148	0.05	0.108	0.187
		Vegetated (Fescue)	0.125	0.166	0.05	0.095	0.214
Darwin	*C. parvum*	Bare	0.128	0.198	0.03		
		Vegetated (Brome)	0.106	0.208	0.02	0.265	0.035
		Vegetated (Fescue)	0.088	0.245	0.01	0.105	0.165
Alvin	Rotavirus	Bare	0.201	0.136	0.05		
		Vegetated (Brome)	0.341	0.046	0.05	0.314	0.084
		Vegetated (Fescue)	0.229	0.131	0.05	0.208	0.116
Catlin	Rotavirus	Bare	0.154	0.184	0.05		
		Vegetated (Brome)	0.228	0.128	0.05	0.156	0.085
		Vegetated (Fescue)	0.236	0.089	0.05	0.186	0.098
Darwin	Rotavirus	Bare	0.161	0.178	0.05		
		Vegetated (Brome)	0.245	0.081	0.05	0.189	0.092
		Vegetated (Fescue)	0.342	0.042	0.05	0.315	0.091

Experimental data showed multiple peaks in many cases, both for bare and vegetated cover conditions which the model could not reproduce. There might be few plausible reasons that may lead to the generation of multiple peaks. For example, it was observed that the rate of sediment transport was very high during large scale experiments under high rainfall intensity and slope conditions that clogged the outflow system temporarily. When the clogging was cleared by backlogged flow periodically, this may have resulted in multiple peaks of pathogens in surface flow. Similarly, pathogens may get driven by a threshold flow velocity or depth. Due to irregularities in bed surface, the flow velocity or depth may reach the threshold value at a particular point in multiple time frames. Furthermore, the bed profile keeps on changing during the experimental time period due to runoff and erosion. The settled pathogens may get buried

under eroded sediment at the beginning. Once the sediment is driven further down due to the flow, the pathogens may get liberated back to flow. In case of vegetated surface, the flow threshold that detaches the pathogens from soil and vegetated surface may be different which may lead to the generation of multiple peaks. Similarly, it should also be noted that the model only incorporates the physical interaction between pathogen and soil particles but it doesn't cover the important chemical interaction phenomenon between them. It should also be noted that there is a procedural difference between data analysis in case of large and small scale *C. parvum* transport experiments.

It is also worth noting that the studies by Trask *et al.* (2004) did not use an infectivity assay for analysis of water samples and hence recovery represented total percent of *C. parvum* oocysts in the sample. Koch (2009) and Davidson (2010) used infectivity assay for water sample analysis and hence their data represented the recovery of oocyst that remained infectious. Since the experimental duration was of very short in both cases, it can be assumed that the fraction of oocyst that got inactivated during the experiment was negligible. A study from Kato *et al.* (2004) indicated that *C. parvum* oocyst can survive in soil in natural environment for many days.

6.3.6 Rainfall and overland flow induced erosion patterns

A series of laboratory experiments were carried out to compare the erosion patterns induced from rainfall and overland flow. Figures 6.78 and 6.79 show the flow rate and sediment concentration patterns induced by 2.25 cm/hr rainfall applied for a 20 minutes duration with soil bed slope of 1.5 and 4.5%, respectively. It was observed that there was no significant change in runoff rate at the end of the bed due to change in bed slope. However, the sediment concentration

generally increased with the increase in the bed slope. With the increase in bed slope, the flow velocity might increase which can contribute to higher erosion rate.

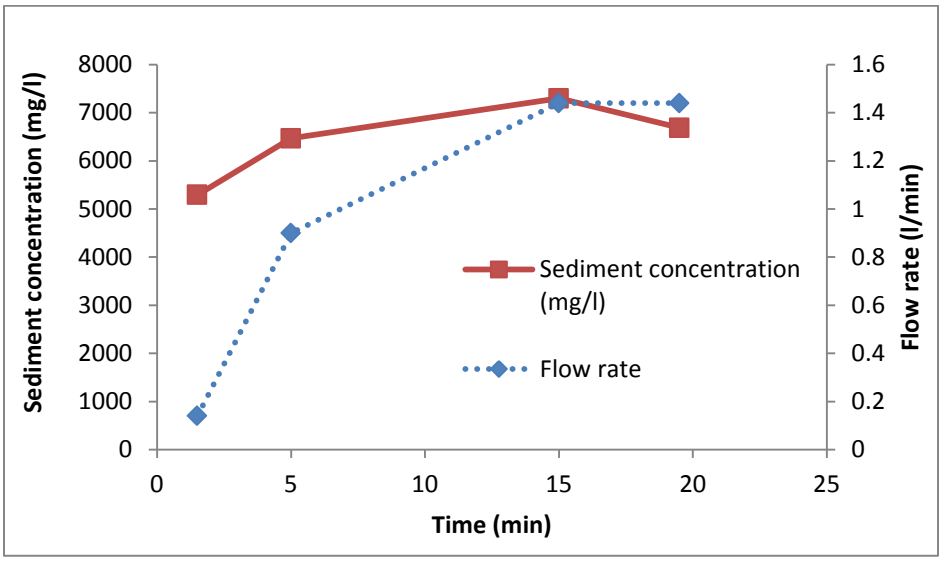

Figure 6.78 Flow rate and sediment concentration pattern from 2.54 cm/hr rainfall applied for 20 minutes to bare soil bed of 1.5% slope.

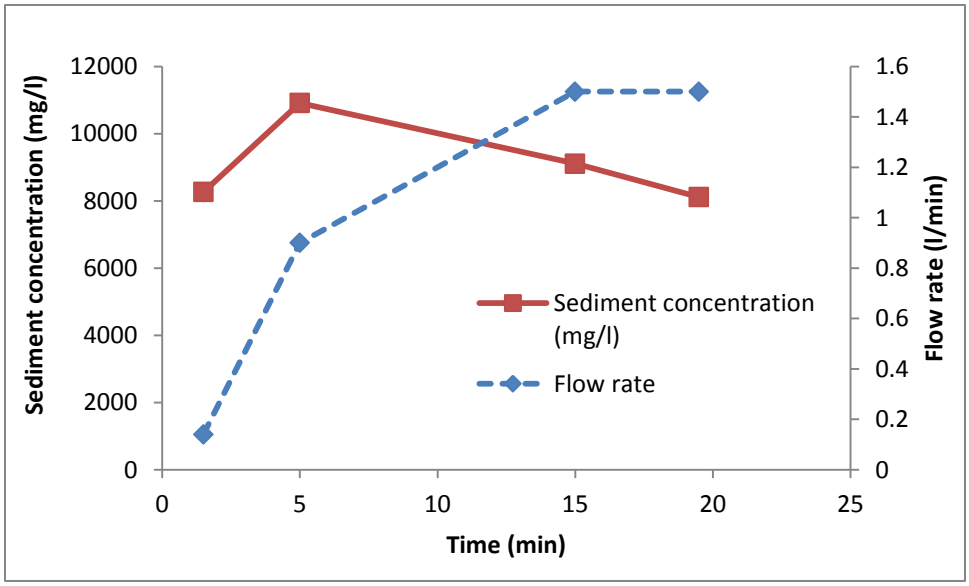

Figure 6.79 Flow rate and sediment concentration pattern from 2.54 cm/hr rainfall applied for 20 minutes to bare soil bed of 4.5% slope.

Figure 6.80 shows the flow rate and sediment concentration patterns induced by 6.35 cm/hr rainfall applied for 20 minutes duration with 1.5% soil bed slope. Similarly, Figure 6.81 shows the flow rate and sediment concentration pattern induced by 6.35 cm/hr rainfall applied for 10 minutes duration with 4.5% soil bed slope. The was collected for only 10 minutes for higher slope condition since the rainfall simulator system broke in the middle of the experiment. The experimental data showed that there was no significant change in runoff rate at the end of the bed due to change in bed slope. However, the sediment concentration increases with the increase in the bed slope. With the increase in bed slope, the flow velocity might increase contributing to higher erosion rate.

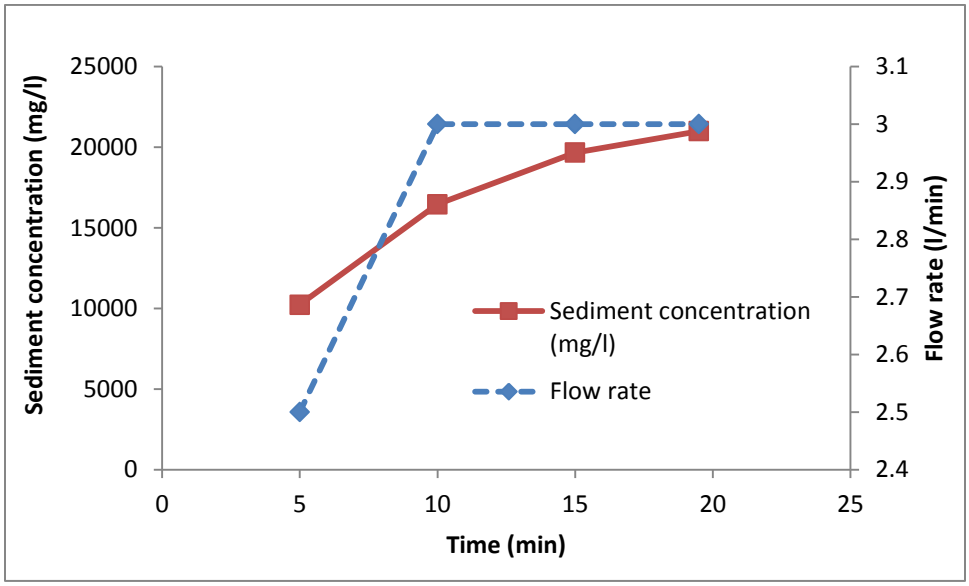

Figure 6.80 Flow rate and sediment concentration pattern from 6.35cm/hr rainfall applied for 20 minutes to bare soil bed of 1.5% slope.

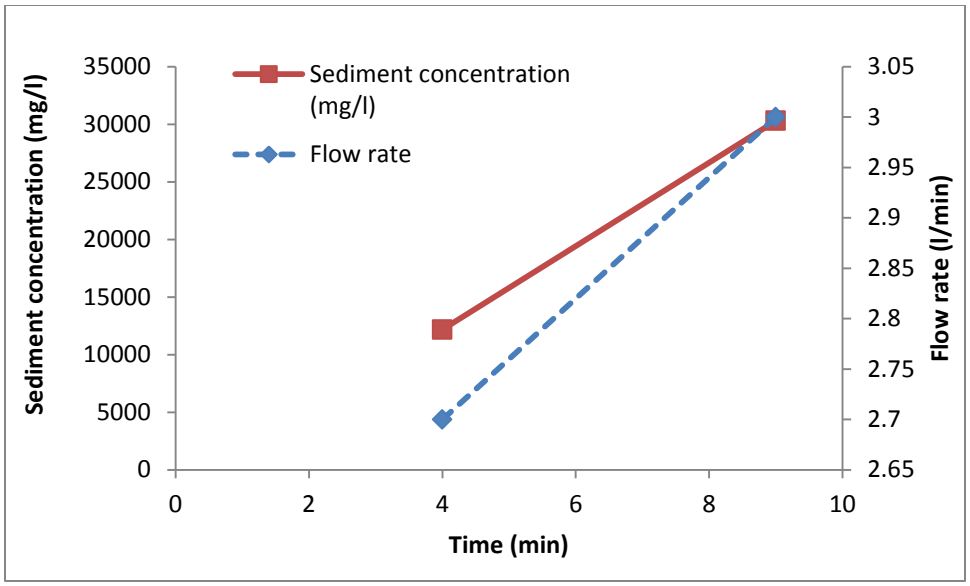

Figure 6.81 Flow rate and sediment concentration pattern from 6.35cm/hr rainfall applied for 20 minutes to bare soil bed of 4.5% slope.

Figures 6.82 and 6.83 show the flow rate and sediment concentration pattern induced by 0.00235 cfs (4 liter/min) inflow applied for 20 minutes duration with soil bed slope of 1.5 and 4.5% respectively. The experimental result showed that there was no significant change in runoff rate at the end of the bed due to change in bed slope. However, the sediment concentration increased with the increase in the bed slope. With the increase in bed slope, the flow velocity might increase causing higher erosion rate. It was also noted that the flow rate increased during the first half interval of the experiment while the sediment concentration decreased during the same interval. The soil bed may have slowly saturated during the experiment gradually increasing the runoff rate at the end of the bed. The flow might have picked loose sediments at the beginning of the experiment generating higher sediment concentration during the first half of the experiment.

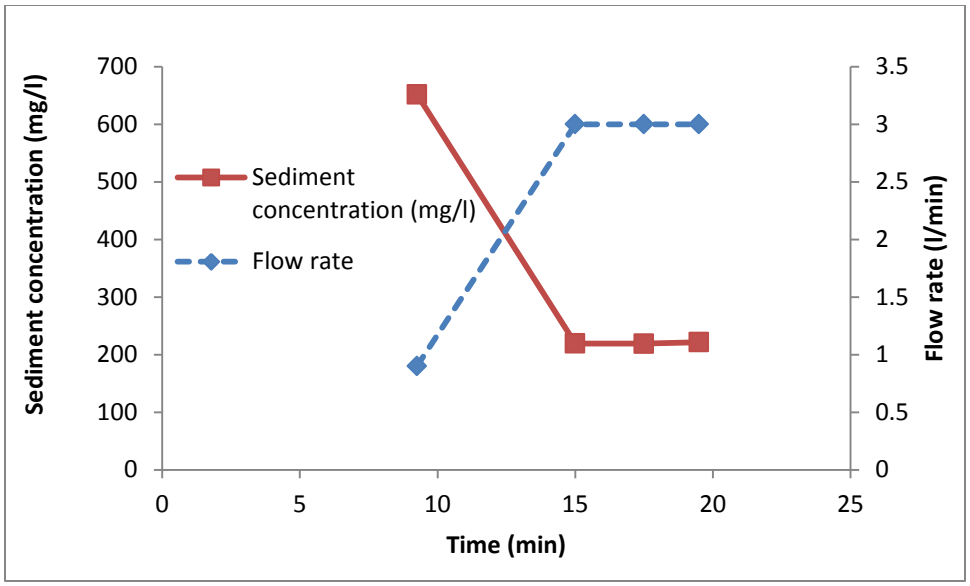

Figure 6.82 Flow rate and sediment concentration pattern from 4 liter/min inflow applied for 20 minutes to bare soil bed of 1.5% slope.

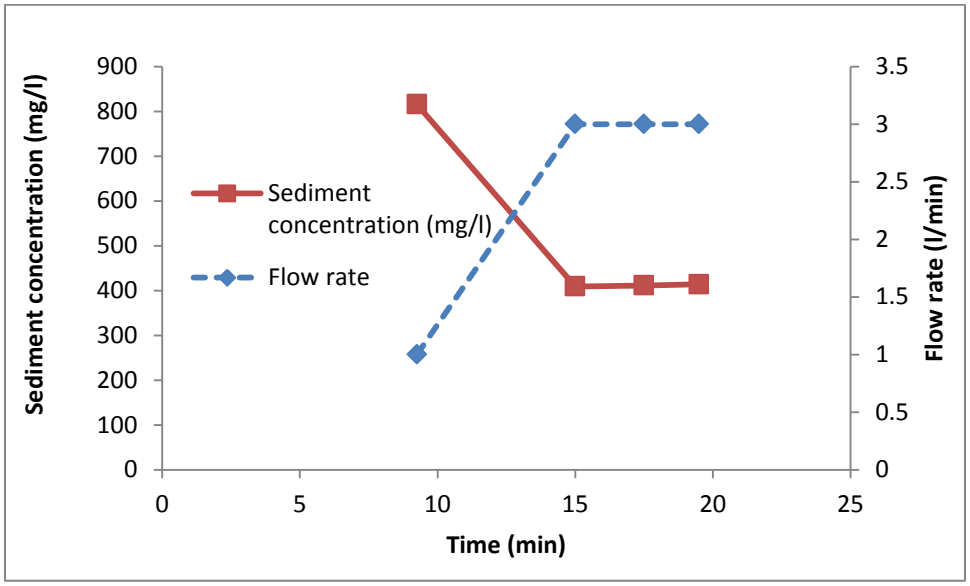

Figure 6.83 Flow rate and sediment concentration pattern from 4 liter/min inflow applied for 20 minutes to bare soil bed of 4.5% slope.

Figure 6.84 and 6.85 show the flow rate and sediment concentration pattern induced by 0.00470 cfs (8 liter/min) inflow applied for 20 minutes duration with soil bed slope of 1.5 and

4.5% respectively. Even though the sediment concentration increased with the increase in the bed slope, there was no significant change in runoff rate due to change in bed slope. The flow velocity might increase with the increase in bed slope, which can contribute to higher erosion rate. This is evident from the experimental data. Since the soil bed was fully saturated before the experiment, it was noted that the flow rate remained constant during the experiment while the sediment concentration decreased gradually.

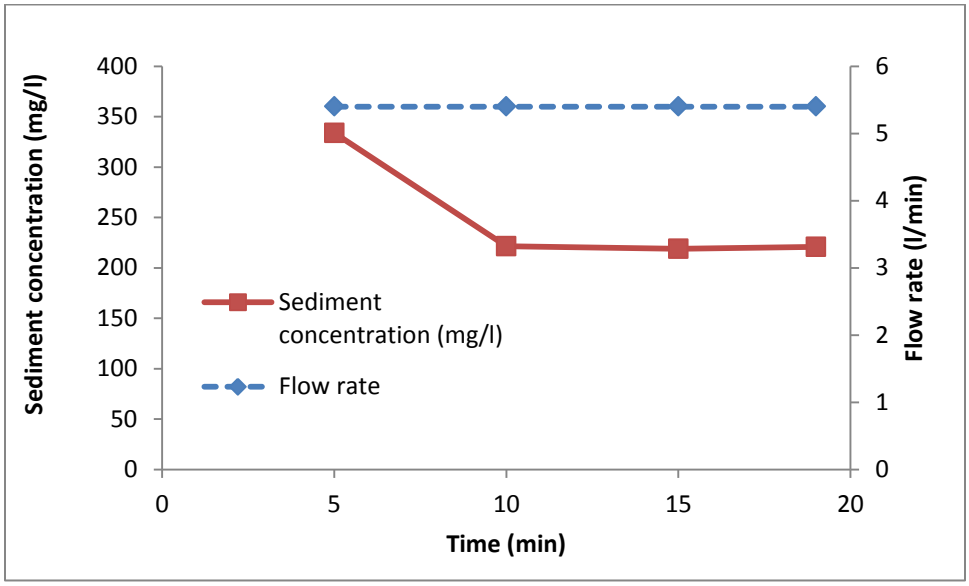

Figure 6.84 Flow rate and sediment concentration pattern from 8 liter/min inflow applied for 20 minutes to bare soil bed of 1.5% slope.

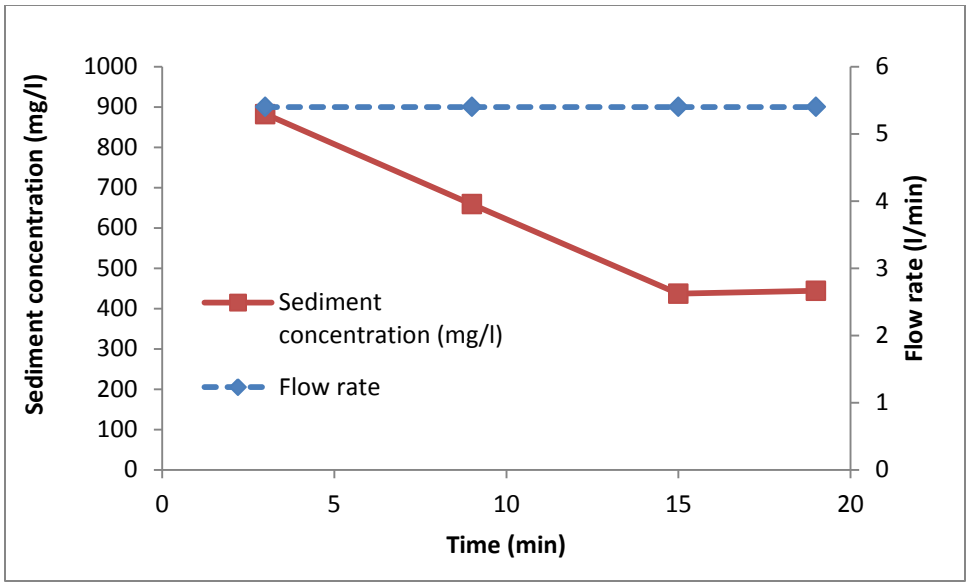

Figure 6.85 Flow rate and sediment concentration pattern from 8 liter/min inflow applied for 20 minutes to bare soil bed of 4.5% slope.

One important finding from these experiments was that the sediment concentration was significantly higher in surface flow generated by rainfall compared to that of flow from runoff only for similar flow condition (Figures 6.80 and 6.82). The implication for this particular phenomenon for pathogen transport could be is such that the pathogens attached to soil particles might move downstream in higher rate when the flow is induced by rainfall compared to the flow generated from overland flow alone for a similar outflow condition.

CHAPTER 7: CONCLUSION

Following key conclusions have been drawn from this study:

1. An extensive review of the literatures related to models developed to simulate microbial pathogens transport processes was carried out. Although a large variety of models exist for pathogen transport, very few models are physically-based and incorporate the dynamic phenomenon of sediment-pathogen interaction. The validation of the existing models is limited due to the scarcity of quality data on pathogen transport. The review effort provided greater insight into the modeling efforts and their applicability, strength and challenges. Major limitation for most modeling effort was unavailability of quality data for model verification. Based on the review study, the basis of the modeling effort of this study was drawn and formulated.
2. A physically-based approach for modeling microbial pathogen transport model for *C. parvum* and rotavirus fate and transport in surface flow has been developed and presented in this study. Deterministic descriptions of the processes have been employed and a correspondence between them has been established. Some of the model parameters have been incorporated based on previous studies. Another feature of the model is the incorporation of an erosion model (WEPP) into the microorganism transport model, thereby establishing a link between the sediment and microbial transport, and highlighting the capability of the suspended sediment to transport microorganisms in the overland flow.
3. Model results were compared with two experimental data sets: large-scale and small-scale laboratory experimental data. The model results showed good agreements with observed data in most cases. Although the model replicated the kinetics of *C. parvum* and

rotavirus recovery from surface runoff, it under-predicted recovery amount in few cases. Experimental data showed multiple peaks in pathogen break-through curve, however this phenomenon could not be simulated by the modeling framework. The model could only replicate the timing and magnitude of the first peak. The multiple peaks observed in experimental data can be attributed to different factors. For example, it was observed that increase in rainfall intensity and slope resulted in high sediment transport that clogged the outflow system temporarily in large scale experiments. When the clogging was cleared periodically by backlogged flow, this may have resulted in multiple peaks of pathogens in surface flow. Similarly, the pathogens may not interact with sediment and vegetation in the same fashion. This may lead to different release rate of the attached pathogen from soil surface and vegetation. Furthermore, the sediment can get deposited over the pathogens due to flow and it may suppress the pathogen movement temporarily till the sediment particle moved downstream.

4. Overall, the new model that has been developed in this study works satisfactorily. The model results have been compared with data observed under different experimental conditions and the model performed well in most cases.
5. It has been realized that further validation of the model results may be required with data collected from field scale experiments. Accordingly, some processes may need to be strengthened and incorporated in the model for greater applicability. This is one of the first modeling efforts to simulate transport of infective (alive) *C. parvum* and rotavirus in the environment. In future activities, other processes (for example biological/growth processes) may be incorporated, although it might add more complications to the modeled processes.

6. With further verification of the model results under various experimental conditions, the model can be used for designing BMP (such as VFS) to control microbial pathogen transport into water resources. This may help in determining size of vegetative filters, location, vegetation type, and soil type of VFS or similar other BMPs for controlling pathogen transport from sources to our water systems.

CHAPTER 8: RECOMMENDATION FOR FUTURE WORK

- Design a series of experiments to evaluate the model parameters (K_{12}, K_{23}, K_{21}, K_{14}, K_{41}) precisely. If the experiments are designed to estimate the model parameters with better precision, it will significantly increase the predictability and reduce the model uncertainty.

- Conduct laboratory experiments under shallow overland flow conditions to observe and collect data on sediment transport and associated pathogen transport. Validating the model with data collected from this set of experiments will increase the applicability of the model.

- Conduct field-scale overland transport studies for pathogens like *C. parvum*, rotavirus, and similar emerging pathogens to evaluate the model. Field-scale studies would be very beneficial for confirming results from the modeling framework proposed in this study.

- Investigate the chemical interactions between pathogen and sediment particles under different environmental conditions. Although the model captures the physical interactions between pathogen and sediment, a better understanding of chemical interactions between them might help to improve the modeling framework. Additional pathogen interactions with various types of vegetation and its associated features like leaves and roots should be investigated.

- Translate the model framework to watershed scale. The proposed modeling framework is simple and has the potential to be transformed to watershed scale.

REFERENCES

Abbaszadegan, M., M. LeChevallier, and C. P. Gerba. 2003. Occurrence of viruses in U.S. groundwaters. *J. Am. Water Works Ass.* 95(9): 107-120.

Ansari, S. A., S. A. Sattar, V. S. Springthorpe, G. A. Wells, and W. Tostowaryk. 1988. Rotavirus survival on human hands and transfer of infectious virus to animate and nonporous inanimate surfaces. *J. Clin. Microbiol.* 26(8): 1513-1518.

Ansari, S. A., V. S. Springthorpe, and S. A. Sattar. 1991. Survival and vehicular spread of human rotaviruses: possible relation to seasonality of outbreaks. *Rev. Infect. Dis.* 13: 448-461.

Arnold, J. G., R. Srinivasan, R. S. Muttiah, and J. R. Williams. 1998. Large area hydrologic modeling and assessment part I : Model development. *J. Am. Water Works As.* 34(1): 73-78.

Atwill E. R., L. Hou, B. M. Karle, T. Harter, K. W. Tate, and R. A. Dahlgren. 2002. Transport of *Cryptosporidium parvum* oocysts through vegetated buffer strips and estimated filtration efficiency. *Appl. Environ. Microbiol.* 68(11): 5517-5527.

Bartlett, A. V., M. Moore, G. W. Gary, K. M. Starko, J. J. Erben, and B. A. Meredith. 1985. Diarrheal illness among infants and toddlers in day care centres I. Epidemiology and pathogens. *J. Pediatr.* 107: 495-502.

Bates, B. C., Z. W. Kundzewicz, S. Wu, and J. P. Palutikof. 2008. Climate Change and Water. Technical Paper of the Intergovernmental Panel on Climate Change. IPCC Secretariat, Geneva.

Beasley, D. B., L. F. Huggins, and E. J. Monke. 1980. ANSWERS: A model for watershed planning. *Trans. ASAE* 23(4): 938-944.

Bicknell, B. R., J. C. Imhoff, J. L. Kittle, A. S. Donigian, and R. C. Johanson. 1997. Hydrological Simulation Program - FORTRAN. User's Manual for Release 10. U.S. Environmental Protection Agency, Environmental Research Laboratory, Athens, GA.

Bines, J. 2006. Intussusception and rotavirus vaccines. *Vaccine* 24(18): 3772–3776.

Bingner, R. L. and F. D. Theurer. 2001. AnnAGNPS: estimating sediment yield by particle size for sheet & rill erosion. In: Proceedings of the Sedimentation: Monitoring, Modeling, and Managing, 7th Federal Interagency Sedimentation Conference, I1- I7. Reno, NV.

Bishop, R. F., G. P. Davidson, I. H. Holmes, and B. I. Ruck. 1974. Detection of a new virus by electron microscopy of faecal extracts from children with acute gastroenteritis. *Lancet*, i: 149-151.

Bishop, R.F. 1994. Chapter 6: Natural history of human rotavirus infection. In: *Viral Infections of the Gastrointestinal Tract*, 131-167. A. Z. Kapikian, ed. New York, USA: Marcel Dekker.

Bishop, R. F. 1996. Natural history of human rotavirus infection. *Arch. Virol. Supp.* 12: 119-28.

Bolin, C., C. Brown, and J. Rose. 2004. Chapter 2: Emerging zoonotic diseases and water. In: *Waterborne Zoonoses: Identification, Causes and Control*, 19-26. J.A. Cotruvo, A. Dufour, G. Rees, J. Bartram, R. Carr, D.O. Cliver, G.F. Craun, R. Fayer, and V.P.J. Gannon, eds. London, UK: IWA Publishing.

Bouraoui, F., I. Braud, and T. A. Dillaha. 2002. Chapter 22: ANSWERS: A nonpoint -source pollution model for water, sediment, and nutrient losses. In: *Mathematical Models of Small Watershed Hydrology and Applications*, 833-882.V.P. Singh and D.K. Frevert, eds. Highlands Ranch, CO, USA: Water Resources Publications.

Brown, K. W., S. G. Jones, and K. C. Donelly. 1980. The influence of simulated rainfall on residual bacteria and virus on grass treated with sewage sludge. *J. Environ.Qual.* 9(2): 261-265.

Brush, C. F., W. C. Ghiorse, L. J. Anguish, J. Parlange, and H. G. Grimes. 1999. Transport of *Cryptosporidium parvum* Oocysts through Saturated Columns. *J. Environ.Qual.* 28: 809-815.

Bryden, A. S., M. E. Thouless, and T. H. Flewett. 1976. A rabbit rotavirus. *Vet. Rec.* 99: 323.

Bukhari, Z., M. M. Marshall, D. G. Korich, C. R. Fricker, H. V. Smith, J. Rosen, and J. L. Clancy. 2000. Comparison of *Cryptosporidium parvum* Viability and Infectivity Assays following Ozone Treatment of Oocysts. *Appl. Environ. Microbiol.* 66(7): 2972-2980.

Canale, R., M. Auer, E. Owens, T. Heidtke, and S. Effler. 1993. Modelling fecal coliform bacteria II. Model development and application. *Water Res.* 27: 703-714.

Capper, J. L., R. A. Cady, and D. E. Bauman. 2009. The environmental impact of dairy production: 1944 compared with 2007. *J. Anim. Sci.* 87(6): 2160-2167.

Casemore, D., S. Wright, and R. Coop. 1997. Chapter 3: Cryptosporidiosis - human and animal epidemiology. In: *Cryptosporidium and Cryptosporidiosis*, 65-92. L. R. Fayer, ed. New York, USA: CRC Press.

CDC. 2009. Bioterrorism Agents/Disease. Atlanta, GA: Centers for disease control and prevention. Available at: http://www.bt.cdc.gov/agent/agentlist-category.asp. Accessed 7 March 2009.

CDC. 2011. Rotavirus. GA: Centers for disease control and prevention. Available at: http://www.cdc.gov/rotavirus/index.html. Accessed 15 June 2011.

Chaplin, M. 2006. Do we underestimate the importance of water in cell biology? *Nat. Rev. Mol. Cell Bio.* 7: 861-866.

Chen, X., J. S. Keithly, C. V. Paya, and N. F. LaRusso. 2002. Cryptosporidiosis. *New Engl. J. Med.* 346: 1723-1731.

Chow, V. T., D. R. Maidment, and L. W. Mays. 1988. *Applied Hydrology*. New York, USA: McGraw-Hill.

Clark, D. P. 1999. New insights into human cryptosporidiosis. *Clin. Microbiol. Rev.* 12(4): 554-563.

Cochrane, T. A. and D. C. Flanagan. 1999. Assessing water erosion in small watersheds using WEPP with GIS and digital elevation models. *J. Soil Water Conser.* 54(4): 678-685.

Coffey, R., E. Cummins, V. O'Flaherty, and M. Cormican. 2010. Analysis of the soil and water assessment tool (SWAT) to model *Cryptosporidium* in surface water sources. *Biosyst. Eng.* 106(3): 303-314.

Collins, R. and K. Rutherford. 2004. Modelling bacterial water quality in streams draining pastoral land. *Water Res.* 38: 700-712.

Connolly, R. D., C. A. A. Ciesiolka, D. M. Silburn, and C. Carroll. 1997. Distributed parameter hydrology model (Answers) applied to a range of catchment scales using rainfall simulator data. IV Evaluating pasture catchment hydrology. *J. Hydrol.* 201 (1-4): 311-328.

Conner, M. E. and R. W. Darlington. 1980. Rotavirus infection in foals. *Am. J. Vet. Res.* 41(10): 1699-703.

Conner, M. E., M. K. Estes and D. Y. Graham. 1988. Rabbit model of rotavirus infection. *J. Virol.* 62(5): 1625-1633.

Cook, N., J. Bridger, K. Kendall, M. I. Gomara, L. El-Attar, and J. Gray. 2004. The zoonotic potential of rotavirus. *J. Infection*, 48(4): 289-302.

Cortis, A., T. Harter, L. Hou, E. R. Atwill, A. I. Packman, and P. G. Green. 2006. Transport of *Cryptosporidium parvum* in porous media: Long-term elution experiments and continuous time random walk filtration modeling. *Water Resour. Res.* 42, W12S13, doi:10.1029/2006WR004897.

Cotruvo, J. A., A. Dufour, G. Rees, J. Bartram, R. Carr, D. O. Cliver, G. F. Craun, R. Fayer, and V. P. J. Gannon. 2004. *Waterborne Zoonoses – Identification, Causes and Control*. London, UK: IWA Publishing.

Craun, G., R. Calderon, and M. Craun. 2004. Chapter 8: Waterborne outbreaks caused by zoonotic pathogens in the USA. In: *Waterborne Zoonoses: Identification, Causes and Control*, J. A. Cotruvo, A. Dufour, G. Rees, J. Bartram, R. Carr, D. O. Cliver, G. F. Craun, R. Fayer, and V. P. J. Gannon, eds. London, UK: IWA Publishing.

Craun, M. F., G. F. Craun, R. L. Calderon and M. J. Beach. 2006. Waterborne outbreaks reported in the United States. *J. Water Health* 4(2): 19-30.

Current, W. L. and L. S. Garcia. 1991. Cryptosporidiosis. *Clin. Microbiol. Rev.* 4(3): 325-358.

Darnault, C. J. G., T. S. Steenhuis, P. Garnier, Y. Kim, M. B. Jenkins, W. C. Ghiorse, P. C. Baveye, and J. Y. Parlange. 2004. Preferential Flow and Transport of *Cryptosporidium parvum* Oocysts through the Vadose Zone: experiments and modeling. *Vadose Zone J.* 3: 262-270.

Davidson, P. C. 2007. Characterization of rotavirus survival in soil. M. S. Thesis. Urbana, Illinois: University of Illinois, Department of Agricultural and Biological Engineering.

Davidson, P. C. 2010. Characterization of pathogen transport in overland flow. Ph.D. Diss. Urbana, Illinois: University of Illinois, Department of Agricultural and Biological Engineering.

Davies, C. M., C. Kaucner, D. Deere, and N. J. Ashbolt. 2003. Recovery and Enumeration of Cryptosporidium parvum from Animal Fecal Matrices. *Appl. Environ. Microb.* 69(5): 2842-2847.

Davies, C. M., C. M. Ferguson, C. Kaucner, N. Altavilla, D. A. Deere and N. J. Ashbolt. 2004. Dispersion and transport of *Cryptosporidium* oocysts from fecal pats under simulated rainfall events. *Appl. Environ. Microbiol.* 70: 1151-1159.

Dennehy, P. H. 2008. Rotavirus vaccines: an overview. *Clin. Microbiol. Rev.* 21(1): 198–208.

Dorner, S. M., W. B. Anderson, R. M. Slawson, N. Kouwen and P. M. Huck. 2006. Hydrologic modeling of pathogen fate and transport. *Environ. Sci. Technol.* 40(15): 4746-53.

Drozd, C. and J. Schwartzbrod. 1996. Hydrophobic and Electrostatic Cell Surface Properties of *Cryptosporidium parvum*. *Appl. Environ. Microbiol.* 62: 1227-1232.

Dun, S., J. Q. Wu, W. J. Elliot, P. R. Robichaud, D. C. Flanagan, J. R. Frankenberger, R. E. Brown, and A. D. Xu. 2009. Adapting the Water Erosion Prediction Project (WEPP) model for forest applications. *J. Hydrol.* 366(1-4): 45-54.

DuPont, H. L., C. L. Chappell, C. R. Sterling, P. C. Okhuysen, J. B. Rose, and W. Jakubowski. 1995. The Infectivity of *Cryptosporidium parvum* in Healthy Volunteers. *New Engl. J. Med.* 332(13): 855-859.

Elshorbagy, A. and L. Ormsbee. 2006. Object-oriented modeling approach to surface water quality management. *Environ. Modell. Softw.* 21: 689-698.

EPA. 2000. National Water Quality Inventory. United States Environmental Protection Agency. Available at: http://water.epa.gov/lawsregs/guidance/cwa/305b/2000report_index.cfm. Accessed 15 February 2011.

Estes, M. K. 1990. Chapter 48: Rotaviruses and their replication. In: *Virology*, 1329-1404. B. N. Fields and D. M. Knipe, eds. New York, USA: Raven Press.

Fayer, R. 1994. Effect of High Temperature on Infectivity of *Cryptosporidium parvum* Oocysts in Water. *Appl. Environ. Microbiol.* 60: 2732-2735.

Fayer, R. and T. Nerad. 1996. Effects of Low Temperatures on Viability of *Cryptosporidium parvum* Oocysts. *Appl. Environ. Microbiol.* 62(4): 1431-1433.

Fayer, R., C.A. Speer and J.P. Dubey. 1997. Chapter 1: The General Biology of *Cryptosporidium*. In: *Cryptosporidium and Cryptosporidiosis*, 1-42. R. Fayer, ed. Boca Raton, Florida, USA: CRC Press.

Fayer, R., J. M. Trout, T. K. Graczyk and E. J. Lewis. 2000. Prevalence of *Cryptosporidium*, Giardia and Eimeria infections in post-weaned and adult cattle on three Maryland farms. *Vet. Parasitol.* 93(2): 103-112.

Fayer, R. 2004. *Cryptosporidium*: a water-borne zoonotic parasite. *Vet. Parasitol.* 126: 37-56.

Feng, N., J. A. Lawton, J. Gilbert, N. Kuklin, P. Vo, B. V. V. Prasad, and H. B. Greenberg. 2002. Inhibition of rotavirus replication by a non-neutralizing, rotavirus VP6–specific IgA mAb. *J. Clin. Invest.* 109(9): 1203-1213.

Ferguson, C. M., A. M. de Roda Husman, N. Altavilla, D. Deere, and N. J. Ashbolt. 2003. Fate and transport of surface water pathogens in watersheds. *Crit. Rev. Environ. Sci. Technol.*, 33: 299-361.

Ferguson, C. M., C. M. Davies, C. Kaucner, M. Krogh, J. Rodehutskors, D. A. Deere, and N. J. Ashbolt. 2007a. Field scale quantification of microbial transport from bovine faeces under simulated rainfall events. *J. Water Health* 5: 83-95.

Ferguson, C. M., B. F. W. Croke, P. J. Beatson, N. J. Ashbolt, and D. A. Deere. 2007b. Development of a process-based model to predict pathogen budgets for the Sydney drinking water catchment. *J. Water Health*, 5(2): 187-208.

Ferrari, M. and G. L. Gualandi. 1986. A serologic survey of rotavirus infection in pigs, *Microbiologica*, 9(1): 29-32.

Fischer, T. K., C. Viboud, U. Parashar, M. Malek, C. Steiner, R. Glass, and L. Simonsen. 2007. Hospitalizations and deaths from diarrhea and rotavirus among children <5 years of age in the United States. 1993-2003, *J. Infect. Dis.* 195(8): 1117-1125.

Flanagan, D. C. and M. A. Nearing. 1995. USDA-Water Erosion Prediction Project (WEPP) Hillslope Profile and Watershed Model Documentation. NSERL Report No. 10, National Soil Erosion Research Laboratory, USDA-Agricultural Research Service, West Lafayette, Indiana.

Flanagan, D. C., J. E. Gilley, and T. G. Franti. 2007. Water Erosion Prediction Project (WEPP): development history, model capabilities, and future enhancements. *Trans. ASABE* 50(5): 1603-1612.

Flewett, T. H., A. S. Bryden, and H. Davies. 1973. Virus particles in gastroenteritis. *Lancet*, ii: 1497.

Flewett, T. H., A. S. Bryden, H. Davies, G. N. Woode, J. C. Bridger, and J. M. Derrick. 1974. Relation between viruses from acute gastroenteritis of children and new born calves. *Lancet*, ii: 61-63.

Flewett, T. H., A. S. Bryden, and H. Davies. 1975. Virus diarrhoea in foals and other animals. *Vet. Rec.* 96: 477.

Fohrer, N., J. Berkenhagen, J. Hecker, and A. Rudolph. 1999. Changing soil surface conditions during rainfall single rainstorm/subsequent rainstorms. *Catena*, 37(3-4): 355-375.

Foster, S. O., E. L. Palmer, G. W. Gary, M. L. Martin, K. L. Herrmann, P. Beasley, and J. Sampson. 1980. Gastroenteritis due to rotavirus in an isolated Pacific Island group: An epidemic of 3,439 cases. *J. Infect. Dis.* 141: 32-39.

Fraser, R., P. Barten, and D. Pinney. 1998. Predicting stream pathogen loading from livestock using a geographical information systems-based delivery model. *J. Environ. Qual.* 27: 935-945.

Gajadhar, A. A. and J. R. Allen. 2004. Factors contributing to the public health and economic importance of waterborne zoonotic parasites. *Vet. Parasitol.* 126 (1-2): 3-14.

Gale, P. 2001. Developments in microbiological risk assessment for drinking water. *J. Appl. Microbiol.* 91(2): 191-205.

Garber, L. P., M. D. Salman, H. S. Hurd, T. Keefe, and J. L. Schlater. 1994. Potential risk factors for *Cryptosporidium* infection in dairy calves. *J. Am. Vet. Med. Assoc.* 205(1): 86-91.

Gerba, C. P., C. Wallis, and J. L. Melnick. 1975. Fate of wastewater bacteria and viruses in soil. *J. Irr. Drain Div.-ASCE* 101: 157-174.

Gleick, P. H. 2002. Dirty Water: Estimated Deaths from Water-Related Disease 2000-2020. Pacific Institute for Studies in Development, Environment, and Security Research Report, Oakland, California.

Goyal, S. M. and C. P. Gerba. 1979. Comparative adsorption of human enteroviruses, simian rotavirus, and selected bacteriophages to soils. *Appl. Environ. Microbiol.* 38(2): 241-247.

Graczyk, T. K., B. M. Evans, C. J. Shiff, H. J. Karreman, and J. A. Patz. 2000. Environmental and Geographical Factors Contributing to Watershed Contamination with *Cryptosporidium parvum* Oocysts. *Environ. Res.* 82(3): 263-271.

Graham, D. Y., G. R. Dufour, and M. K. Estes. 1987. Minimal infective dose of rotavirus. *Arch. Virol.* 92: 261-271.

Groisman, P. Y. and D. R. Easterling. 1994. Variability and trends of total precipitation and snowfall over the United States and Canada. *J. Climate* 7(1): 184-205.

Groisman, P., R. Knight, and T. Karl. 2001. Heavy precipitation and high streamflow in the contiguous United States: Trends in the 20th century. *B. Am. Meteorol. Soc.* 82: 219– 246.

Harter, T., S. Wagner, and E. R. Atwill. 2000. Colloid Transport and Filtration of *Cryptosporidium parvum* in Sandy Soils and Aquifer Sediments. *Environ. Sci. Technol.* 34: 62-70.

Haydon, S. and A. Deletic. 2006. Development of a coupled pathogen-hydrologic catchment model. *J. Hydro.* 328: 467-480.

Hoadley, A. W. and S. M. Goyal. 1976. Public health implications of the application of wastewater to land. In: *Land treatment and disposal of municipal and industrial wastewater*, 101-132. R.L. Sanks and T. Asano, eds. Ann Arbor, Michigan, USA: Ann Arbor Science.

Hoxie, N. J., J. P. Davis, J. M. Vergeront, R. D. Nashold, and K. A. Blair. 1997. Cryptosporidiosis-associated mortality following a massive waterborne outbreak in Milwaukee, Wisconsin. *Am. J. Public Health*, 87(12): 2032-2035.

Hrudey, S. E., P. M. Huck, P. Payment, R. W. Gillham and E. J. Hrudey. 2002. Walkerton: lessons learned in comparison with waterborne outbreaks in the developed world. *J. Environ. Eng. Sci.*, 1: 397-407.

Hunter, P. R. 2003. Climate change and waterborne and vectorborne disease. *J. Appl. Microbiol. Suppl.* 94: 37-46.

Jamieson, R., R. Gordon, D. Joy, and H. Lee. 2004. Assessing microbial pollution of rural surface waters: a review of current watershed scale modeling approaches. *Agr. Water Manage.* 70: 1-17.

Kapikian, A.Z. and R.M. Chanock. 1985. Rotaviruses. In: *Virology*, 863-906. B. N. Fields, D. M. Knipe, R. M. Chanock, J. L. Melnick, B. Roizman, and R. E. Shope. eds. New York, USA: Raven Press.

Karanis, P., C. Kourenti, and H. Smith. 2007. Waterborne transmission of protozoan parasites: A worldwide review of outbreaks and lessons learnt. *J. Water Health*, 5(1): 1-38.

Kato, S., M. Jenkins, E. Fogarty, and D. Bowman. 2004. *Cryptosporidium parvum* oocyst inactivation in field soil and its relation to soil characteristics: analyses using the geographic information systems. *Sci. Total Environ.* 321: 47-58.

Kaucner, C., C. M. Davies, C. M. Ferguson, and N. J. Ashbolt. 2005. Evidence for the existence of *Cryptosporidium* oocysts as single entities in surface runoff. *Water Sci. Technol.* 52: 199-204.

Kim, S. B. and M. Y. Corapcioglu. 2004. Analysis of *Cryptosporidium parvum* oocyst transport in porous media. *Hydrol. Process.* 18(11): 1999-2009.

Koch, D. J. 2009. Fate and transport of *Cryptosporidium parvum* under small-scale rainfall simulator. M.S. Thesis. Urbana, Illinois: University of Illinois, Department of Agricultural and Biological Engineering.

Korich, D. G., J. R. Mead, M. S. Madore, N. A. Sinclair and C. R. Sterling. 1990. Effects of ozone, chlorine dioxide, chlorine, and monochlorine on *Cryptosporidium parvum* oocyst viability. *Appl. Environ. Microbiol.* 56(5): 1423-1428.

Kouwen, N. and S.F. Mousavi. 2002. WATFLOOD/ SPL9 Hydrological Model and Flood Forecasting System. In: *Mathematical Models of Large Watershed Hydrology*, 649-685. V. P. Singh and D. K. Frevert. eds. Highlands Ranch, Colorado, USA: Water Resource Publications.

Kramer, M. H., B. L. Herwaldt, G. F. Craun, R. L. Calderon, and D. D. Juranek. 1996. Surveillance for waterborne-disease outbreaks-United States, 1993-1994, *MMWR CDC Surv. Summ.* 45(1): 1-33.

Kuczynska, E. and D. R. Shelton. 1999. Method for detection and enumeration of *Cryptosporidium parvum* oocysts in feces, manures, and soils. *Appl. Environ. Microbiol.* 65: 2820-2826.

LaBelle, R.L. and C. P. Gerba. 1979. Influence of pH, salinity, and organic matter on the adsorption of enteric viruses to estuarine sediment. *Appl. Environ. Microbiol.* 38: 93-101.

Laflen, J. M., L. J. Lane, and G. R. Foster. 1991. WEPP – a next generation of erosion prediction technology. *J. Soil Water Conserv.* 46(1): 34-38.

LeChevallier, M. W., W. D. Norton, and R. G. Lee. 1991. Occurrence of Giardia and *Cryptosporidium* spp. in surface water supplies. *Appl. Environ. Microbiol.* 57: 2610-2616.

LeChevallier, M. W., M. Abbaszadegan, A. K. Camper, C. J. Hurst, G. Izaguirre, M. M. Marshall, D. Naumovitz, P. Payment, E. W. Rice, J. Rose, S. Schaub, T. R. Slifko, D. B. Smith, H. V. Smith, C. R. Sterling, and M. Stewart. 1999a. Committee Report: Emerging Pathogens – Bacteria. *J. Am. Water Works Ass.* 91(9): 101-109.

LeChevallier, M. W., M. Abbaszadegan, A. K. Camper, C. J. Hurst, G. Izaguirre, M. M. Marshall, D. Naumovitz, P. Payment, E. W. Rice, J. Rose, S. Schaub, T. R. Slifko, D. B. Smith, H. V. Smith, C. R. Sterling, and M. Stewart. 1999b. Committee Report: Emerging Pathogens – Viruses, Protozoa, and Algal Toxins. *J. Am. Water Works Ass.* 91(9): 110-121.

Ling, T. Y., E. C. Achberger, C. M. Drapcho, and R. L. Bengtso. 2003. Quantifying adsorption of an indicator bacteria in a soilwater system. *Trans. ASAE* 45: 669-674.

Linhares, A. C., Y. B. Gabbay, J. D. Mascarenhas, R. B. Freitas, T. H. Flewett, and G. M. Beards. 1988. Epidemiology of rotavirus subgroups and serotypes in Belem, Brazil: a three-year study. *Ann. Inst. Pasteur. Virol.* 139(1): 89–99.

MacKenzie, W. R., N. J. Hoxie, M. E. Proctor, M. S. Gradus, K. A. Blair, D. E. Peterson, J. J. Kazmierczak, D. G. Addiss, K. R. Fox, J. B. Rose, and J.P. Davis. 1994. A massive outbreak in Milwaukee of *Cryptosporidium* infection transmitted through the public water supply. *New Engl. J. Med.* 331: 161-167.

Mawdsley, J. L., R. D. Bardgett, R. J. Merry, B. F. Pain, and M. K. Theodorou. 1995. Pathogens in livestock waste, their potential for movement through soil and environmental pollution. *Appl. Soil Ecol.* 2(1): 1-15.

Mawdsley, J. L., A. E. Brooks, and R. J. Merry. 1996a. Movement of the protozoan pathogen *Cryptosporidium parvum* through three contrasting soil types. *Biol. Fert. Soils* 21: 30-36.

Mawdsley, J. L., A. E. Brooks, R. J. Merry, and B. F. Pain. 1996b. Use of a novel soil tilting table apparatus to demonstrate the horizontal and vertical movement of the protozoan pathogen *Cryptosporidium parvum* in soil. *Biol. Fert. Soils* 23: 215-220.

McLaughlin, S. J. 2003. Adsorption kinetics of *Cryptosporidium parvum* to soils and vegetation. M.S. Thesis. Urbana, Illinois: University of Illinois, Department of Agricultural and Biological Engineering.

McNulty, M. S., G. M. Allen, G. R. Pearson, J. B. McFarren, W. L. Curran, and R. M. McCracken. 1976. Reovirus-like agent (rotavirus) from lambs. *Infect. Immun.* 14: 1332-1338.

McNulty, M. S. 1978. Rotaviruses. *J. Gen. Virol.* 40: 1-18.

McNulty, M. S. and E. F. Logan. 1983. Longitudinal survey of rotavirus infection in calves. *Vet. Rec.* 113: 333-335.

Mead, P. S., L. Slutsker, V. Dietz, L. F. McCaig, J. S. Bresee, C. Shaprio, P. M. Griffin, and R. V. Tauke. 1999. Food-related illness and death in the United States. *Emerg. Infect. Dis.* 5(5): 607-625.

Mebus, C. A., N. R. Underdahl, M. B. Rhodes, and M. J. Twiehaus. 1969. Calf diarrhoea (scours): reproduced with a virus from a field outbreak, University of Nebraska Agricultural Experiment Station Research Bulletin, No. 233.

Medema, G. J., F. M. Schets, P. F. M. Teunis, and A. H. Havelaar. 1998. Sedimentation of Free and Attached *Cryptosporidium* Oocysts and Giardia Cysts in Water, *Appl. Environ. Microbiol.* 64(11): 4460-4466.

Medema, G. J. and J. F. Schijven. 2001. Modelling the sewage discharge and dispersion of *Cryptosporidium* and Giardia in surface water. *Water Res.* 35(18): 4307-4316.

Middleton, P. J., M. T. Szymanski, G. D. Abbott, R. Bortolussi , and J. R. Hamilton. 1974. Orbivirus of acute gastroenteritis of infancy. *Lancet*, i: 1241-1244.

Moore, J. A., J. D. Smyth, E. S. Baker, J. R. Miner and D. C. Moffitt. 1989. Modeling bacteria movement in livestock manure systems. *Trans. ASAE*, 32: 1049-1053.

Nakagomi, O. and T. Nakagomi. 1993. Interspecies transmission of rotaviruses studied from the perspective of genogroup, *Microbiol. Immunol.* 37: 337-348.

Nash, J. E. and J. V. Sutcliffe. 1970. River flow forecasting through conceptual models part I - A discussion of principles. *J. Hydrol.* 10(3): 282-290.

Nearing, M. A., G. R. Foster, L. J. Lane, and S. C. Finkner. 1989. A process based soil erosion model for USDA-water erosion prediction project technology. *Trans. ASAE* 32(5): 1587-2593.

Neelakantan, T. R., G. M. Brion, and S. Lingireddy. 2001. Neural network modelling of *Cryptosporidium* and *Giardia* concentrations in the Delaware River, USA. *Water Sci. Technol.* 43(12): 125-132.

Neitsch, S. L., J. G. Arnold, J. R. Kiniry, R. Srinivasan, and J. R. Williams. 2002. Soil and Water Assessment Tool User's Manual Version 2000. GSWRL Report 02-02, BRC Report 02-06, Texas Water Resources Institute TR-192: College Station, TX, USA.

Neitsch, S. L., J. G. Arnold, J. R. Kiniry, and J. R. Williams. 2005. Soil and Water Assessment Tool Theoretical Documentation Version 2005. Grassland, Soil and Water Research Laboratory, Agricultural Research Service 808 East Blackland Road, Temple, Texas, USA.

Oates, P. M., C. Castenson, C. F. Harvey, M. F. Polz, and P. Culligan. 2005. Illuminating reactive microbial transport in saturated porous media: Demonstration of a visualization method and conceptual transport model, *J. Contam. Hydrol.* 77(4): 233-245.

Ogden, F. L. and P.Y. Julien. 2002. Chapter 4: CASC2D: A Two-Dimensional, Physically-Based, Hortonian Hydrologic Model. In: *Mathematical Models of Small Watershed Hydrology and Applications*, 69-112. Singh, V. P. and D. Frevert. eds. Highlands Ranch, CO, USA: Water Resources Publications.

Olson, M. E., J. Goh, M. Phillips, N. Guselle, and T. A. McAllister. 1999. Giardia Cyst and *Cryptosporidium* oocyst survival in water, soil, and cattle feces. *J. Environ. Qual.* 28: 1991-1996.

Overcash, M. R., K. R. Reddy, and R. Khaleel. 1983. Chemical processes and transport of animal waste pollutants. In: *Agricultural management and water quality*, 109–125. F.W. Shaller and G.W. Bailey. eds. Ames, Iowa, USA: Iowa State Univ. Press.

Pachepsky, Y. A., A. M. Sadeghi, S. A. Bradford, D. R. Shelton, A. K. Guber, and T. H. Dao. 2006. Transport and fate of manure-borne pathogens: Modeling perspective. *Agr. Water Manage.* 86: 81–92.

Parajuli, P. B., K. R. Mankin, and P.L. Barnes. 2008. Applicability of targeting vegetative filter strips to abate fecal bacteria and sediment yield using SWAT. *Agr. Water Manage.* 95: 1189-1200.

Parashar U. D., E. G. Hummelman, J. S. Bresee, M. A. Miller, and R I. Glass. 2003. Global illness and deaths caused by rotavirus disease in children. *Emerg. Infect. Dis.* 9(5): 565-572.

Parashar, U. D., C. J. Gibson, J. S. Bresee, and R. I. Glass. 2006. Rotavirus and severe childhood diarrhea. *Emerg. Infect. Dis.*, 12(2): 304-306.

Park, Y., L. Yeghiazarian, J. R. Stedinger, and C. D. Montemagno. 2008. Numerical approach to Cryptosporidium risk assessment using reliability method. *Stoch. Env. Res. Risk A.* 22(2): 169-183.

Patel, M. M., P. Haber, J. Baggs, P. Zuber, J. E. Bines, and U. D. Parashar. 2009. Intussusception and rotavirus vaccination: a review of the available evidence. *Expert Rev. Vaccines* 8(11): 1555-1564.

Paul, S., P. L. Haan, M. D. Matlock, S. Mukhtar, and S. D. Pillai. 2004. Analysis of the HSPF water quality parameter uncertainty in predicting peak in-stream fecal coliform concentrations. *Trans. ASAE* 47(1): 69-78.

Prüss-Üstün A., R. Bos, F. Gore and J. Bartram. 2008. *Safer water, better health: costs, benefits and sustainability of interventions to protect and promote health.* Geneva, Switzerland: World Health Organization.

Ramig, R. F. 1997. Genetics of the rotaviruses. *Annu. Rev. Microbiol.* 51: 225-255.

Refsgaard, J. C. and B. Storm. 1995. MIKE SHE. In: *Computer models of watershed hydrology*, 809–846. V.P. Singh, ed. Highlands Ranch, CO, USA: Water Resources Publications.

Renschler, C. S. 2003. Designing geo-spatial interfaces to scale process models: the GeoWEPP approach. *Hydrol. Process.* 17(5): 1005-1017.

Robertson, L. J. and H. V. Smith. 1992. *Cryptosporidium* and cryptosporidiosis - Part I: current perspective and present technologies. *Europ. Microbiol.* 1: 20-29.

Robertson, L. J., A. T. Campbell, and H. V. Smith. 1992. Survival of *Cryptosporidium parvum* oocysts under various environmental pressures. *Appl. Environ. Microbiol.* 58: 3494-3500.

Rodger, S. M., J. A. Craven, and I. Williams. 1975. Demonstration of reovirus-like particles in intestinal contents of piglets with diarrhea. *Aust. Vet. J.* 51: 536.

Rolsma, M. D., T. B. Kuhlenschmidt, H. B. Gelberg and M. S. Kuhlenschmidt. 1998. Structure and function of a ganglioside receptor for porcine rotavirus. *J. Virol.* 72: 9079-9091.

Rose, J. B. 1997. Environmental Ecology of *Cryptosporidium* and Public Health Implications. *Annu. Rev. Public Health* 18: 135-161.

Sadeghi, A. and J. Arnold. 2002. A SWAT/Microbial sub-model for predicting pathogen loadings in surface and groundwater at watershed and basin scales. In: *Proceedings of the March 11–13, 2002 Conference*, 56–63, Total Maximum Daily Load (TMDL) Environmental Regulations, Fort Worth, Texas.

Sagar, M. G. and C. P. Gerba. 1979. Comparative adsorption of human enteroviruses, simian rotavirus, and selected bacteriophages to soils. *Appl. Environ. Microbiol.* , 38: 241-247.

Santos, N. and Y. Hoshino. 2005. Global distribution of rotavirus serotypes/genotypes and its implication for the development and implementation of an effective rotavirus vaccine, *Rev. Med. Virol.* 15(1): 29-56.

Santosham, M., R. H. Yolken, R. G. Wyatt, R. Bertrando, R. E. Black, W. M. Spira, and R. B. Sack. 1985. Epidemiology of rotavirus diarrhea in a prospectively monitored American Indian population. *J. Infect. Dis.* 152: 778-783.

Sattar, S. A., R. A. Raphael, and V. S. Springthorpe. 1984. Rotavirus survival in conventionally treated drinking water. *Can. J. Microbiol.* 30:(5) 653-656.

Schaub, S. A. and C. A. Sorber. 1977. Virus and bacteria removal from wastewater by rapid infiltration through soil. *Appl. Environ. Microbiol.* 33: 609-619.

Schets, F. M., G. B. Engles, M. During ,and A. M. D. Husman. 2005. Detection of infectious *Cryptosporidium* oocysts by cell culture immunofluorescence assay: applicability to environmental samples. *Appl. Environ. Microbiol.* 71(11): 6793-6798.

Shamshad, A., C. S. Leow, A. Ramlah, W. M. A. Wan Hussain and S. A. Mohd. Sanusi. 2008. Applications of AnnAGNPS model for soil loss estimation and nutrient loading for Malaysian conditions. *Int. J. Appl. Earth Obs.* 10(3): 239-252.

Shaw, A. R. 2006. The rotavirus vaccine saga. *Annu. Rev. Med.* 57: 167-180.

Silvestri, L. S., Z. F. Taraporewala, and J. T. Patton. 2004. Rotavirus replication: plus-sense templates for double-stranded RNA synthesis are made in viroplasms. *J. Virol.* 78(14): 7763-7774.

Singh, P., J. Q. Wu, D. K. McCool, S. Dun, C. H. Lin, and J. R. Morse. 2009. Winter hydrologic and erosion processes in the U.S. Palouse region: field experimentation and WEPP simulation. *Vadose Zone J.* 8(2): 426-436.

Smith, M. and S. Tzipori. 1979. Gel electrophoresis of rotavirus RNA derived from six different animal species. *Aus. J. Exp. Biol. Med.* 57: 583–585.

Snelling, W. J., L. Xiao, G. Ortega-Pierres, C. J. Lowery, J. E. Moore, J. R. Rao, S. Smyth, B. C. Millar, P. J. Rooney, M. Matsuda, F. Kenny, J. Xu, and J.S. Dooley. 2007. Cryptosporidiosis in developing countries. *J. Inf. Dev. Count.* 1(3): 242-56.

Snodgrass, D. R., K. W. Angus, and E. W. Gray. 1977. Rotavirus infection in lambs: Pathogenesis and pathology. *Arch. Virol.* 55(4): 263-274.

Springer, E. P., G. F. Gifford, M. P. Windham, R. Thelin, and M. Kress. 1983. Fecal coliform release studies and development of a preliminary nonpoint source transport model for indicator bacteria. Hydraulics and Hydrology Series, UWRL/H-83/02, Utah Water Research Laboratory, Utah State University, Logan, Utah.

Starkey, S. R., S. E. Wade, S. Schaaf, and H. O. Mohammed. 2005. Incidence of *Cryptosporidium* parvum in the dairy cattle population in a New York City Watershed, *Vet. Parasitol.* 131(3-4): 197-205.

Sureshbabu, J., P. Venugopalan and A. P. Kourtis. 2010. Cryptosporidiosis. Available at: http://emedicine.medscape.com/article/996876-overview. Accessed 28 December 2010.

Tate, K. W., M. D. Pereira, and E. R. Atwill. 2004. Efficacy of vegetated buffer strip for *Cryptosporidium parvum. J. Environ. Qual.* 33(6): 2243-51.

Tian, Y., P. Gong, J. Radke, and J. Scarborough. 2002. Spatial and temporal modeling of microbial contaminants on grazing farmland. *J. Environ. Qual.* 31: 860–869.

Torres, J., M. Gracenea, M. S. Gomez, A. Arrizabalaga, and O. Gonzalez-Moreno. 2000. The occurrence of *Cryptosporidium parvum* and *C. muris* in wild rodents and insectivores in Spain. *Vet. Parasitol.* 92: 253-260.

Trask, J. R. 2002. Transport of *Cryptosporidium parvum* in overland and near-surface flow. M.S. Thesis, Urbana, Illinois: University of Illinois, Department of Agricultural Engineering.

Trask, J. R., P. K. Kalita, M. S. Kuhlenschmidt, R. D. Smith, and T.L. Funk. 2004. Overland and near-surface transport of *Cryptosporidium parvum* from vegetated and nonvegetated surfaces. *J. Environ. Qual.* 33: 984–993.

Tufenkji, N. 2007. Modeling microbial transport in porous media: traditional approaches and recent developments. *Adv. Water Resour.* 30: 1455-1469.

Tzipori, S., L. W. Caple, and R. Butler. 1976. Isolation of a rotavirus from deer, *Vet. Rec.* 99: 398.

Ungar, B. L. P. 1990. Cryptosporidiosis in humans (*Homo sapiens*). In: *Cryptosporidiosis of man and animals*, 59-82. J. P. Dubey, C. A. Speer and R. Fayer. eds. Boca Raton, Florida, USA: CRC Press.

USDA. 2008. Soil survey of Champaign County, Illinois. United States Department of Agriculture, Natural Resources Conservation Service.

USEPA. 1998. Announcement of the Drinking Water Contaminant Candidate List. United States Environmental Protection Agency notice, *Federal Register*, 63(40): 10274–10287.

USEPA. 1999. 25 Years of the Safe Drinking Water Act: History and Trends, EPA 816-R-99-007 report, United States Environmental Protection Agency.

Vaughn, J. F., E. F. Landry, L. J. Baranosky, C. A. Beckwith, M. C. Dahl, and N. C. Delihas. 1978. Survey of human virus occurrence in wastewater-recharged groundwater on Long Island. *Appl. Environ. Microbiol.* 36: 47-51.

Velázquez F. R., D. O. Matson, J. J. Calva, L. Guerrero, A. L. Morrow, S. Carter-Campbell, R. I. Glass, M. K. Estes, L. K. Pickering, and G. M. Ruiz-Palacios. 1996. Rotavirus infections in infants as protection against subsequent infections. *New Engl. J. Med.* 335(14): 1022-1028.

Walker, S. E., S. Mostaghimi, T. Dillaha, and F. Woeste. 1990. Modeling animal waste management practices: Impacts on bacteria levels in runoff from agricultural lands. *Trans. ASAE* 33: 807–817.

Walker, F. R. and J. R. Stedinger. 1999. Fate and Transport model of *Cryptosporidium*, *J. Environ. Eng.-ASCE* 125(4): 325-333.

Walker, M. J., C. D. Montemagno, and M. B. Jenkins. 1998. Source water assessment and nonpoint sources of acutely toxic contaminants: a review of research related to survival and transport of *Cryptosporidium parvum*. *Water Resour. Res.* 34(12): 3383-3392.

Wellings, F. M., A. L. Lewis, and C. W. Mountain. 1974. Virus survival following wastewater spray irrigation of sandy soils. In: *Virus survival in water and wastewater systems*, 253-260. J. F. Malina Jr. and B. P. Sagik. eds. Austin, USA: University of Texas Press.

Wellings, F. M., A. L. Lewis, C. W. Mountain, and L. V. Pierce. 1975. Demonstration of virus in groundwater after effluent discharge into soil. *Appl. Microbiol.* 29: 751-757.

WHO. 2009. World health statistics 2009 Report. Geneva, Switzerland: World Health Organization.

Widmer, G., M. Carraway, and S. Tzipori. 1996. Water-borne *Cryptosporidium*: A perspective from the USA. *Parasitol. Today* 12(7): 286-290.

Wilkinson, J., A. Jenkins, M. Wyer, and D. Kay. 1995. Modelling faecal coliform dynamics in streams and rivers. *Water Res.* 29: 847–855.

Woode, G. N., J. C. Bridger, G. A. Hall, and M. J. Dennis. 1974. The isolation of a reovirus-like agent associated with diarrhoea in colostrum deprived calves in Great Britain. *Res. Vet. Sci.* 6: 102-104.

Woode, G. N., J. Bridger, G. A. Hall, J. M. Jones, and G. Jackson. 1976. The isolation of reovirus-like agents (rotavirus) from acute gastroenteritis of piglets. *J. Med. Microbiol.* 9: 203-209.

Woolhiser, D. A., R. E. Smith, and D. C. Goodrich. 1990. KINEROS, A kinematic runoff and erosion model: documentation and user manual. ARS-77, USDA-Agricultural Research Service.

Wray, C., M. Dawson, A. Afshar, and M. Lucas. 1981. Experimental Escherichia coli and rotavirus infection in lambs. *Res. Vet. Sci.* 30(3): 379-81.

Wu, J., P. Rees, S. Storrer, K. Alderisio, and S. Dorner. 2009. Fate and transport modeling of potential pathogens: the contribution from sediments. *J. Am. Water. Resour. As.* 45(1): 35-44.

Yeghiazarian, L. L., M. J. Walker, P. Binning, J. Y. Parlange, and C. D. Montemagno. 2006. A combined microscopic and macroscopic approach to modeling the transport of pathogenic microorganisms from nonpoint sources of pollution. *Water Resour. Res.* 42, W09406, doi:10.1029/2005WR004078.

Young, R. A., C. A. Onstad, D. D. Bosch, and W. P. Anderson. 1987. AGNPS, Agricultural nonpoint source pollution model: A large watershed analysis tool. ARS Conservation Research Report # 35, United States Department of Agriculture.

Young, R. A., C. A. Onstad, D. D. Bosch, and W.P. Anderson. 1995. AGNPS: An agricultural nonpoint source model. In: *Computer Models of Watershed Hydrology*, 1011-1020. V.P. Singh. ed. Highlands Ranch, CO, USA: Water Resources Publications.